

DEPT. NAT. RES & ENV

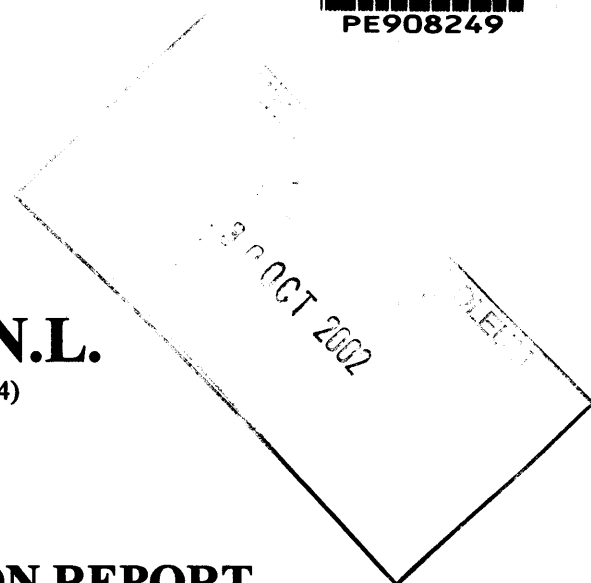


PE908249



Lakes Oil N.L.

(A.C.N. 004 247 214)



WELL COMPLETION REPORT

HUNTERS LANE-1 WELL

PEP 135 VICTORIA

Prepared for Petro Tech Pty Ltd
A subsidiary of Lakes Oil NL
by
Mulready Consulting Services Pty Ltd

August 2002

VOLUME 1



Lakes Oil N.L.

(A.C.N. 004 247 214)

WELL COMPLETION REPORT

HUNTERS LANE-1 WELL

PEP 135 VICTORIA

Prepared for Petro Tech Pty Ltd
A subsidiary of Lakes Oil NL
by
Mulready Consulting Services Pty Ltd

August 2002

LIST OF CONTENTS

	Page
SUMMARY & CONCLUSIONS	4
1. INTRODUCTION	5
2. WELL HISTORY	6
2.1 Location	6
2.2 General Data	7
2.3 Drilling Data	7
2.3.1 Drilling Contractor	7
2.3.2 Drilling Rig	7
2.3.3 Casing and Cementing	7
2.3.4 Drilling Bits	7
2.3.5 Drilling Fluids	8
2.3.6 Water Supply	8
2.4 Formation Sampling and Testing	8
2.4.1 Cuttings	8
2.4.2 Core	8
2.4.3 Tests	9
2.5 Logging and Surveys	9
2.5.1 Mud Logging	9
2.5.2 Wireline Logging	9
2.5.3 Deviation Surveys	9
2.5.4 Velocity Surveys	9
3. RESULTS OF DRILLING	10
3.1 Stratigraphic Table Hunters Lane-1	10
3.2 Lithological Descriptions	10
3.2.1 Jemmy's Point Formation	10
3.2.2 Tambo River Formation	10
3.2.3 Gippsland Limestone	10
3.2.4 Lakes Entrance Formation	11
Greensand Member	
Colquhoun Gravels	
Weathered Granite	
Fresh Granite	
3.3 Hydrocarbon Shows	11
3.3.1 Mud Gas	11
3.3.2 Sample Fluorescence	11
3.3.3 Liquid Hydrocarbons	11
4. GEOLOGY	12
4.1 Structure	12
4.2 Stratigraphy	13
4.3 Porosity and Water Saturations	13
4.4 Core Description & Core Analyses	13
4.5 Petrology	13

	Page
5. INITIAL BAILING TESTING	14
6. WORKOVER OPERATIONS	16
7. FINAL BAILING TESTING	18
8. PLUGGING & ABANDONMENT	20

FIGURES

Figure 1	Gippsland Permits Location Map
Figure 2	Well Location Map
Figure 3	Air Photo Lakes Entrance Field Area
Figure 4	Time vs. Depth Curve
Figure 5	Structure Map, Greensand Member
Figure 6	Isopach Map, Greensand Member
Figure 7	Correlation Petro Tech-1, Woodside Lakes Entrance & Hunters Lane-1
Figure 8	Well Diagram Hunters Lane pre-workover

TABLES

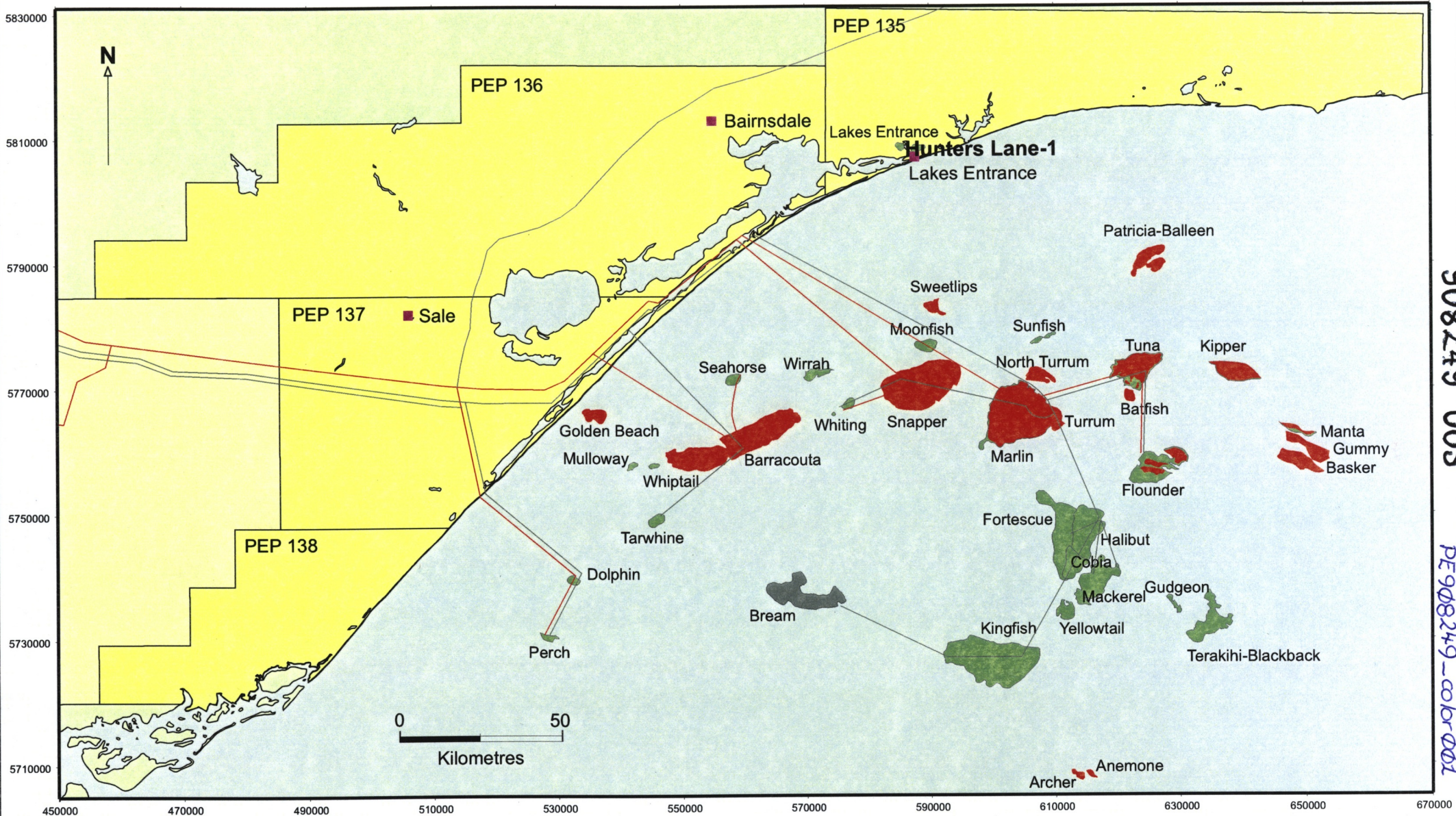
Table 1	Drilling Bit Record
Table 2	Drilling Fluids Record
Table 3	Lithostratigraphy Gippsland Basin
Table 4	Stratigraphic Table Hunters Lane-1

APPENDICES

I	Core Description and Porosity Analyses
II	Palynological Age Dating
III	Petrology Report Greensand Member
IV	Wellsite Survey
V	Water Analysis
VI	Oil Analysis
VII	Thermal History Reconstruction, Basement Granite, Hunters Lane-1

ENCLOSURES

1. Composite Well Log 1:500 Scale
2. Halliburton Formation Evaluation Log
3. Schlumberger Wireline Logs
 - Platform Express
 - Sonic MGT



908249 005

PE 908249-color 001



LAKES OIL N.L.

Figure 1: Permit Location Map

SUMMARY & CONCLUSIONS

Hunters Lane-1 was the second of two appraisal wells drilled by Lakes Oil into the Lakes Entrance oil field. The first was Petro Tech-1, drilled in March 1997 and located near the centre of the field as mapped, approximately 300 m. from the oil shaft sunk in the 1940s. Hunters Lane-1 was designed to provide control in the western portion of the field, to the north of Kalimna, and immediately west of North Arm.

In drilling these wells Lakes was concerned to provide an adequate modern set of data, which could be used for planning the development of the field. Correlation between the two wells, located 2-1/4 km apart, is good - both have similar Tertiary sections unconformably overlying Early Devonian granodiorite. The Woodside Lakes Entrance-1 well, drilled in 1966 also correlates well, and is included in Figure 7.

Two cores were cut within the Lakes Entrance Formation before oil shows were encountered in the Greensand Member. The well then drilled through the Greensand and the underlying Colquhoun gravel equivalent before intersecting basement (granodiorite) at 407.5 m. Electric logs were run at TD (422.5 m. KB). Repeated attempts at fluid recovery from the Greensand interval failed, and a barefoot completion of the Greensand was achieved cementing 178 mm (7 inch) casing at 395.5 m., then dressing a plug at 400.3 m. and under-reaming the Greensand section in preparation for bailing operations.

Over the next 10 months approximately 1700 litres of oil/oil water emulsion were produced from Hunters Lane-1 during bailing tests, representing of order 11% of the gross fluid recovery, which includes formation water.

The oil is similar to that recovered from the "Oil Shaft" near the centre of the field, showing evidence of biodegradation and water washing. Its API gravity is 16.14 rendering it a medium range oil which nonetheless flows readily at room temperature (pour point -18 deg. C). Its kinematic viscosity @ 40 deg. C is 78.16 cSt, (refer Appendix VI). An attempt to increase the fluid flow by opening up the underlying water-wet Colquhoun gravel section also failed, and the well was plugged and abandoned August 13th, 2001.

The results of the well indicate the reservoir has limited permeability and thickness, and is unlikely to be suited to steam injection stimulation. Nonetheless the field is open to the north, where both the Greensand and Colquhoun gravel will be at higher elevation, and future exploration will be focused on this portion of the field.

LOCATION MAP

PE908249-cob-rd2
908249 007

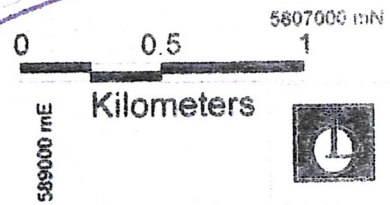
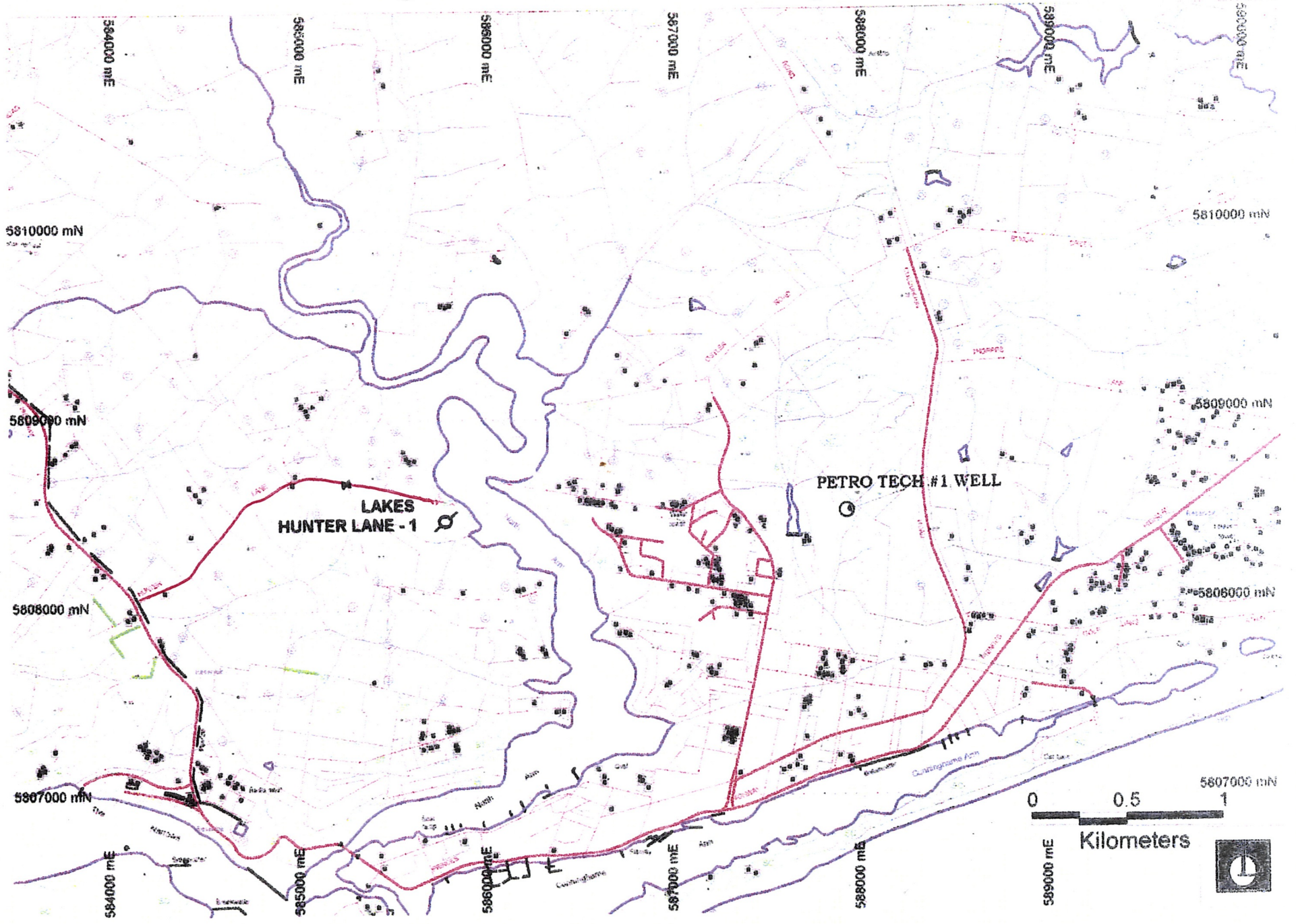
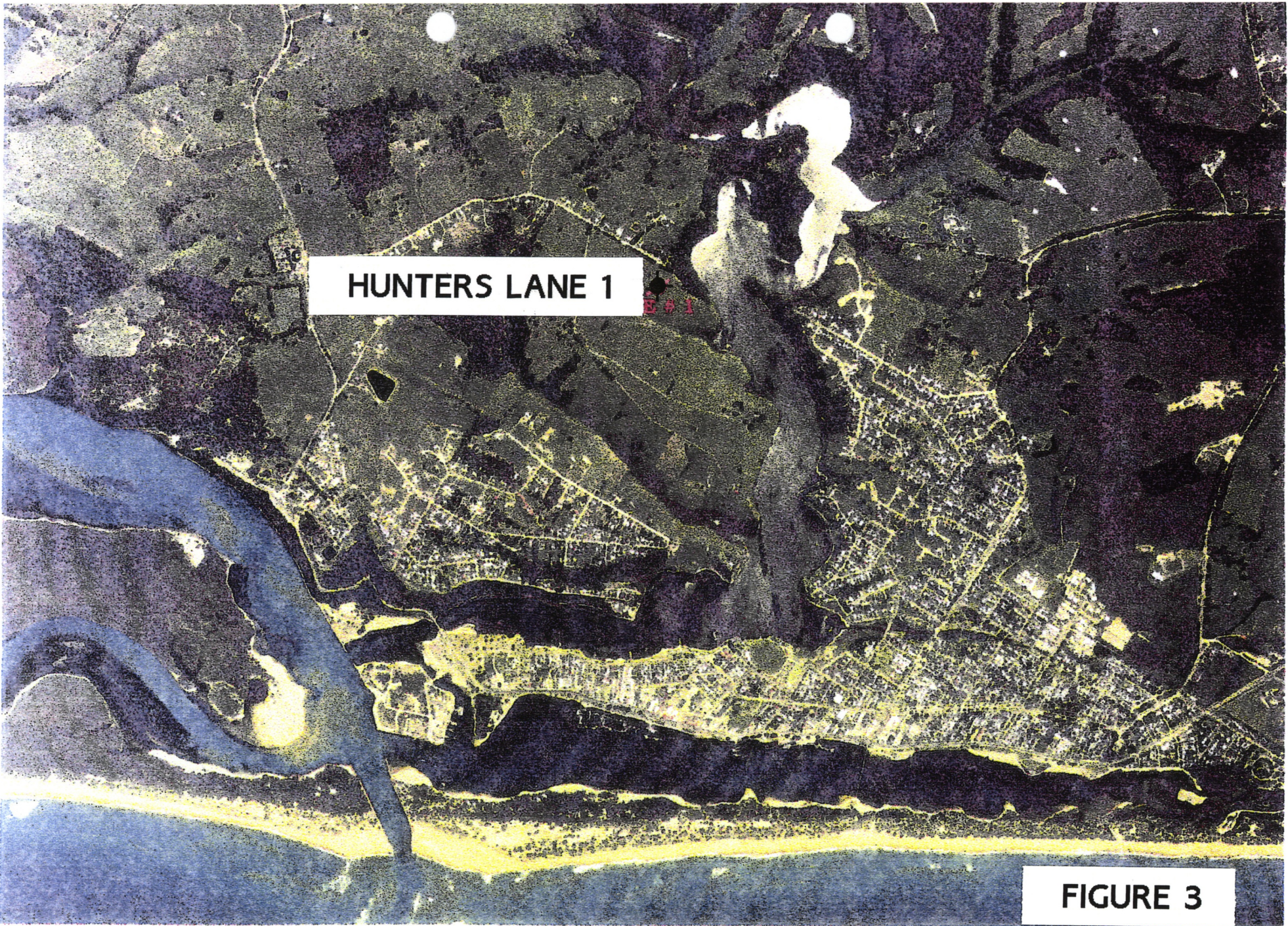


FIGURE 2



HUNTERS LANE 1

B # 1

FIGURE 3

PE998249-color003
903249 008

1. INTRODUCTION

The initial discovery well of the Lakes Entrance Oilfield (Lake Bunga-1) was drilled in 1924. Since that time over 60 wells have been drilled at Lakes Entrance targeting the Greensand reservoir at the base of the Lakes Entrance Formation.

Hunters Lane-1 was drilled by Lakes Oil NL as the second of a two well programme located within the boundaries of known production for the Lakes Entrance Oilfield, (*Figures 2,5&6*). Both the Hunters Lane-1 and Petro Tech-1 wells were designed to evaluate the potential of that field by providing up to date information on reservoir fluids and the Greensand reservoir, and in particular the potential for steam injection as a means of stimulating production from the field.

The Hunters Lane-1 location was chosen because of its close proximity to the Colquhoun-10 well, (also known as Oil Search-2). Colquhoun-10 appears to have been drilled in the 1940s, and was one of the highest producing wells in the western half of the field (36 gallons per day). The implication was thus that the well would be located either within or close to a 'reservoir fairway'. Additionally access was readily available from Hunters Lane. Housing development on Hunters Lane required that the site be positioned approximately 100 metres south of the Colquhoun-10 well.

HUNTERS LANE-1 TIME DEPTH CURVE

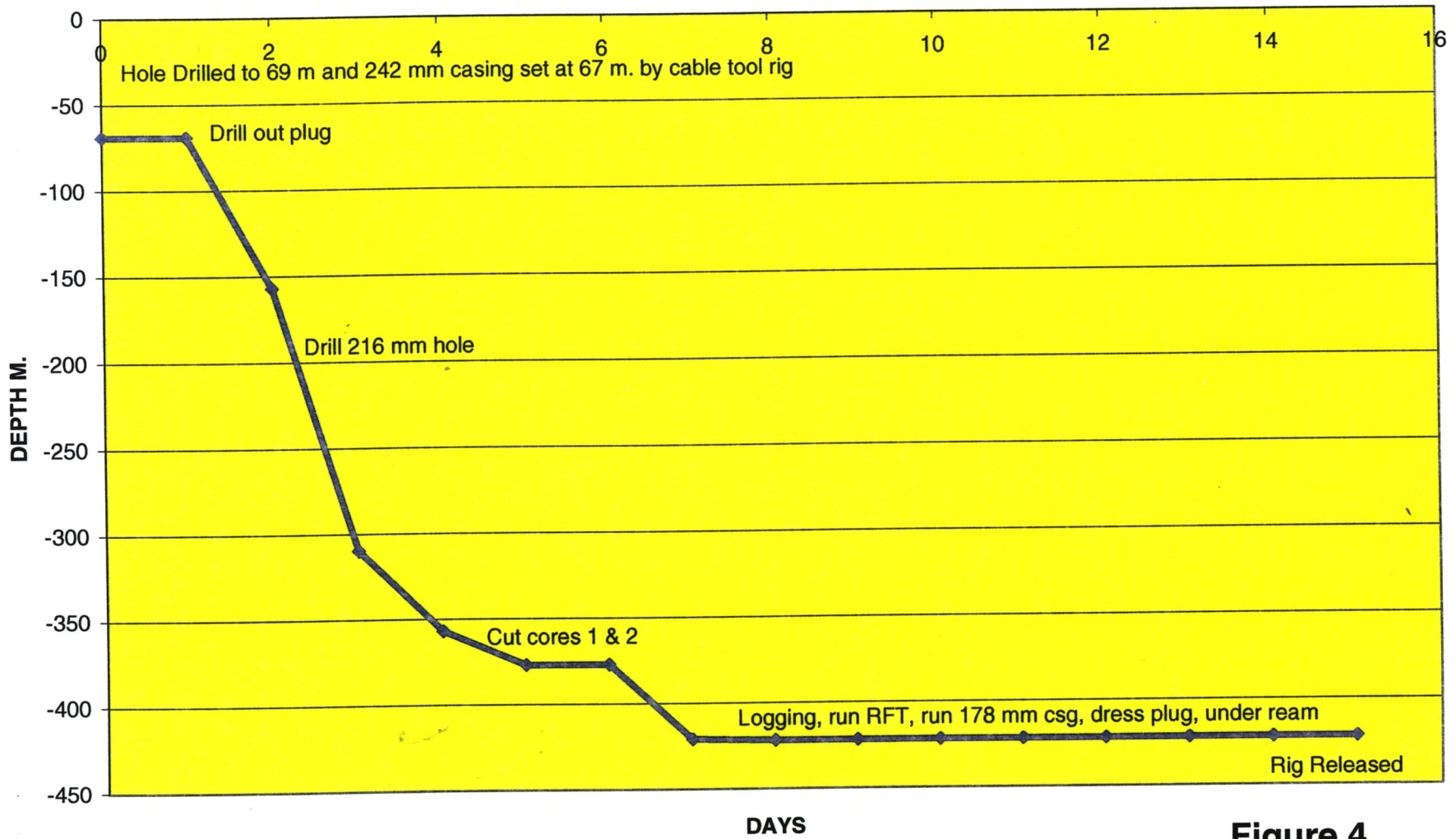


Figure 4

PE908249-color 004
908249 010

2. WELL HISTORY

2.1 Location (See Figures 1 & 2)

The well is located 2 km north-northwest of the Lakes Entrance Post Office.

Co-ordinates	Latitude	37° 51' 59.75" S
	Longitude	147° 58' 25.40" E

Australian Map Grid Co-ordinates, Zone 55

E 585646.21

N 5808526.47

Description: Eastern end of Hunters Lane, south side.
Property "Arren Dene"

Access to Location: Via Hunters Lane off the Princes Highway

2.2 General Data

Well Name: Hunters Lane-1

Operator: Lakes Oil NL
Level 11
500 Collins Street
Melbourne 3000

Elevation: Ground Level: 42.73 m.
Kelly Bushing (KB) 50.23 m (OKB)
Note: *Unless otherwise stated, all depths refer to KB, but note that three rigs were engaged in operations at Hunters Lane-1, each with their own unique KB elevation. These are NKB= 44.93 for the Speedstar Workover rig, and CKB= 43.43 m. for the cable tool rig.*

Total Depth:	Driller:	422.5 m
	Logger:	419.5 m

Pre-spud Surface Casing: 21st September 1997

Spudded: 29th September 1997

T.D. Reached: 9th October 1997.

Rig Released: 15th October 1997

Bailing Commenced: 23rd October 1997 (Cable Tool Rig)

Re-entry to open up
Colquhoun Gravel section: 8th September 1998

Speedstar Rig Released: 19th September 1998

Baling recommenced: 8th December 1998
 Bailing Ceased: 10th August 1999
 Status: Plugged and Abandoned at conclusion of bailing operations, 11th August 1999.

2.3 Drilling Data

2.3.1 Drilling Contractor

Imperial Snubbing Services
 P.O. Box 1506
 Sale
 Victoria 3850

2.3.2 Drilling Rig

Imperial Snubbing ISS Longstroke

2.3.3 Casing & Cementing Details

(i) Casing

Conductor

340 mm (13.3/8") set at 15 m KB

Grade/Weight J55, (81.3 kg/m or 54.5 lb/ft) BTC

Surface Casing

Size: 242 mm (9.5/8") set at 67 m KB

Grade/Weight K55 (53.7 kg/m or 36 lb/ft) BTC

Completion

Size 178 mm (7") set at 395.5 m. (driller) 392.5 m. (logger)

Grade /Weight P110 (43.1 kg/m or 29 lb/ft).

137 sx (5840 kg) Class G cement

82 sx (2180 kg) Silica Flour

(ii) Cement Plugs

(a) Initial phase

After reaching TD a cement plug was inserted over the interval 422-386.5 m. The plug was then dressed to 400 m. prior to under-reaming over the interval 397 to 400 m.

The hole was then displaced with brine prior to rig release.

(b) Abandonment

An abandonment plug was run from TD to approximately 30 m. above the casing shoe (dumped by the cable tool rig bailer).

Finally a surface plug was spotted prior to rig release.

2.3.4 Drilling Bits

The well was drilled from surface to 69 m by cable tool rig and 242 mm surface casing set at 67 m.

The Longstroke rig then moved on site and rigged up to drill 216 mm (8 ½”) hole out of the casing shoe

Table 1 Drilling Bit Record

Bit No.	1 (RR)	2(RR)	3
Size	216 mm	156 mm	To 356 mm
Make	Varel	Hughes	
Type	L117 1.1.7	STR-1 1.1.6	Under-reamer
Jets	3 x 11/32	3 x 11/32	
Depth in	69 m	413.58	397
Depth out	422.3 m		400
Total metres	353.3 m		3
Total Hours	12.5	15.5	
WOB (dN)	4	12	
RPM	60	60	
Condition		8-5-3/16	

2.3.5 Drilling Fluids

The 156 mm hole was drilled from 69 m to TD of 422.3 m over 6.5 days using an aquagel/starch/KCl mud system.

Typical mud properties close to TD were as follows:

Table 2 Drilling Fluids Record

Density	9.3 lb/gall	Gels	3/6 10s/10m
Viscosity	42 sec.	Sand	0.75%
Water Loss	9.6 ml.	Solids	7.0%
Ph	10.0	K+	9000 mg/l
Filter Cake	2 mm	Chlorides	8000 mg/l
PV/YP	10/6 cp/Pa	Calcium	220 mg/l

2.3.6 Water Supply

Town water was used for drilling and was transported by tanker from the Shire depot at Lakes Entrance

2.4 Formation Sampling and Testing

2.4.1 Cuttings

Cuttings samples were collected at 5 m. intervals from surface to surface casing point and at 3 m. intervals thereafter. Samples for immediate analysis were washed and a split stored in clear plastic "samplex" sample trays, which have been retained by the Operator. One separate washed split has also been retained by the Operator, and a second washed split forwarded to the Department of Manufacturing and Industry for storage.

Larger sample volumes were not washed but allowed to air dry before being forwarded to the Department of Manufacturing and Industry for storage.

2.4.2 Cores

Two conventional cores were cut in the well.

Core No. 1 was cut over the interval 357-366 m. (Lakes Entrance Formation) Recovery was 6.5 m. (72%). Whilst running in the hole to cut core No. 2 an error in pipe tally resulted in the barrel being washed/ drilled to 368 m before coring commenced.

Core No. 2 was cut over the interval 368-377.3 m. (Lakes Entrance Formation) Recovery was 9.3 m (100%).

The core was sent to Amdel in Adelaide for analysis. A Core Description and Core Analysis results are included in Appendix 1. No sidewall cores were taken in the well.

2.4.3 Testing

No conventional drill stem tests were run in the well.

The RFT was run following electric logging, but 17 attempts at sampling proved unsuccessful, (Refer RFT log in Enclosure 3).

The well was then completed utilising a barefoot technique for the Greensand target zone. 7 inch (178mm) casing was set at 395.5 m. (driller) 392.5 m (logger). After setting a bottom hole plug which was dressed to 400.3 m (driller), the well was left for bailing testing of the interval 392.5-400.3 m. (driller).

2.5 Logging and Surveys

2.5.1 Mudlogging (Refer Enclosure 2)

A Halliburton mudlogging unit was on site to record penetration rate, continuous mud gas monitoring, intermittent mud and cuttings gas analysis, pump rate and mud volume data. The mud log, (Halliburton Formation Evaluation Log), is included as Enclosure 2.

2.5.2 Wireline Logging (Refer Enclosure 3)

Wireline logging was performed by Schlumberger SEACO utilising a truck mounted offshore unit from their Sale base. The following logs were run at total depth:

Run 1 DLL-MSFL-SP-CAL (Platform Express Resistivity)
415 to 66.5 m

Density-Neutron (Platform Express Nuclear)
415 to 66.5 m

Gamma to Surface

Run 2 Spectral Gamma ray
411 to Surface

Run 3 RFT with Gamma

17 attempts at flow testing were undertaken over the gross interval 400 to 272 m. 5 attempts failed for lack of seal.

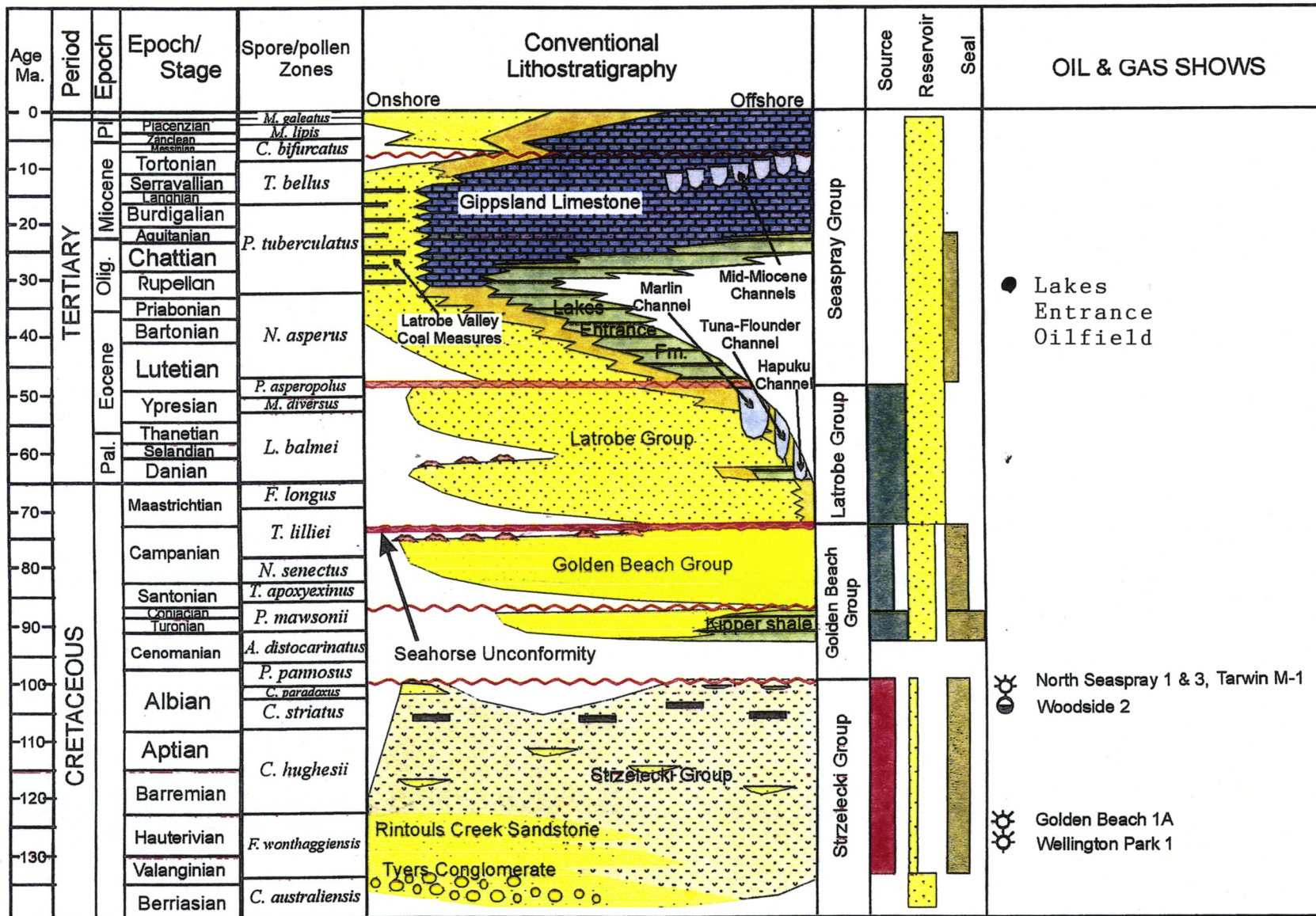
No fluid was recovered. Pressure data from RFT test is included in the RFT log in Enclosures 3.

2.5.3 Deviation Surveys

Nil.

2.5.4 Velocity Survey

No velocity survey was recorded.



LITHOSTRATIGRAPHY
GIPPSLAND BASIN

TABLE 3

908249 015 PE 908249-color.doc

3 RESULTS OF DRILLING

3.1 Stratigraphic Table Hunters Lane-1

The stratigraphy of the Gippsland Basin is summarised in Table 3.

For Hunters Lane-1 the following stratigraphic intervals have been identified utilising penetration rate, cuttings descriptions and wireline logs.

Table 4 Stratigraphic Table Hunters Lane-1

AGE	FORMATION	DEPTH K.B. (M)	DEPTH S.S. (M)	THICKNESS (M)
Miocene Oligocene	Jemmy's Point	Surface	+ 42.7	20
	Tambo River	27	+ 26	40
	Gippsland Limestone	67	-24	251
	Lakes Entrance	318	-266	76
	Greensand Member	394	-342	10
	Colquhoun Gravel	404	-352	7.5
Devonian	Granodiorite	411.5	-359	
	Total Depth	422.5		

3.2 Lithological Descriptions

3.2.1 Jemmy's Point Formation (surface to 27 m KB)

SANDSTONE: greyish orange, fine-medium grained, occasionally coarse grained, poorly sorted, subangular to occasionally rounded, common dispersed clay matrix, good visual porosity.

3.2.2 Tambo River Formation (27-67 m KB)

LIMESTONE: Off-white, pale yellow, orange brown, common fossil fragments, common dispersive clay matrix, and traces of muscovite and chert. Interbedded with

CLAYSTONE: grey-orange, very dispersive, soft, amorphous and

CALCAREOUS SILTSTONE: grey orange, very argillaceous, with very fine grained quartz and mica, including biotite, grading to very fine grained silty sandstone.

Also medium-dark grey, with a dispersive argillaceous matrix, and common fossil fragments. Soft, friable, grades to very fine grained sandstone and

SANDSTONE: dark yellow brown, well sorted, very fine to fine grained, rounded, very common fossil fragments, soft.

3.2.3 Gippsland Limestone (67-318 m KB)

LIMESTONE: (Calcarenite) Pale yellow brown, with coarse fossil fragments, common echinoid spines, bryozoa & coralline algae, traces of loose sand, hard.

MARL: grey, light brown in part, soft, sub blocky, traces of glauconite, traces of fossil fragments, traces of pyrite & rare traces of glauconite.

CLAYSTONE: light grey and olive grey to grey brown, silty, very calcareous in part, with common dispersed glauconite, traces of carbonaceous specks, commonly micromicaceous, traces of pyrite, soft, sub blocky to blocky.

3.2.4 Lakes Entrance Formation (318-394 m KB)*Interval 318-358*

SILTSTONE: grey brown, very argillaceous, traces of very fine grained quartz, traces of foraminifera fossils, with common carbonaceous specks, commonly micromicaceous, soft, slightly pyritic.

SANDSTONE: white, black speckled in part, very fine grained to silty, with clear quartz grains, common green black glauconite pellets in part, well sorted, rounded, generally as loose grains, with an argillaceous matrix in the occasional aggregates. No fluorescence.

Interval 358-377 m.

Refer core descriptions.

Interval 377 - 394 m

SILTSTONE AND SANDSTONE as above

Greensand Member (394-404 m)

SANDSTONE: green black, very fine to fine grained, predominantly black glauconitic pellets with very fine to occasionally coarse grained quartz, local fair sorting, with a glauconitic matrix. Aggregates have poor-fair visual porosity. Tr-20% fluorescence.

Colquhoun Gravel (404-411 m)

QUARTZ SANDSTONE: White to pale yellow brown, fine to predominantly coarse grained well rounded quartz grains, poorly sorted, with traces of mica. Good porosity inferred, no fluorescence.

Granodiorite (411 -)

White with common black biotite, predominant plagioclase feldspar and quartz. Medium to coarse crystalline aggregates.

3.3 Hydrocarbon Shows**3.3.1 Mud Gas Readings**

Gas detection equipment was operational from the casing shoe at 67 m to total depth. Initial readings of methane were first detected by the chromatograph within the Gippsland Limestone at 205 m. and these persisted virtually to total depth, reaching a maximum of approximately 8000-ppm between 280 - 355 m. Total gas readings became evident from 255 m, reaching a maximum of 20 units over the gross interval 280-320 m. As usual readings decreased during coring, but also remained low thereafter.

3.3.2 Fluorescence

Fluorescence was noted within the Greensand Member between 397 and 401 m. The fluorescence was moderately bright green, spotty, with weak background fluorescence. Moderately fast streaming cut with a thick residual ring.

3.3.2 Liquid Hydrocarbons

Oil was recovered during post-drill bailing operations. Refer Sections 5 and 7 below.

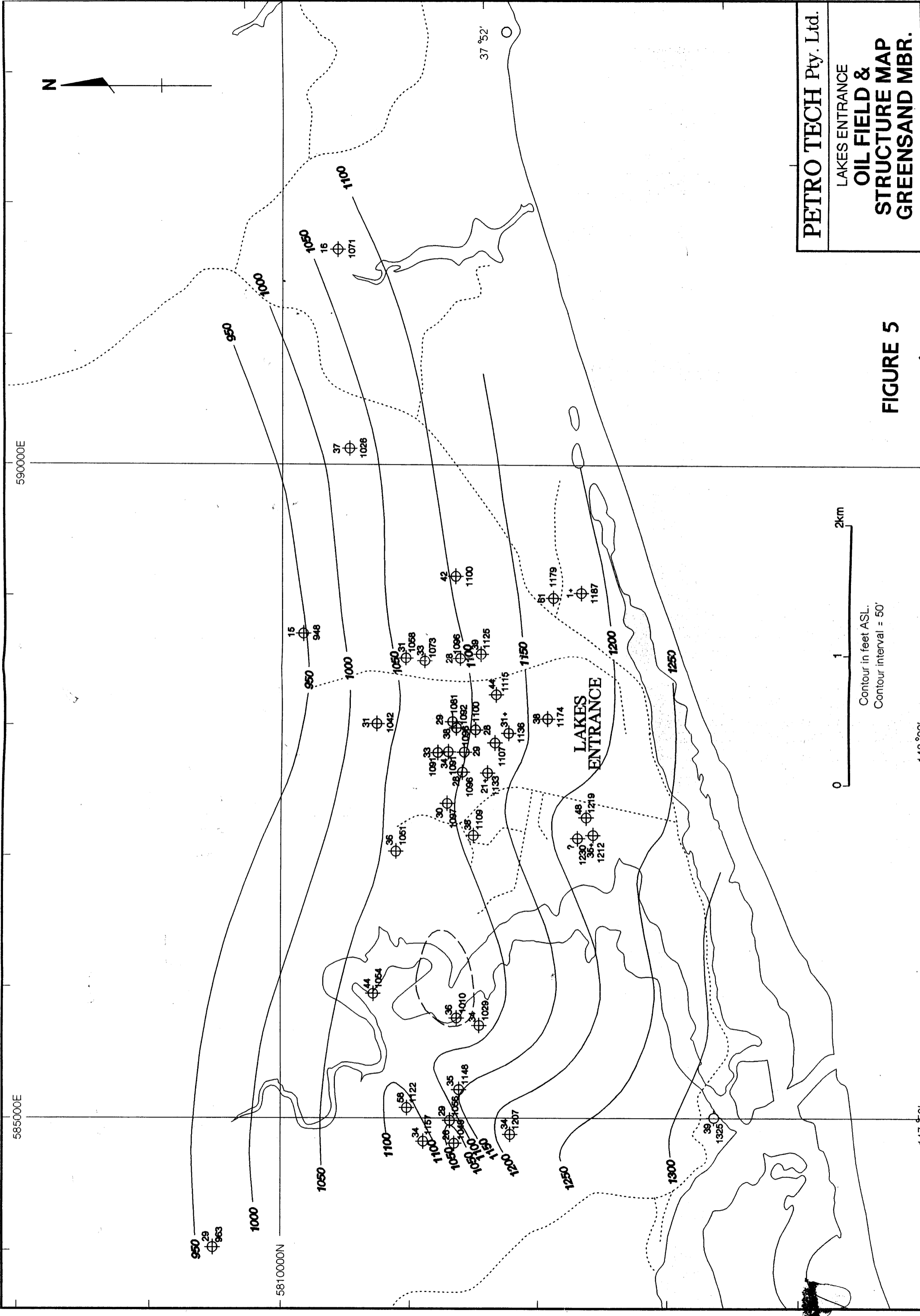
This is Page Number **908249_018X**

This is an enclosure indicator page.

The page that follows this page is an uncatalogued fold-out with page number:

908249_018Y

and is enclosed within the document PE908249 at this page.



PETRO TECH Pty. Ltd.
 LAKES ENTRANCE
 OIL FIELD &
 STRUCTURE MAP
 GREENSAND MBR.

FIGURE 5

0 1 2km
 Contour interval = 50'

Contour in feet ASL.
 Contour interval = 50'

148°00'

147°58'

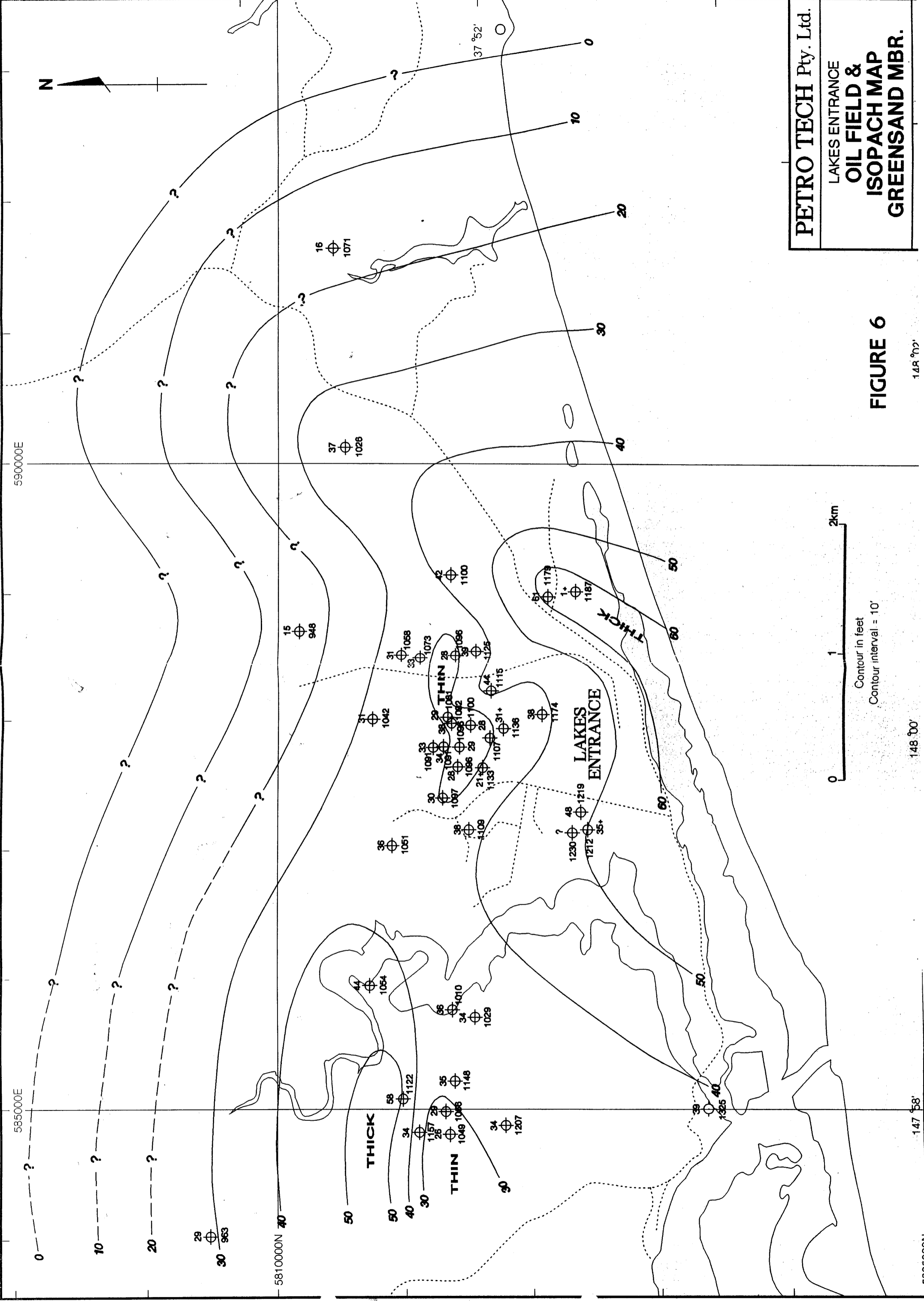
This is Page Number **908249_019X**

This is an enclosure indicator page.

The page that follows this page is an uncatalogued fold-out with page number:

908249_019Y

and is enclosed within the document PE908249 at this page.



PETRO TECH Pty. Ltd.
 LAKES ENTRANCE
 OIL FIELD &
 ISOPACH MAP
 GREENSAND MBR.

FIGURE 6

148 00'

148 00'

147 58'

4. GEOLOGY

4.1 Structure

Whilst there is virtually no effective seismic coverage over the Lakes Entrance oilfield, over 60 wells have been drilled within the field and its vicinity since the first discovery of oil in Lake Bunga #1 at the eastern end of the field in 1924, (Refer Figures 5 and 6). Unfortunately very little reliable stratigraphic information is available for the vast majority of the wells.

Despite these limitations two maps have been prepared from previously existing data and interpretations, viz.

Figure 5 Structure Map, Greensand Member

Figure 6 Isopach Map, Greensand Member

(Note that these figures are included for their historical interest, rather than for precise technical merit).

Hunters Lane-1 is located in the western portion of the field, west of North Arm and 2 km north-northwest of the Lakes Entrance Post Office. Although the well came in low to prognosis this is considered to be related to the inadequacy of the old well data used to prepare the well prognosis.

4.2 Stratigraphy

The section penetrated at Hunters Lane-1 was in reasonable agreement with the prognosis, with the exception of the pick for the top of the Greensand Member.

Confusion regarding this pick is believed to be related to the occurrence of varying amounts of glauconite in the overlying Lakes Entrance Formation section.

In an attempt to provide additional resolution within the Lakes Entrance Formation section a spectral gamma ray log was run at Hunters Lane-1. Relatively subtle variations in this log have been of assistance in selecting picks for the top of the Lakes Entrance Formation and the Greensand member.

Dr Alan Partridge of Biostrata Pty Ltd undertook palynological analysis of core and cuttings samples from the well, confirming an Early Oligocene age for the section.

His report is included as Appendix II.

4.3 Porosity and Water Saturation

Problems related to log interpretation of the Tertiary sediments of the Lakes Entrance region were discussed in section 4.2 of the Petro Tech-1 Well Completion Report.

In particular the unconsolidated nature of the section renders the Sonic log largely ineffective, whilst the gamma and resistivity logs are believed to be affected by the exotic mineral assemblage of the Greensand interval.

In Hunters Lane-1 the caliper log indicates significant washout in the hole of up to 13.1/2 inches (343 mm) within the Lakes Entrance Formation between the interval between 330 and 375 m. Filter cake build up was evident within the Gippsland Limestone and over the Colquhoun gravel interval, but not over the Greensand Member.

4.4 Core Descriptions and Core Analyses

Cores Nos. 1 & 2 were both cut within the Lakes Entrance Formation section above the Greensand Member as the result of an erroneous top Greensand Member pick in the existing well card. Accordingly the cores are dominated by mudstone lithology, and no plugs were taken for permeability measurements. Porosity analyses were undertaken using the summation of fluids technique.

Amdel's report on the core includes the core description and analytical results, and is included as Appendix I

4.5 Petrology

A sample collected from the Greensand Member section below the casing during bailing operations was submitted to Dr N.Lemon of the NCPGG in Adelaide for petrological analysis.

This is included as Appendix III.

A sample of the basal granodiorite was submitted to Dr Ian Duddy of Geotrack International for Thermal History Reconstruction using AFTA techniques. (See Appendix VII).

The conclusions of this study are:

- (i) Significant (kilometre scale) uplift has occurred on the Granodiorite/Tertiary unconformity, possibly removing Cretaceous sediments associated with rifting.
- (ii) The Oligocene and younger sedimentary section is immature for oil generation
- (iii) The age of the intrusion is assumed to be Late Devonian (370 Ma) based on regional information.

Note that similar results were obtained from the basement section at Petro Tech-1 well.

5. INITIAL BAILING TESTS

A new wellhead was installed prior to commencement of bailing operations.

Phase 1

On October 23rd 1997, (8 days after rig release), a cable tool rig was installed over the wellhead and bailing operations were carried out during daylight hours over the next four days.

The top of the brine was found to be 12m below ground level.

The well was bailed down progressively to approx. 391 metres CKB.

Approx. 250 ml. of oil/oil water emulsion was recovered at 360 m. CKB, whilst eight metres of fill (green silty sand) were retrieved from the bottom of the hole.

The well was then shut in for build up and the rig released.

Phase 2

The cable tool rig returned on December 2nd, 1997. Pressure was noted at the wellhead, and the well blew down air for 1 minute. Bailing then recommenced.

The top of the fluid was encountered at 358 m. CKB. The well was then bailed down to the top of the fill. The recovery included an estimated 50-60 litres of oil/oil water emulsion. The well was then allowed to build up for two hours, after which over 1 litre of oil/oil water emulsion and 20 litres of water were recovered.

Screens were then installed over the interval 393.9 to 400.3 m. OKB. (with the top 1.6 m. CKB inside the 7" casing).

Phase 3

The rig returned on the 8th January 1998. The surface valve bled air for 1 minute 20 sec. before bailing recommenced. The top of the fluid column was encountered at 347 m. CKB i.e. 47 m. above the screens and approx. 53 m. off bottom.

The well was bailed down to the top of the screens, yielding 40 litres of oil and 600 litres of water.

Bailing continued the next day, recovering an additional 35 litres of oil and 90 litres of water.

The well was then shut in to allow further build up.

Phase 4

The rig returned on February 9th, 1998. The top of the fluid column was again encountered at 347 m.

Bailing recovered a total of 72 litres of oil/oil water emulsion and 370 litres of water. A water sample was collected and analysed by Amdel (see Appendix V).

In total bailing operations to this date had recovered of order 200 litres of oil and over 2000 litres of water.

Note that it was found after standing that the oil is recovered as an emulsion, with approximately 30% of the 'oil' settling out as water.

A sample of oil recovered from the well was submitted to Amdel for analysis, and their report is included as Appendix VI

The oil has a specific gravity of 16.14, and viscosity of 78.16 cSt.

As expected there is a strong imprint of biodegradation and water washing, as was the case for the sample retrieved from the 'oil shaft'

This is Page Number **908249_024X**

This is an enclosure indicator page.

The page that follows this page is an uncatalogued fold-out with page number:

908249_024Y

and is enclosed within the document PE908249 at this page.

HUNTERS LANE 1

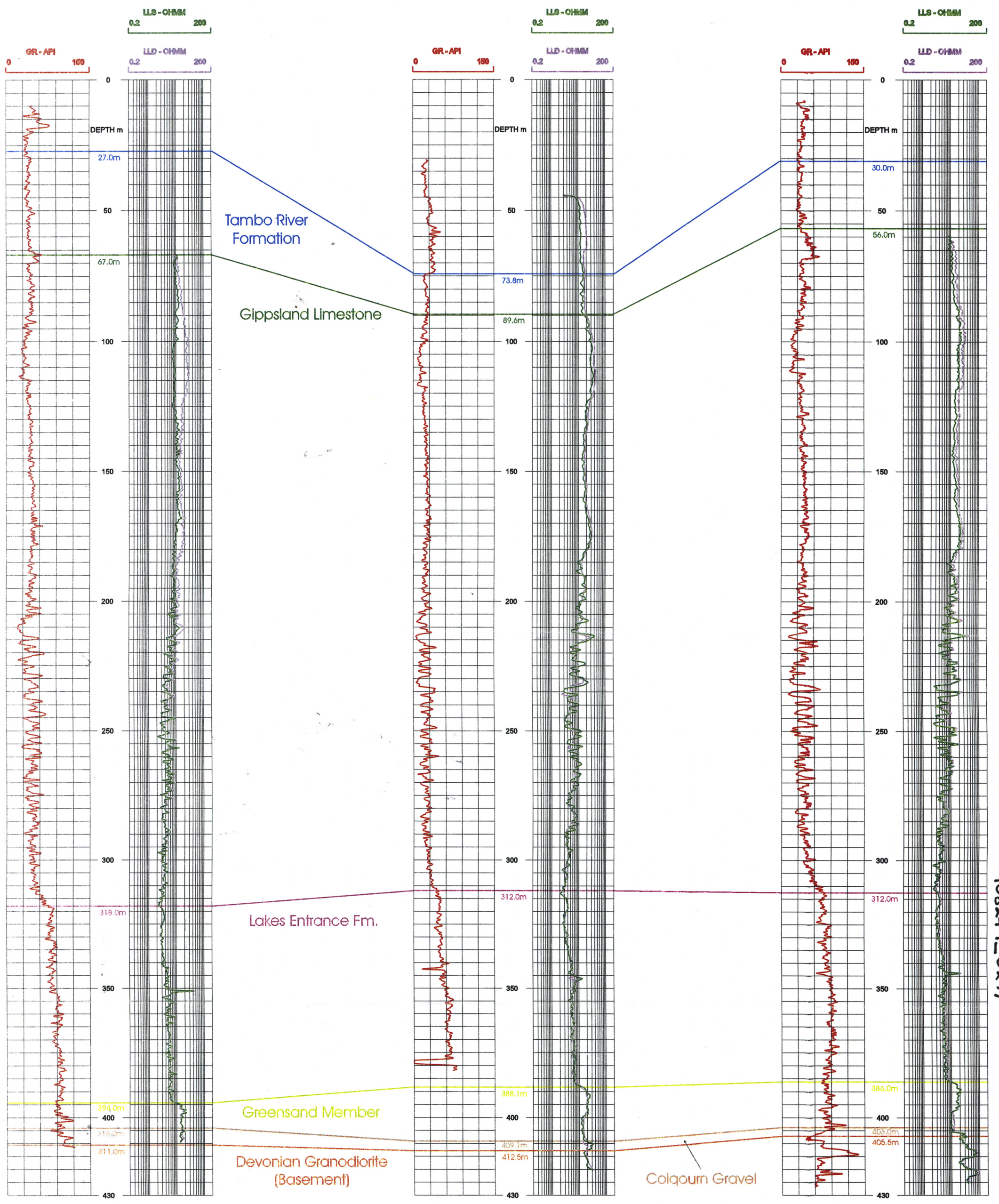
LAKES ENTRANCE 1

PETRO-TECH 1

KB: 50.5m

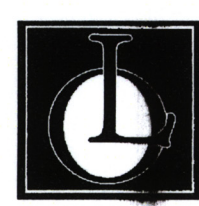
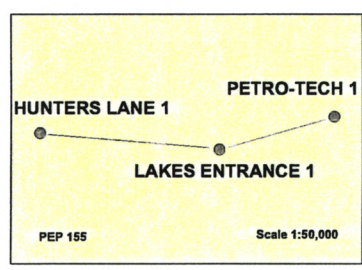
KB: 52.1m

KB: 50.2m



908249_0247

FIGURE 7



LAKES OIL LIMITED
PEP 155 - Onshore Gippsland Basin
 Hunters Lane 1 - Lakes Entrance 1 - Petro-tech 1
 Stratigraphic Correlation

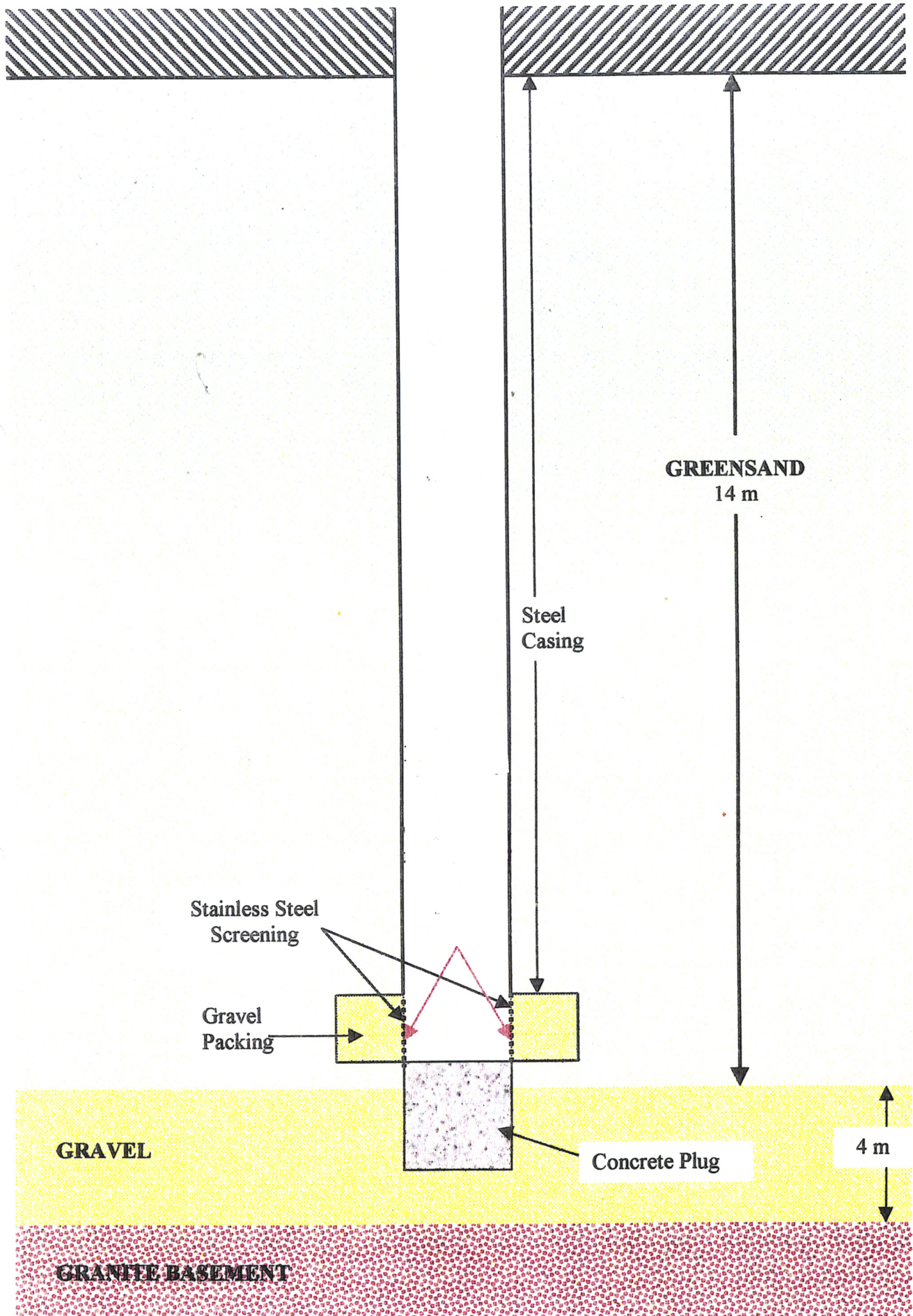


FIGURE 8

6. WORKOVER OPERATIONS

Daily reports for the Workover Operations are included in Appendix V.

After the completion of the initial bailing test programme, it was apparent that oil flow from the Greensand reservoir was not sufficient for commercial development. Pressure data from the RFT run at TD in the well (Enclosure 3) suggested the underlying Colquhoun Gravel sands should be capable of artesian flow at surface. Accordingly it was decided to re-enter the well, drill out the bottom hole plug and open up the underlying 'Colquhoun Gravel' section, (*Figure 8*) in the hope that the artesian flow would bring with it an increase in the rate of the oil produced.

On September 8th 1998 Sides Engineering's Speedstar SS40 HP rotary rig moved on site and set up to re-enter the hole and carry out the workover program. Difficulties were experienced in retrieving the screens, but finally these were recovered from the hole on 11/9/98.

After mudding up the top of the cement plug was tagged at 395 m. new KB.

Note: This is equivalent to 400.3 m. original KB. Thus
New KB (NKB) = Original KB-5.3 m. or
Original KB (OKB) = New KB+5.3 m.

The cement was then drilled out to 400 m. NKB (=405.3 m OKB). The hole was then opened up to 10 inches diameter over the interval 395-400 m. NKB (=400.3-405.3 m. OKB).

The mud column was then displaced with water - no flow was observed. After pulling back to 120 m NKB the BOPs were closed and an attempt was made to circulate out the hole with air, but the compressor was not able to displace the column. It was then decided to pull back to 82 m. NKB, where the BOP was closed and the well blown dry. After bleeding off pressure the BOPs were opened and the above procedure was repeated at 112 m., 130 m., 190 m. and 220 m. NKB. At 250 m. NKB the compressor was again unable to lift water to surface. The standing water level was estimated at 220 m. NKB. After pulling back to 130 m. the well was shut in overnight for 16 hours of build up.

Next morning the top of the water column was encountered at 190 m. NKB, a rise of 30 m., equivalent to approximately 3.7 barrels, or roughly 5.5 bbls fluid per day.

After changing out the under reamer and mudding up, 6 inch hole was then drilled to 407.8 m. NKB. The hole was then under reamed from 393 to 402.5m NKB. After displacing mud with water and pulling back to 120 m. NKB, a further unsuccessful attempt was made to unload the hole. A second attempt at 90 m. proved successful, and after running in to 120 it was again found to be possible to unload water from the hole. This procedure was repeated at 180m., 210 m., 240 m., and 260 m. NKB.

The circulation at this depth indicated the compressor was at the limit of its capacity. The well was then closed in for 3 hours before running in to 260 m. and establishing circulation, recovering approx. 1/2 barrel of water.

After pulling back to 120 m. the well was shut in over night.

Next morning after an 18 hours shut in the top of the fluid was encountered at approx. 240 m., a rise of 18 m, roughly equivalent to a flow of 3 bbls of fluid per day.

At this stage it was decided to suspend operations and release the rig, with bailing operations to be resumed at a later date using a cable tool rig.

Sides Engineering's Speedstar SS40 HP rotary rig was released 19/9/98.

7. FINAL BAILING TESTING

Note: Cable tool rig KB (CKB) is 6.8 m less than original KB of the Longstroke rig. Operations were concluded during daylight hours only.

Phase 1

On October 12th Killeen Drilling's cable tool rig was used to bail the well dry. The rig then moved off location to allow build up of fluids in the well.

Phase 2

On December 8th 1998 the cable tool rig returned and set up over the hole. Two 20 bbl tanks were located on site for storage of produced fluids.

The top of the fluid was encountered at 117 m. CKB, and thereafter 220 litres of oil/oil water emulsion were bailed before the top of the water column was intersected at 135 m.

The next day the fluid level was found to have risen 6 m. The well was then bailed dry to the top of the screens, recovering an additional 20 litres of oil/oil emulsion, and then shut in.

Finally acid was spotted over the uncased portion of the hole, and the well allowed to build up once again for a period of 2 months.

Phase 3

On the 8th of February 1999 Pincott Drilling's cable tool rig again set up over location, and bailing recommenced.

The top of the fluid was encountered at 224 m. CKB, and thereafter 370 litres of oil/oil water emulsion were bailed before the top of the water column was intersected at 243 m., suggesting an oil/oil emulsion content of 11%, with an oil percentage of order 8%.

In order to drill out the fill at the bottom of the hole the casing was part filled with water.

An additional 20 litres of oil/oil emulsion were recovered at this stage.

3 metres of fill were drilled before an obstruction was encountered at 391 m. CKB.

An impression block was run and this indicated the presence of a sharp metallic object located near the circumference of the hole. Attempts at recovery of the fish with a magnet proved unsuccessful, but the fish was eventually by-passed and the well cleaned out to 402.5m. CKB (=409.3 m OKB).

After pulling out of the hole a 15.7 m. x 4-1/2" OD liner was made up, with the bottom 3 metres being slotted.

The liner was successfully set at TD, with the top of the liner sitting 1.9 metre within the casing at 386.8 m. CKB.

The well was then bailed down to the top of the liner, but only traces of oil were recovered throughout.

The next morning the fluid level had risen 23 m. overnight.

The well was then bailed to the top of the liner, recovering 140 litres of oil/oil water emulsion and 300 litres of water. At 11 a.m. the well was shut in for 5 hours to allow build up. After this time the rise of the fluid level was 3.1 metres. 10 litres of oil/oil water emulsion and 50 litres of water were recovered. The well was then shut in and the rig released on February 17th 1999.

Phase 4

On the 9th of March 1999 Pincott Drilling's cable tool rig returned and set up over the well.

The top of the fluid was encountered at 298 m. CKB (305 m OKB). The rig then bailed approximately 80 litres of oil/oil water emulsion, with the remainder of the fluid (97%) being water. The well having been bailed to the top of the liner, the well shut in overnight.

Next morning the fluid level was found to have risen 9 m. The well was bailed to the top of the liner and 10+ litres of oil/oil water emulsion and approximately 150 litres of water were recovered.

The well was then shut in and the rig released on March 12th 1999.

Phase 5

After evaluation of the bailing test results it was decided to abandon the well in accordance with DNRE requirements, having first conducted another bailing test.

After 6 months Pincott Drilling's cable tool rig returned and set up over the well on the 9th of August 1999.

The top of the fluid was encountered at 113 metres CKB. 450 litres of oil/oil water emulsion were recovered before encountering the top of the water column at 137 m.

The liner was then removed and the well allowed to build up over night.

Next morning the top of the fluid was encountered at 145 m.

80 litres of oil/oil water emulsion were bailed before the top of the water was intersected at 149 m. The well was then bailed to within 6 m. of TD.

Next morning 80 litres of additional oil/oil water emulsion were recovered, then water.

Total oil/oil water emulsion produced in the second round of bailing tests was approx. 1500 litres, with over 20,000 litres of water.

Overall of order 1700 litres of oil/oil water emulsion were produced from Hunters Lane-1 during bailing tests.

8. PLUGGING AND ABANDONMENT

On August 11th a 22-sack bottom hole cement plug was then set with the rig's dump bailer, and allowed to set overnight.

On August 12th the bottom plug was bumped at 368 m. CKB (375 m. OKB).

A surface plug was then set using 2 sacks of cement, with the top of the plug at 3 m.

The rig was then released on the morning of August 13th, 1999.

Subsequently the wellhead was retrieved and the well capped.

Finally a sign was erected on the adjacent fence.

903249 031

**HUNTERS LANE-1 WELL COMPLETION
REPORT**

APPENDIX 1

**CORE ANALYSIS &
CORE DESCRIPTION**

BY AMDEL

Amdel Limited
A.C.N. 008 127 802

Petroleum Services
PO Box 338
Torrensville Plaza SA 5031

Telephone: (08) 8416 5240

Facsimile: (08) 8234 2933

12 November, 1997

Lakes Oil NL
GPO Box 427G
MELBOURNE VIC 3000

Attention: Jack Mulready

REPORT LQ6330

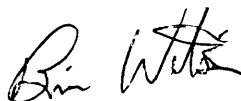
CLIENT REFERENCE: PEP135-CA-01

WELL NAME/RE: Hunters Lane

MATERIAL: Core

WORK REQUIRED: Routine Core Analysis

Please direct technical enquiries regarding this work to the signatory below under whose supervision the work was carried out.



Brian L. Watson
Manager
Petroleum Services

1. INTRODUCTION

Two (2) cores were cut in Hunters Lane-1 over the interval 356.85 to 377.30 metres in the Greensand Member of the Lakes Entrance Formation.

Core #1 (356.85-365.35 m) 6.5 m (76% recovery) of mudstone while Core #2 (368.0-377.3 m) recovered 9 m (97% recovery) also of mud stone.

This report is a formal presentation of results forwarded as they became available.

2. ANALYTICAL PROCEDURES

Gamma ray analysis was determined every fifteen centimetres over the length of Cores #1 and #2. Porosity and saturation data were determined by summation of fluids.

3. RESULTS AND DISCUSSION

Results are presented on the following pages.

All of Cores #1 and #2 appeared to be mudstone and water wet. Therefore no plug samples were cut.

3.1 Notes on the Logging of Hunters Lane-1

The entire interval from 357 m to 377 m was dominated by mudstone. The interval also has a number of marine indicators, including abundant bioturbation, glauconite pellets and some shelly fauna (oysters, turreted gastropods, and possible bryozoans and echinoids). The burrows are mainly simply subhorizontal tubes (Planolites) with a few more complex forms showing working up and down in the sediment pile (Techichnus).

The distribution of shelly material and glauconite pellets allows the muddy sequence to be broken up into depositional cycles. This is evident around 370-373 m and again around 375 m. Glauconite pellets and fossil hash collects at the base of thin cycles, effectively raising the average grainsize to fine sand. This does not infer there is any clastic sand in these intervals, merely coarser "intraclastic" material, glauconite mud pellets supported by a mud matrix.

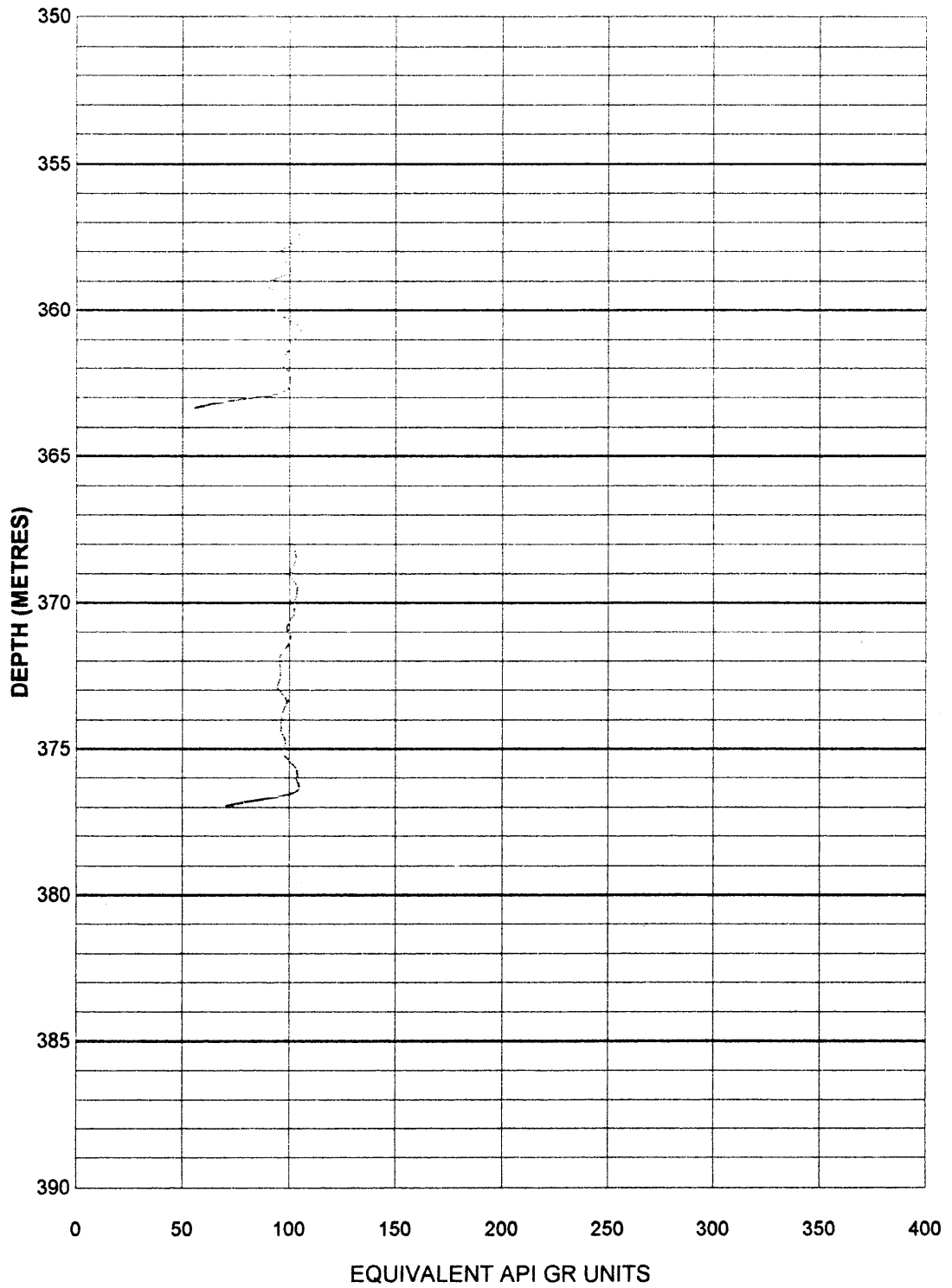
The tightly cemented zones within the core are very calcareous. These are also zones with a higher shelly fossil content and zones where there are fossil moulds and other evidence of aragonite dissolution. It is highly likely that the dissolved aragonite has re-precipitated in the immediate vicinity as calcite cement.

Table 1
Summation of Fluids Data

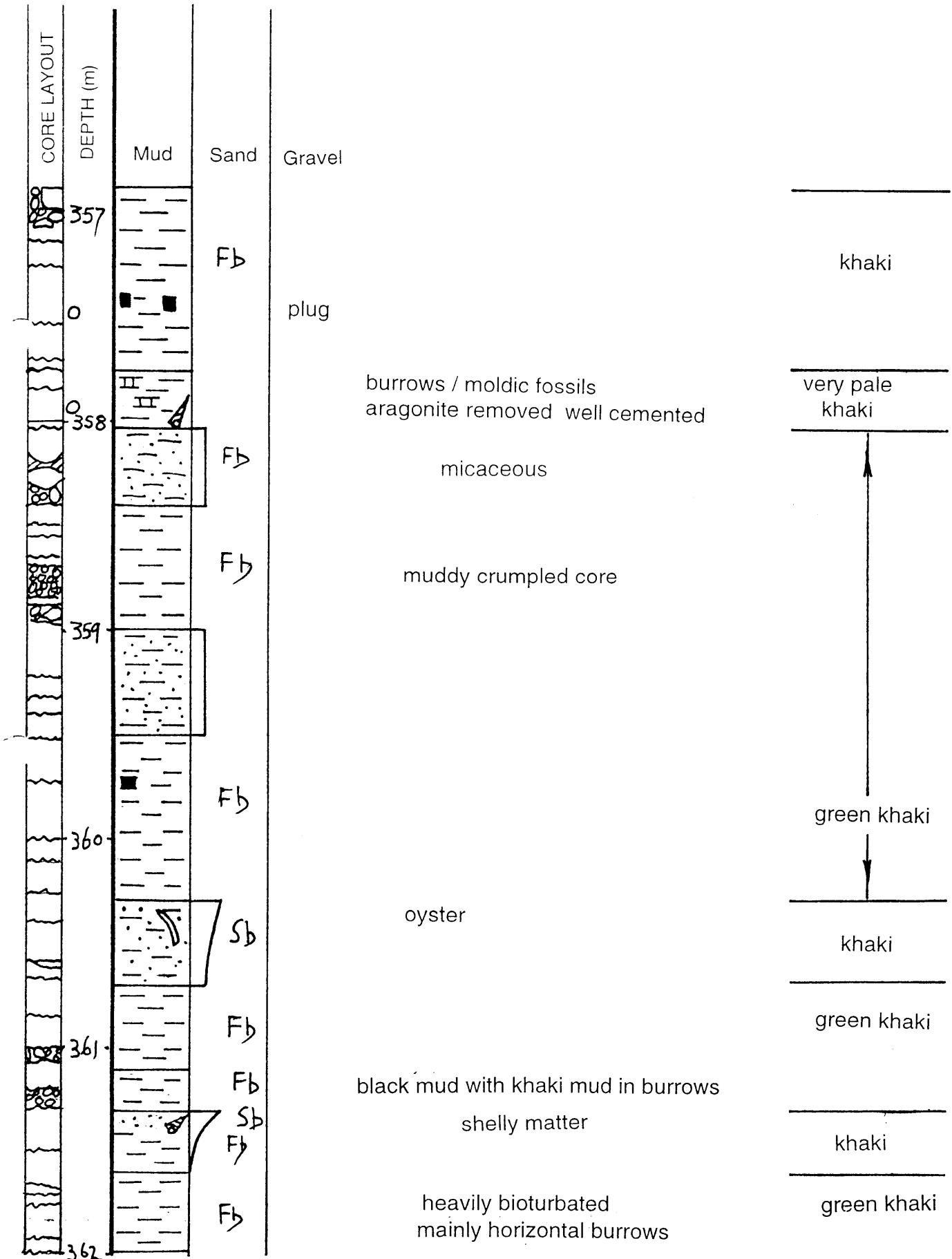
Sample Number	Depth (m)	Porosity Percent	Residual Liquid Saturation		
			Oil		Total Water
			% Vol	% Pore	% Pore
CORE #1					
1	357	37.3		0.0	95.5
2	358	33.4		0.0	94.7
3	359.25	28.1		0.0	92.1
4	360.05	29.8		0.0	92.0
5	361.05	33.5		0.0	93.4
6	362.05	27.1		0.0	86.4
7	362.95	19.3		0.0	90.1
8	363.20	3.8		0.0	70.7
CORE #2					
9	369.05	22.3		0.0	89.9
10	370.05	34.8		0.0	57.5
11	371.05	30.5		0.0	91.8
12	372.10	29.5		0.0	88.8
13	373.30	27.8		0.0	93.6
14	374.10	28.0		0.0	92.4
15	375.25	29.6		0.0	88.7
16	376.40	27.7		0.0	90.7

HUNTERS LANE NO.1, CORES 1 & 2

GAMMA RAY

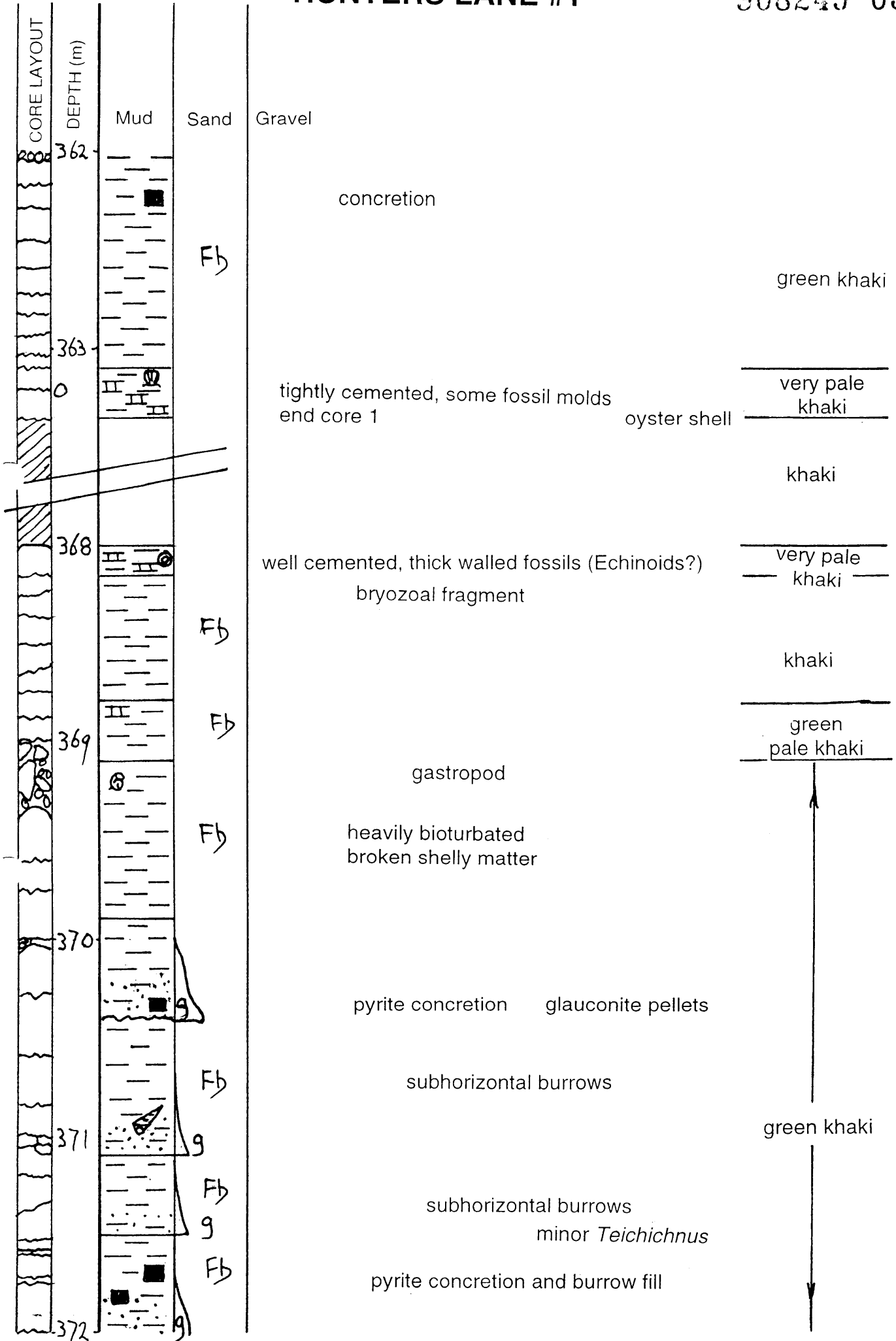


HUNTERS LANE #1



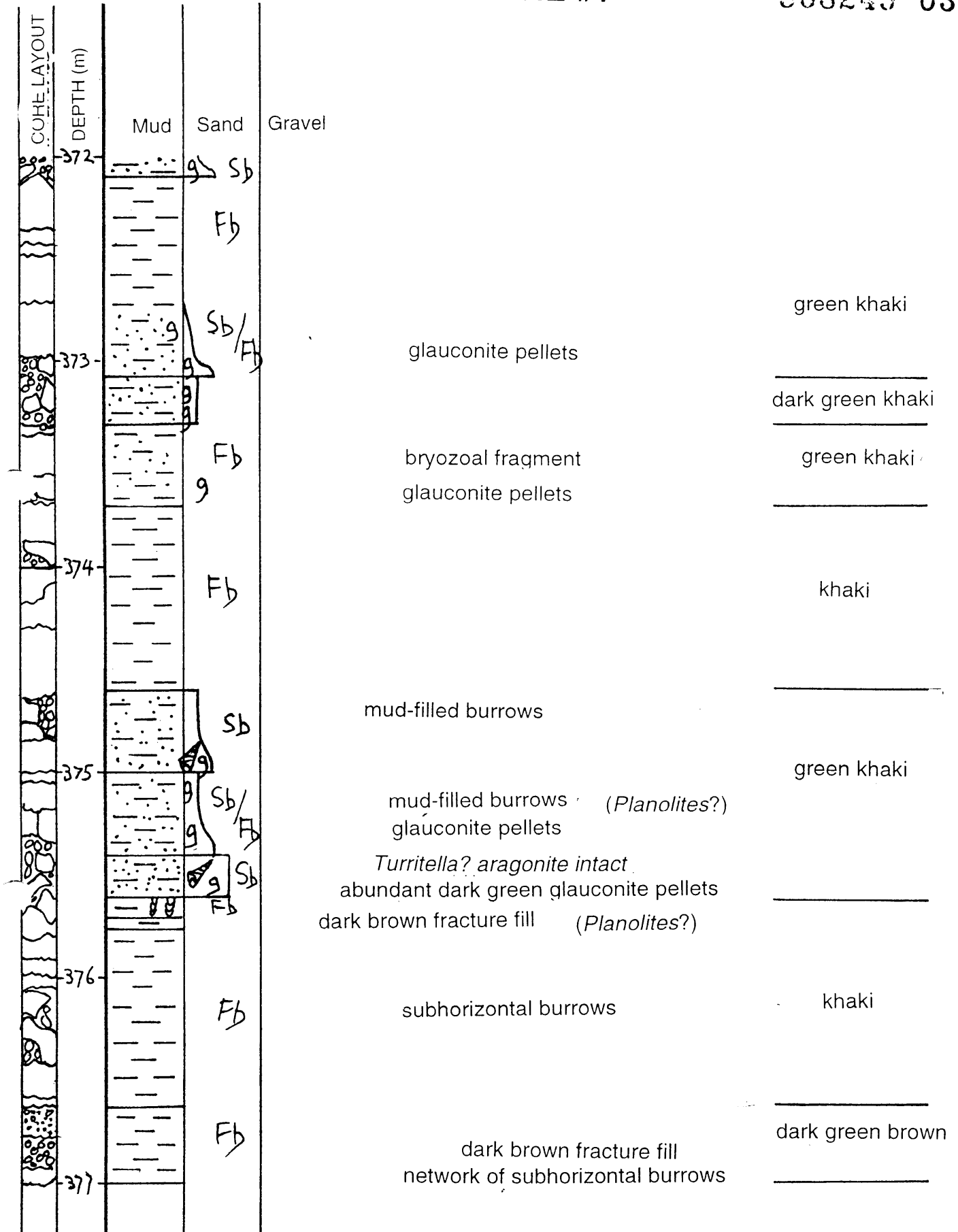
HUNTERS LANE #1

903249 038



HUNTERS LANE #1

903249 039



903249 040

**HUNTERS LANE-1 WELL COMPLETION
REPORT**

APPENDIX II

PALYNOLOGICAL AGE DATING

Dr. A. Partridge

Biostrata Pty Ltd

**Palynological analysis of
core and cuttings samples from
Hunters Lane-1, onshore Gippsland Basin**

by

Alan D. Partridge

Biostrata Pty Ltd
A.C.N. 053 800 945

Biostrata Report 1998/7

10 July 1998

Palynological analysis of core and cuttings samples from Hunters Lane-1, onshore Gippsland Basin.

by Alan D. Partridge

INTERPRETATIVE DATA

Summary

This report provides the results of palynological analysis of two core and three cuttings samples from the Hunters Lane-1 well located near the township of Lakes Entrance, onshore Gippsland Basin. The conventional cores were sampled to investigate the age and stratigraphic assignment of the cores. The cuttings were analysed to investigate the age of the quartz sands immediately above the granite basement and to clarify their relationship to the overlying stratigraphic units. The key findings are:

- All samples gave well preserved, abundant and diverse spore-pollen assemblages assignable to the Early Oligocene portion of the *P. tuberculatus* Zone.
- All samples also contained marine microplankton assigned to the broad *Operculodinium* Superzone. In the two core samples the microplankton were abundant (17% and 36% of count) but of low diversity. The three deeper cuttings samples contained higher diversity assemblages reflecting a significant caved component. The shallowest two cuttings at 405 and 408m could also be more precisely assigned to the *Fromea leos* Zone.
- The two core samples are interpreted to lie in the Metung Marl Member of the Lakes Entrance Formation.
- The three cuttings are interpreted to contain mixed assemblages derived from the Metung Marl Member of the Lakes Entrance Formation, basal greensand (Cunninghame Greensand Member), as well as in all probability the basal quartz sandstone (Colquhoun Sandstone Member). However, as there is nothing new or particularly characteristic in the assemblages recorded the most reasonable conclusion is that no significant age difference can be distinguished between the three units in Hunters Lane-1 using palynology.

Introduction

This study is of two samples from the top and bottom of a conventionally cored section within the marl or mudstone member of the Lakes Entrance Formation (= Metung Marl Member) and three cuttings samples from the interpreted basal sands or gravel section (= Colquhoun Sandstone Member) that overlies the granite basement.

The samples analysed were collected at the Geological Survey of Victoria core store on 15 June 1998; forwarded to Laola Pty Ltd in Perth for palynological processing and returned on 24 June. A provisional report on the results was submitted on 28 June. Final results are given on Table 1.

Between 17 to 18 grams of the samples were processed to give moderate residue yields with high concentration of palynomorphs on the microscope slides (Table 2). High diversity spore-pollen assemblages and low to moderate diversity marine microplankton assemblages were recorded from the samples. Preservation of the assemblages is uniformly good. A list of all species identified is presented in Table 3. The assemblage counts of the two core samples were made on oxidised slides filtered with a 10 μ m sieve cloth and counted under a x40 objective. The counts were terminated when ~100 specimens of spores and pollen had been counted. Although the counts give a representative approximation of the changes in the abundance of the major species groups necessary to distinguish gross assemblage changes they are only considered accurate to $\pm 5\%$.

Geological Discussion

The results of the palynological study of samples from Hunters Lane-1 conform to the general accepted understanding of the stratigraphic sequence in the Lakes Entrance area. The results however highlight the potential unreliability of stratigraphic data from early wells and bores and the difficulties in providing more detailed subdivision of the sequence.

The two conventional cores taken in Hunters Lane-1 between 356.8m to 377.3m were originally intended to drill the greensand facies (= Cunninghame Greensand Member of Hocking, 1976; 1988) but instead encountered the overlying marl or mudstone facies (= Metung Marl Member of Hocking, 1976; 1988) of the Lakes Entrance Formation. This is confirmed by the lithology and palynology. The lithology is described as a khaki to green-khaki calcareous mudstone with abundant bioturbation, common glauconite pellets and frequent shelly fauna such as pelyceps, gastropods, bryozoa and echinoids. Although the glauconite pellets are conspicuous their abundance is estimated at <10%, considerably lower than the underlying greensands. The glauconite is also not associated with

“clastic” quartz sand. The palynological assemblages from the two core samples contain abundant marine dinoflagellates (17% and 36%) dominated by *Spiniferites* spp. and *Operculodinium centrocarpum* and are considered typical of the marine calcareous mudstones and marls of the Lakes Entrance Formation.

The analysis of the three cuttings to confirm the possible presence of “Latrobe coarse clastic” facies in Hunters Lane-1 gave equivocal results. The three samples contained assemblages with a mixture of material from the Lakes Entrance Formation, the underlying greensands facies and possibly the Latrobe coarse clastic facies. In the cores examined from Petro Tech-1 these three “facies” were found to contain assemblages with much the same species and only differed from each other by changes in the abundance of selected species (see Partridge, 1998). Unfortunately these “abundance” differences cannot be discriminated in the cuttings from Hunters Lane-1, because the cuttings contain a significant caved component which distorts the abundances. The presence of the known Early Oligocene dinoflagellate *Fromea leos* ms and absence of any Eocene dinoflagellates in the cuttings is strong evidence for the absence of any Eocene age “Latrobe coarse clastic facies” at Hunters Lane-1. It does not however exclude the possible presence of Early Oligocene age “Latrobe coarse clastic facies”.

A few rare Eocene spore-pollen species were recorded in the cuttings. These are believed to represent reworked Eocene fossils from the Lakes Entrance Formation that have caved into the cuttings. Such Eocene reworking has previously been recorded by the author as common in the Lakes Entrance Formation in the Lakes Entrance Oil Shaft (Partridge, 1971).

Overall the assemblages from the five samples are remarkable similar and this suggest they are also closely similar in age. Further subdivision of the sequence will depend on looking for and documenting the rarer microplankton species such as *Fromea leos*. This would require more detailed sampling and more intensive microscope analysis than was request for this report.

Biostratigraphy

Zone and age determinations are based on the spore-pollen zonation scheme proposed by Stover & Partridge (1973) which was originally partly derived from Partridge (1971). The microplankton zones are based on the scheme outlined by Partridge (1975, 1976) which has been modified and embellished in the many subsequent palynological reports prepared on well drilled in the Gippsland Basin. Unfortunately this latter work has not yet been collated or synthesised into a single report.

Author citations for most spore-pollen species can be sourced from Stover & Partridge (1973, 1982). Other, less frequently recorded species can be found in Pocknall & Mildenhall (1984) and/or Mildenhall & Pocknall (1989). Author citations for microplankton can be found in the indexes of Lentin & Williams (1993). Species names followed by "ms" are unpublished manuscript names.

Lower *Proteacidites tuberculatus* Spore-Pollen Zone

Interval: 356.85 to 411 metres

Age: Early Oligocene.

The five samples analysed assigned to the zone based on the presence of the key index species *Cyatheacidites annulatus* and absence of the younger index species *Foveotriletes lacunosus* and *Cyathidites subtilis* which define the base of the Middle *P. tuberculatus* Zone (Stover & Partridge, 1973; fig.2). Of the six species considered to range no younger than the Lower subzone by Stover & Partridge (1973) only *Granodiporites nebulosus* is still considered reliable. Unfortunately this species is generally rare and was only recorded from the deepest cuttings (Table 3). Other rare but significant species include *Proteacidites stipplatus* at 376.78m and *Triporopollenites chnosus* at 411m. The occurrences of manuscript species *Reticuloidosporites escharus* and *Verrucatosporites attinatus* originally described by Partridge (1971) are also notable, and potentially important, as these species have been rarely found in offshore Eocene sediment in the intervening ~30 years. The occurrence of *Acaciapollenites myriosporites* in the cuttings at 405m is considered to be caved.

Overall the assemblages have high diversity and are dominated by *Nothofagidites* angiosperm pollen. Only the two core samples were counted and in these the most abundant species include *Nothofagidites* spp. averaging 27%, *Haloragacidites harrisii* (= modern *Casuarina* pollen) averaging ~12% and *Podocarpidites* spp. averaging ~9%. The relative high abundances of the alete gymnosperm pollen *Araucariacites australis* averaging 15% and *Dilwynites* spp. averaging ~5% can be interpreted as the manifestation of a Neves effect as described by Traverse (1988) and indicates the samples were deposited in distal offshore environments.

***Operculodinium* Microplankton Superzone**

Interval: 356.85 to 411 metres

Age: Early Oligocene.

All samples analysed contain dinoflagellates characteristic of the *Operculodinium* Superzone which has a broad Oligocene to Miocene age range. The superzone is identified by the dominance of *Spiniferites* spp. and *Operculodinium centrocarpum* and absence of known Eocene dinoflagellates. Many of the key species in the microflora are still undocumented or are only identified by manuscript names (eg. *Nematosphaeropsis rhizoma* and *Protoellipsoidinium simplex*). Because the superzone has not been subdivided into smaller zones it is of limited value for detailed age

dating and correlation. The only range zone currently identified is the *Fromea leos* Zone which occurs at the base of the superzone and is identified in a limited number of wells.

***Fromea leos* Microplankton Zone**

Interval: 405 to 408 metres

Age: basal Oligocene.

The *Fromea leos* Zone is defined as interval above the acme of *Phthanoperidinium comatum* to the Last Appearance Datum (LAD) of *Fromea leos* ms. The species was first recorded from the greensand at 365.8m in the Lakes Entrance Oil Shaft during the author's MSc research nearly 30 years ago but was neither illustrated nor described in my thesis which concentrated on the associated spore-pollen assemblages (Partridge, 1971). Although, the species has occasionally been recorded in offshore wells in the Gippsland Basin it was only demonstrated to have a diagnostic range and therefore erected as a discrete zone interval in the relatively recent Blackback-3 well (Partridge, 1994). Subsequently, the zone has been identified in additional outer shelf wells where it is found in the distal deep water calcareous mudstones at the base of the Seaspray Group and has an Early Oligocene age based on associated planktonic foraminifera.

The index species *Fromea leos* is recorded as a rare form in the two shallowest cuttings. It is interpreted to be caved or derived from the Cunninghame Greensand Member rather than the underlying Colquhoun Sandstone Member, based on the species occurrence in the former member in the Lakes Entrance Oil Shaft. The occurrence of this zone indicates the interval sampled is no older than Early Oligocene, which supports the evidence from the associated spore-pollen assemblages.

References

- HOCKING, J.B., 1976. Definition and revision of Tertiary stratigraphic units, onshore Gippsland Basin. *Department of Minerals and Energy Geological Survey of Victoria Report 1976/1*, p.1-40
- HOCKING, J.B., 1988. Gippsland Basin. **In** *Geology of Victoria*, J.G. Douglas & J.A. Ferguson, (editors), Victorian Division Geological Society Australia Inc., Melbourne. p.322-347.
- LENTIN, J.K. & WILLIAMS, G.L., 1993. Fossil Dinoflagellates: Index to genera and species, 1993 Edition. *AASP Contribution Series No. 28*, p.1-856.
- MILDENHALL, D.C. & POCKNALL, D.T., 1989. Miocene-Pleistocene spores and pollen from Central Otago, South Island, New Zealand. *New Zealand Geological Survey Palaeontological Bulletin 59*, 12-128.
- PARTRIDGE, A.D., 1971. Stratigraphic palynology of the onshore Tertiary sediments of the Gippsland Basin, Victoria. MSc thesis, University of NSW (unpubl.).
- PARTRIDGE, A.D., 1975. Palynological zonal scheme for the Tertiary of the Bass Strait Basin (Introducing Paleogene Dinoflagellate Zones and Late Neogene Spore-Pollen Zones). *Geol. Soc. Aust. Symposium on the Geology of Bass Strait and Environs, Melbourne, November, 1975. Esso Aust. Ltd. Palaeo. Rept. 1975/17* (unpubl.).
- PARTRIDGE, A.D., 1976. The geological expression of eustacy in the early Tertiary of the Gippsland Basin. *APEA Journal vol. 16*, pt.1, p.73-79.
- PARTRIDGE, A.D., 1994. Palynological analysis of sidewall cores from Blackback-3, Gippsland Basin. *Biostrata Report 1994/6*, p.1-23.
- PARTRIDGE, A.D., 1998. Palynological analysis of core samples from Petro Tech-1, onshore Gippsland Basin. *Biostrata Report 1998/6*, p.1-12.
- POCKNALL, D.T. & MILDENHALL, D.C., 1984. Late Oligocene-Early Miocene spores and pollen from Southland, New Zealand. *New Zealand Geological Survey Paleontological Bulletin 51*, p.1-66.
- STOVER, L.E. & PARTRIDGE, A.D., 1973. Tertiary and late Cretaceous spores and pollen from the Gippsland Basin, southeastern Australia. *Proceedings Royal Society of Victoria, vol. 85*, pt.2, p.237-286.
- STOVER, L.E. & PARTRIDGE, A.D., 1982. Eocene spore-pollen from the Werillup Formation, Western Australia. *Palynology 6*, p.69-95.
- TRAVERSE, A., 1988. *Paleopalynology*. Unwin Hyman Ltd, Boston, p.1-600.

Table-1: Interpretative Palynological Data for Hunters Lane-1

Sample Type	Depth (m)	Unit	Spore-Pollen Zone	*CR Microplankton Zone	*CR MP%	Comments and Key Species Present
Core 1	356.85	Metung Marl Member	Lower <i>P. tuberculatus</i>	A2	A3	36% <i>Cyatheacidites annulatus</i> present. Superzone
Core 2	376.78	Metung Marl Member	Lower <i>P. tuberculatus</i>	A1	A3	17% <i>C. annulatus</i> present. Superzone
Cuttings	405	Cunningham and/or Colquhoun Members	Lower <i>P. tuberculatus</i>	D1	A3	NA LAD of dinoflagellate <i>Fromea leos</i> .
Cuttings	408	Cunningham and/or Colquhoun Members	Lower <i>P. tuberculatus</i>	D1	A3	NA <i>F. leos</i> and <i>C. annulatus</i> present.
Cuttings	411	Cunningham and/or Colquhoun Members	Lower <i>P. tuberculatus</i>	D1	Indeterminate	NA <i>Grandiporites nebulosus</i> and <i>C. annulatus</i> present.

*CR = Confidence Ratings MP = Microplankton

Table-2: Basic Sample and Palynomorph Data for Hunters Lane-1

Sample Type	Depth (m)	Lithology	Wt (g)	Vol (cc)	O/Yield	HCl Reaction	Visual Yield	Palynomorph Concentration	Preservation	Number SP Species	Number MP Species
Core 1	356.85	Micaceous marl	18.1	2.8	0.154	Slight	Moderate	High	Good	24	4
Core 2	376.78	Micaceous marl	17.8	3.0	0.168	Reactive	Moderate	High	Good	27	4
Cuttings	405	Mixed greensand & quartz sand	17.1	1.0	0.058	Reactive	Moderate	High	Good	34	9
Cuttings	408	Mixed greensand & quartz sand	17.3	0.7	0.040	Reactive	Low	High	Good	35	12
Cuttings	411	Mixed greensand & quartz sand	18.6	0.8	0.043	Reactive	Moderate	High	Good	30	10

Wt = Weight of samples in grams

Vol (cc) = Volume of aqueous suspension of kerogen residue recovered by Laola Pty Ltd

O/yield = Volume (cc) divided by Weight (grams)

Confidence Ratings

The Confidence Ratings assigned to the zone identifications on Table-2 are quality codes used in the STRATDAT relational database developed by the Australian Geological Survey Organisation (AGSO) as a National Database for interpretive biostratigraphic data. Their purpose is to provide a simple relative comparison of the quality of the zone assignments. The alpha and numeric components of the codes have been assigned the following meanings:

Alpha codes: Linked to sample type

- A** Core
- B** Sidewall core
- C** Coal cuttings
- D** Ditch cuttings
- E** Junk basket
- F** Miscellaneous/unknown
- G** Outcrop

Numeric codes: Linked to fossil assemblage

- 1 Excellent confidence:** High diversity assemblage recorded with key zone species.
- 2 Good confidence:** Moderately diverse assemblage recorded with key zone species.
- 3 Fair confidence:** Low diversity assemblage recorded with key zone species.
- 4 Poor confidence:** Moderate to high diversity assemblage recorded without key zone species.
- 5 Very low confidence:** Low diversity assemblage recorded without key zone species.

Diversity:

When diversity is used in the text it has the following numerical equivalence:

Very low	=	1-5	species
Low	=	6-10	species
Moderate	=	11-25	species
High	=	26-74	species
Very high	=	75+	species

Table-3: Species Distribution and Abundance in Hunters Lane-1.

Sample Type:	Core 1	Core 2	Cts	Cts	Cts
Depth in metres:	356.85	376.78	405.0	408.0	411.0
SPORE-POLLEN					
Acaciapollenites myriosporites			Caved		
Araucariacites australis	12.3%	18.4%	X	X	X
Baculatisporites spp.	4.9%	1.6%	X	X	X
Clavifera triplex		0.8%			X
Cupanieidites orthoteichus		X			
Cupressacites sp.			X	X	X
Cyatheadites annulatus	X	X	X	X	X
Cyathidites paleospora	9.0%	13.6%	X	X	X
Dacrycarpites australiensis	X	0.8%			X
Dictyophyllidites arcuatus	0.8%	1.6%		X	X
Dilwynites granulatus	5.7%	4.8%	X	X	X
Dilwynites tuberculatus	X			X	X
Ericipites crassiexinus/scabratus				X	
Granodiporites nebulosus					X
Haloragacidites harrisii	15.6%	8.8%	X	X	X
Haloragacidites trioratus				X	
Herkosporites elliotii			X	X	X
Ilexpollenites anguloclavatus			X		
Ischyosporites gremius			X		X
Ischyosporites irregularis ms	X			X	
Laevigatosporites ovatus	2.5%	4.0%	X	X	X
Lygistepollenites florinii	4.1%	1.6%	X	X	X
Malvacipollis subtilis			X		X
Matonisporites ornamentalis	X	X	X	X	
Microcachrydites antarcticus	0.8%				
Nothofagidites asperus		0.8%	X	X	X
Nothofagidites brachyspinulosus	2.5%	3.2%	X		
Nothofagidites deminutus				X	X
Nothofagidites emarcidus/heterus	18.9%	28.0%	X	X	X
Nothofagidites falçatus	X	X	X	X	X
Nothofagidites flemingii		X	X	X	X
Nothofagidites goniatus			X		
Nothofagidites longispina			X		
Nothofagidites vansteenensii		0.8%	X	X	
Parvisaccites catastus				X	X
Periporopollenites demarcatus	0.8%		X	X	
Peromonolites vellosus		X		X	X
Phyllocladiidites mawsonii	X	1.6%	X	X	X
Podocarpidites spp.	13.9%	3.2%	X	X	X
Proteacidites spp.		2.4%	X	X	X
Proteacidites adenantoides			RW	RW	
Proteacidites annularis			X	X	
Proteacidites grandis					RW
Proteacidites pachypolus			RW		
Proteacidites stipplatus		X			

Table-3: Species Distribution and Abundance in Hunters Lane-1 cont...

Sample Type:	Core 1	Core 2	Cts	Cts	Cts
Depth in metres:	356.85	376.78	405.0	408.0	411.0
Proteacidites symphonemoides					X
Proteacidites xestiformis ms		RW			
Reticuloidosporites escharus ms	1.6%	0.8%	X		X
Retitriletes sp.	X	X	X	X	
Rugulatisporites mallatus	X	X			
Santalumidites cainozoicus	RW				
Sapotaceoidaepollenites rotundus				X	
Stereisporites antiquisporites		X	X	X	X
Stereisporites (Tripunctisporis) sp.					X
Tricolporites adelaidensis			X		
Trilete spores undiff.	5.7%	0.8%			
Tripoporollenites ambiguus	0.8%				
Tripoporollenites chnosus					X
Verrucatosporites attinatus ms					X
Verrucosisporites cristatus				X	
Verrucosisporites kopukuensis		X	X		X
Total spore-pollen count:	122	125			
MICROPLANKTON					
Dinoflagellates undiff.	7%	4%			
Achomosphaera ramulifera	1%		X		X
Crassosphaera concinnia				X	
Cyclopsiella vieta		X		X	X
Fromea sp. cf F. chytra			X	X	
Fromea leos ms			X	X	
Hystriochokolpoma rigaudae			X	X	X
Hystriochosphaeridium spp.				X	
Impagidinium spp.			X		
Lingulodinium machaerophorum			X	X	X
Nematosphaeropsis rhizoma ms		X			
Operculodinium centroporum	34%	28%	X	X	X
Paralecaniella indentata			X	X	
Protoellipsodinium simplex ms	4%	8%	X		X
Rottnestia borussica				X	X
Spiniferites spp.	53%	68%	X	X	X
Systematophora placacanthum				X	X
Tectatodinium pellitum				X	X
Total spore-pollen count:	68	25			
MICROPLANKTON as % of SP & MP count.	36%	46%			
OTHER PALYNOMORPHS					
Botryococcus sp.	X				
Microforaminiferal liners		X	X		X
Scolecodont	X				
Fungal fruiting bodies		X	X	X	X
Fungal spores/hyphae	X	X			

RW = Reworked palynomorphs

**HUNTERS LANE-1 WELL COMPLETION
REPORT**

APPENDIX III

PETROLOGICAL REPORT

GREENSAND MEMBER

**Dr. N.M. Lemon
NCPGG**

PETROGRAPHIC ANALYSIS REPORT

HUNTERS LANE - 1

Dr.N.M. LEMON

*National Centre for Petroleum Geology and Geophysics
G.P.O. Box 498
ADELAIDE,
S.A. 5001.*

MARCH 1998

DISCLAIMER

These analyses, opinions and interpretations are based on observations and material supplied by the client to whom, and for whose exclusive and confidential use, this report is made. The interpretations or opinions expressed represent the best judgement of the authors (all errors and omissions excepted). These interpretations and opinions are not necessarily those of the National Centre for Petroleum Geology and Geophysics and its officers and employees assume no responsibility and make no warranty or representations as to the connection with which such report is used or relied upon.

1. INTRODUCTION

The client, Lakes Oil NL, through JN Mulready, submitted a single sample to the NCPGG from below the casing (around 400m) in the well Hunters Lane-1, onshore Gippsland Basin. The instructions were to prepare a thin section of the sample and describe it petrographically with specific reference to the porosity of the sample and its likelihood as the unit from which the oil in the hole is produced.

A thin section was prepared by Pontifex and Associates using blue-dyed araldite to impregnate the sample prior to sectioning to allow easy identification of the porosity. Grainsize and porosity of the sample was measured using a Videopro 32 (3) image analyser. The same image analysis system was used to quantify some of the framework components, thereby constraining the visual estimation of the minor components of the rock. A number of photomicrographs were taken of the sample, usually in transmitted light. In order to image the dark and opaque grains, some photos were taken in reflected light, merely using an unshielded globe above the stage as the light source.

5. PETROGRAPHIC DESCRIPTION

Macro description

The sample received was a 3cm by 2cm block of poorly sorted, silty, very to fine grained, green, glauconitic arenite. There were areas of mud up to 2cm long that appeared to be burrows. The whole rock reacted weakly to 10% HCl as if there were a calcite cement throughout.

Micro description

In thin section, the sample is poorly sorted with angular, very fine to medium grains of quartz unevenly distributed throughout the slide. Figure 1 shows a typical field of view of the more porous parts of the rock. The grain size distribution is bimodal with larger grains composed of goethite pellets and ooids, glauconitic pellets and fossils (mainly foraminifers but also bryozoans, gastropods and bivalves). There is some green matrix, composed of glaucony and other indeterminate clays. Detail of a more porous zone in Figure 2 shows most of the porosity to be intergranular although the fossils in Figure 1 show intragranular pores to be common. Finely dispersed pyrite cubes and spheres act as cement between the quartz and other framework grains. Figure 3 is of a burrow area and shows some of the rock is very muddy with no effective porosity. These zones are matrix supported but not continuous through the rock. Figure 4 encompasses a larger field of view and shows a muddy burrow in a zone of cleaner, high porosity rock.

The average porosity of this specimen is around 15% but this is quite unevenly distributed. Highly porous zones with up to 20% porosity occur where there is a concentration of quartz grains with little matrix. The background porosity where matrix is common is around 10% but the mud-filled burrows have no effective pores. As this specimen is quite glauconitic, some of the porosity might be expected to be a result of clay shrinkage. This can occur naturally but is also certainly induced during thin section preparation when the slide is heated to set the resins used to glue the sample to the glass slide. About 3%, however, is all that is estimated to be present from shrinkage.

The only clearly identified cement in the rock is pyrite but glauconite could well act a cement as well. Carbonate distribution is not as hinted at in the acid reaction in the macro description. There is no obvious calcite cement and the occurrence of intact aragonitic shells (gastropods and bivalves) confirms there has been no movement of calcium carbonate in the rock.

Glauconite and related iron-rich clays shows 4 modes of occurrence in the rock, as globular grains, ooids and homogenous grains now oxidised to goethite, as pellets and in the matrix, as the alteration product of micas and possibly as cement. The glauconite and pyrite show that the sediment was deposited and remained in mildly reducing conditions but this is at odds with the goethite grains. Most of the goethite grains are larger than the rest of the framework grains and appear to have come from a different source. This idea is supported by the fact that goethite is formed and is only stable in oxidising conditions. Figure 5 shows a number of goethite grains, dark reddish brown in transmitted light, with a range of grainsizes and types. Figure 6, in reflected light, gives a better indication of the nature of some of these grains. The round grains in the centre of the field of view are clearly ooids with concentric growth or cortex. The core of one grain is a quartz grain and another grain has become incorporated during growth. the core of the ooid is unstructured goethite, similar to the globular mass in the lower right of the scene. Shrinkage cracks around the core are similar to those observed on other globular grains. Thin layers of pyrite within the ooids point to later reduction or alternating reducing and oxidising conditions during ooid growth.

Despite the interesting mineralogies and depositional conundrums apparent in the rock, there are enough large pore spaces in this rock with good interconnectedness to both store a heavy oil and to allow it to flow. This rock could well be the reservoir for the oil occurrence observed in Hunters Lane-1.

Hunters Lane-1

Composition

Framework			
	Quartz		35%
	Hematite ooids and grains		14%
	Fossils and fragments		5%
	Pellets (glauconite and other clays)		10%
	Feldspar		Tr
	Muscovite		Tr
	Biotite		Tr
	Heavies		Tr
	Organic matter		Tr
Matrix			
	Glauconite and other clays		13%
Alteration products			
	Glauconite		1%
Cement			
	Pyrite		6%
Porosity			
	Primary	intergranular	9%
		intragranular	3%
	Secondary	shrinkage	3%

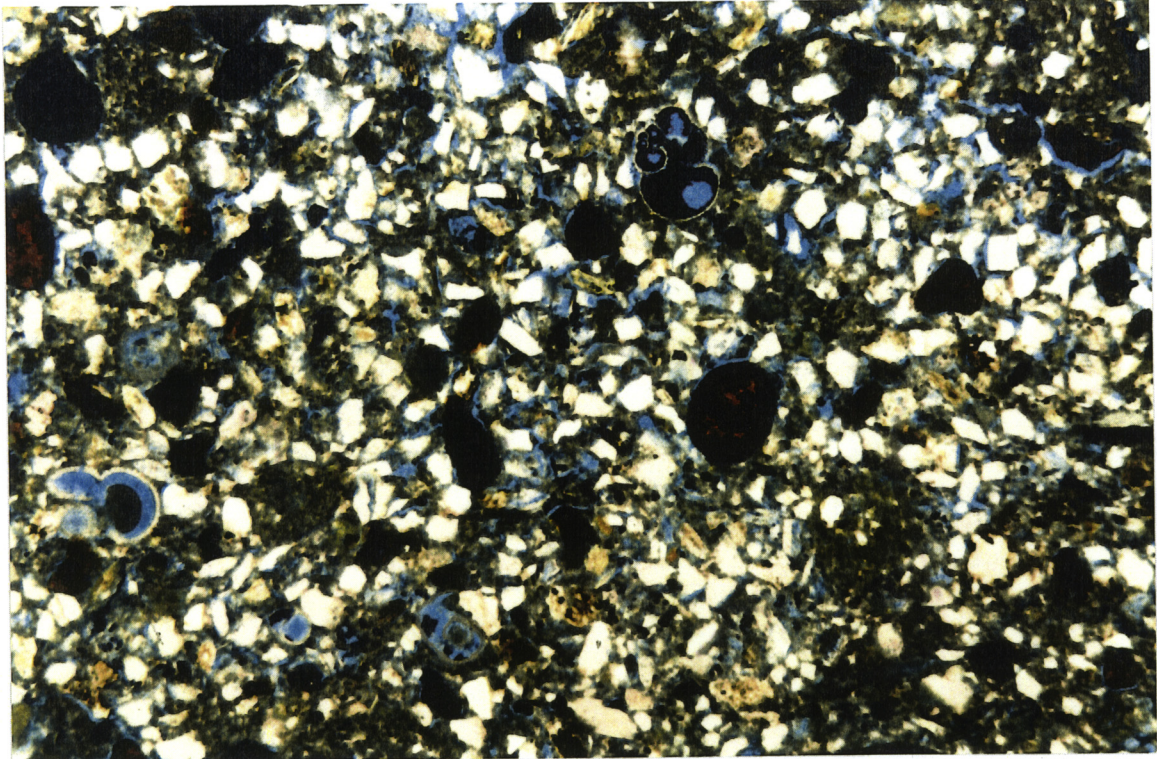


Figure 1. *Hunters Lane-1.* (Plane polarised light). A general view of this slide shows good intergranular porosity supported by fine to very fine, angular quartz grains. Reddish goethite grains, foraminifers and glauconitic pellets make up the larger grains. Porosity is slightly occluded by green clay matrix and some pyrite cement.

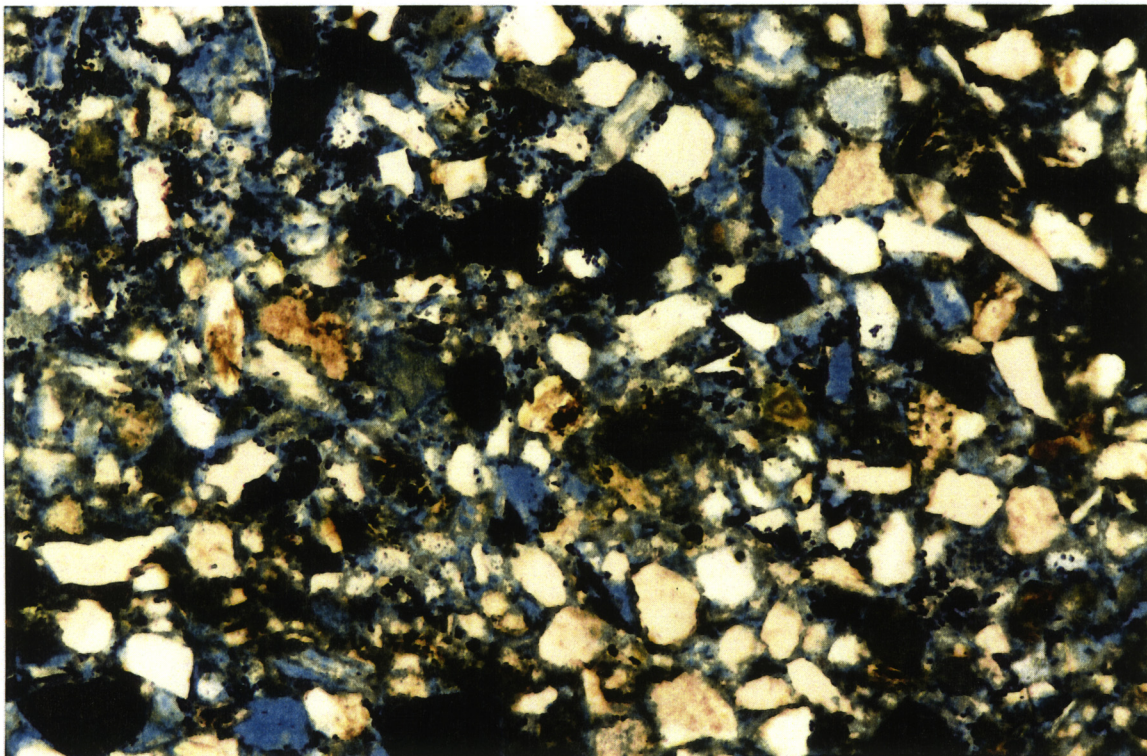


Figure 2. *Hunters Lane-1.* (Plane polarised light). Detail of a porous zone in the rock shows intergranular pores supported by angular quartz grains and some usually larger dark goethite grains. Pyrite cement and minor green clay matrix (glauconite plus probably kaolin and illite) partially occlude the pores.

Hunters Lane-1

7

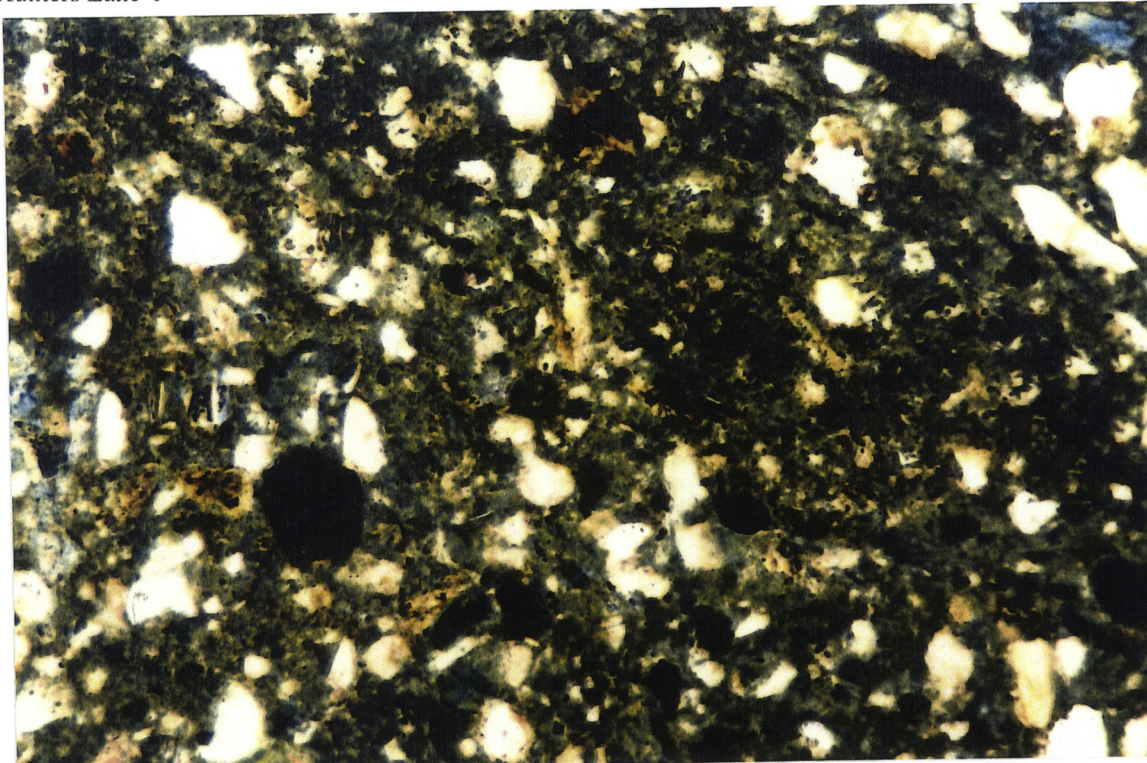


Figure 3. *Hunters Lane-1.* (Plane polarised light). A very tight section of the rock where a green clay matrix (glaucanite plus probably kaolin and illite) support a few angular quartz grains. The dark grains are commonly larger than the quartz and are composed of goethite.

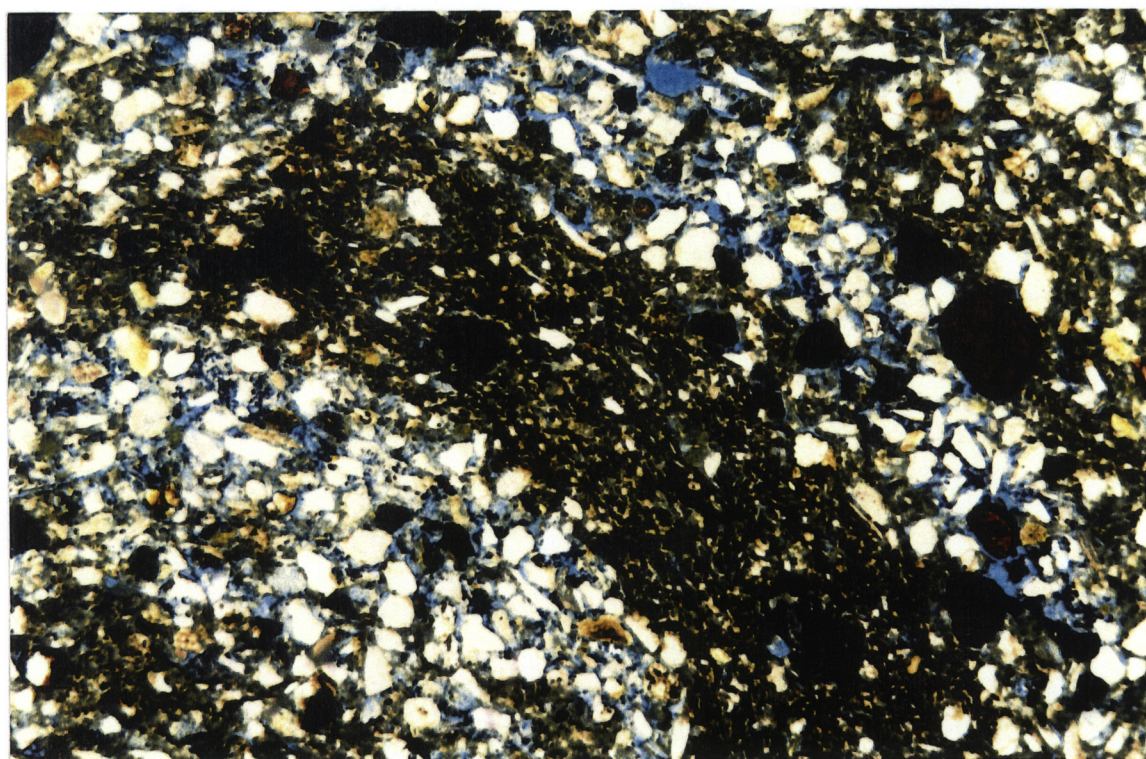


Figure 4. *Hunters Lane-1.* (Plane polarised light). A wider field of view of a tight zone shows it to be a muddy burrow infill in a zone of high porosity. Some dark reddish brown goethite grains show internal cracks and a globular texture reminiscent of glauconitic pellets.

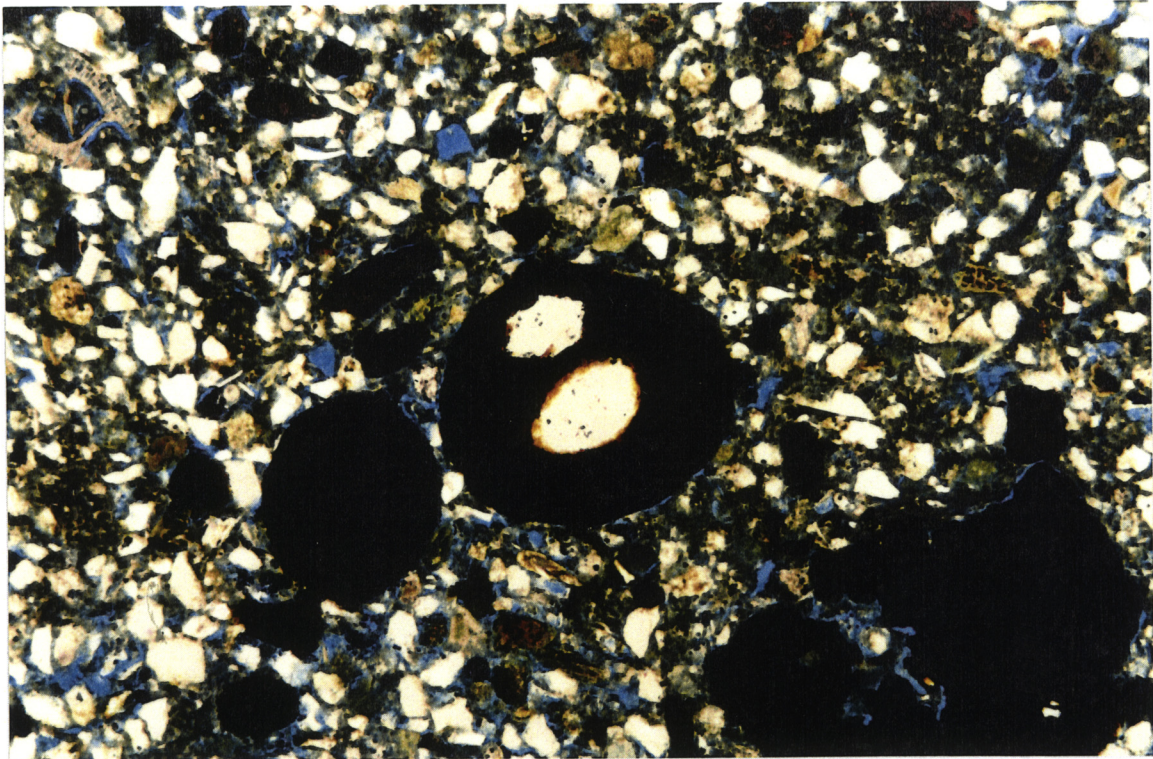


Figure 5. *Hunters Lane-1.* (Plane polarised light). This field of view displays numerous goethite grains. The smaller grains are angular and the same size as the quartz grains but the larger grains are either well rounded or irregular.

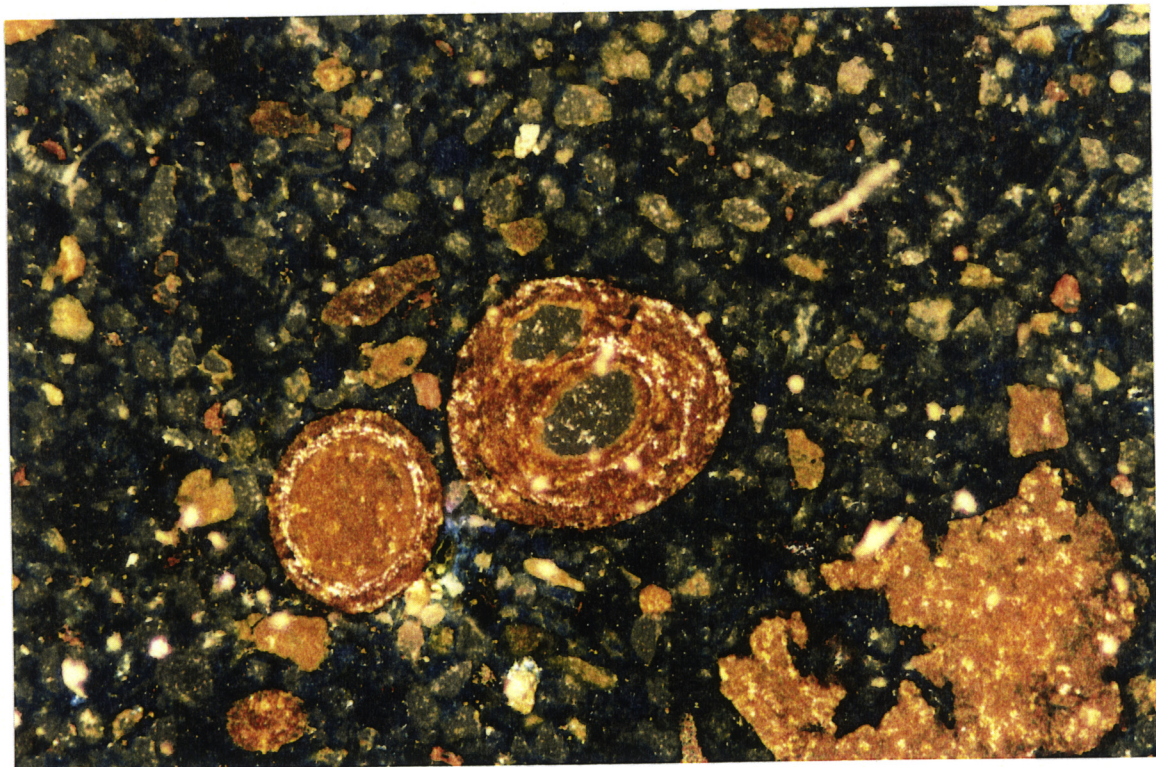


Figure 6. *Hunters Lane-1.* The same field of view as Figure 5 viewed under reflected light shows the internal structure of the goethite grains. The rounded grains are clearly ooids, one with a quartz grain core and another quartz grain included during growth while the other has an unstructured goethite core. Thin pyrite layers sparkle among the cortical layers. The amorphous globular goethite at lower right is similar to the core of the smaller ooid.

903249 063

**HUNTERS LANE-1 WELL COMPLETION
REPORT**

APPENDIX IV

WELLSITE SURVEY

AUSTEC SURVEYING CONSULTANTS



AUSTEC SURVEYING CONSULTANTS PTY LTD
 ACN 006 347 100
 TITLE & ENGINEERING SURVEYORS :: LAND DEVELOPMENT CONSULTANTS

Ref 98004.C03
 05/02/98

Lakes Oil N.L.
 GPO Box 427G
 Melbourne, 3000.

Att: Mr Jack Mulready
 Re: Metung Gravity Survey

9 FEB 1998

The following sheets list the results of our levelling survey around the Metung Gravity Stations, and below is the co-ordination of the Borehole at the end of Hunters Lane.

Centreline of the Borehole at ground level

E 585646.21	N5808526.47	RL 42.730
-------------	-------------	-----------

Datum Permanent Marks

PSM 16	E 584126.669	N 5808066.635	RL 66.360
PSM 107	E 584490.660	N 5807610.810	RL 59.390
PSM 174	E 587261.196	N 5808733.860	RL 58.790

Co-ords are AMG and AHD. A traverse was made from PM 107 to 174 and checked onto 16. Closures were obtained to 0.050m and the co-ords to the borehole adjusted thereto. Levels closed to 0.01m by trig levelling, no adjustment applied.

Yours Faithfully,

Bruce Bowden.



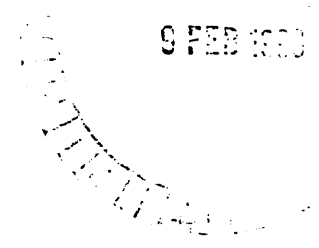
903249 066

AUSTEC SURVEYING CONSULTANTS PTY LTD
ACN 006 347 100
TITLE & ENGINEERING SURVEYORS :: LAND DEVELOPMENT CONSULTANTS

Ref 98004.C03
05/02/98

Lakes Oil N.L.
GPO Box 427G
Melbourne, 3000.

Att: Mr Jack Mulready
Re: Metung Gravity Survey



The following sheets list the results of our levelling survey around the Metung Gravity Stations, and below is the co-ordination of the Borehole at the end of Hunters Lane.

Centreline of the Borehole at ground level
E 585646.21 N5808526.47 RL 42.730

Datum Permanent Marks

PSM 16	E 584126.669	N 5808066.635	RL 66.360
PSM 107	E 584490.660	N 5807610.810	RL 59.390
PSM 174	E 587261.196	N 5808733.860	RL 58.790

Co-ords are AMG and AHD. A traverse was made from PM 107 to 174 and checked onto 16. Closures were obtained to 0.050m and the co-ords to the borehole adjusted thereto. Levels closed to 0.01m by trig levelling, no adjustment applied.

Yours Faithfully,

Bruce Bowden.



908249 067

AUSTEC SURVEYING CONSULTANTS . PTY. LTD
ACN 006 347 100

TITLE & ENGINEERING SURVEYORS :: LAND DEVELOPMENT CONSULTANTS

AHD LEVELS FOR GRAVITY STATIONS IN THE KALIMNA TO SWAN REACH SURVEY AREA

NO.	RL.	COMMENT	NO.	RL.	COMMENT
101	69.28	132	36.46	
102	68.85	133	30.33
103	74.86	134	2.66
104	74.79	135	2.28
105	68.08	136	2.24	
106	70.44	137	1.51	
107	77.69	138	9.68	
108	85.48	139	2.89	
109	83.50	140	1.34	base of 'light tower'
110	72.07	141	25.86
111	66.87	142	21.68
112	63.53	143	23.09
113	50.96	only tape found, not stake	144	28.15
114	23.08	145	24.37
115	23.07	146	28.49
116	22.39	147	24.98
117	18.92	148	38.89
118	20.51	149	19.07
119	6.82	not found, level of PM 19 used ~ fence intersection	150	10.75
120	4.16	151	8.64
121	1.89	152	11.26
122	2.82	153	27.70
123	3.45	154	16.28
124	1.95	155	1.52
125	15.77	156	2.57
126	28.59	157	8.60
127	33.17	158	35.82
128	45.37	159	38.72	missing
129	32.95	160	9.12
130	43.17	161	16.34
131	51.50	162	9.92
			163	2.26

****Note changes to preliminary results are highlighted



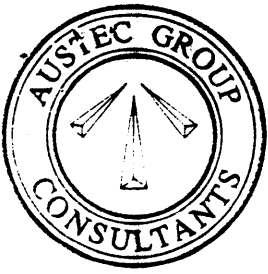
AUSTEC SURVEYING CONSULTANTS

PTY LTD
ACN 006 347 100

TITLE & ENGINEERING SURVEYORS :: LAND DEVELOPMENT CONSULTANTS

NO.	RL.	COMMENT	NO.	RL.	COMMENT
164	79.33	197	70.90
165	72.77	not found, cnr of Telecom pit used, at fence int.	198	68.55
166	77.91	199	50.17
167	67.92	200	41.93
168	59.53	201	66.31
169	66.33	202	61.18
170	69.12	203	76.96
171	80.85	204	74.45
172	76.73	205	56.09
173	77.13	206	41.29
174	73.98	207	42.38
175	51.18	208	2.50
176	48.45	209	81.41
177	19.04	210	76.70
178	3.14	211	71.20	fence intersection, no stake
179	31.85	212	71.17
180	47.22	213	39.04
181	50.20	214	33.27
182	49.50	stake out of ground	215	52.68
183	34.02	216	47.99
184	41.41	217	29.99
185	58.33	218	17.94
186	68.08	219	43.23
187	74.50	220	33.73
188	67.45	221	2.84
189	52.18	222	2.61
190	36.97	223	31.94
191	26.15	224	23.35
192	1.87	225	7.26
193	62.43	226	4.15
194	57.12	227	2.86
195	59.53	228		survey not required
196	53.03	229		survey not required

****Note changes to preliminary results are highlighted



903249 063

AUSTEC SURVEYING CONSULTANTS . PTY LTD
ACN 006 347 100

TITLE & ENGINEERING SURVEYORS :: LAND DEVELOPMENT CONSULTANTS

PERMANENT SURVEY MARKS USED IN THE CO-ORDINATION OF GRAVITY STATIONS IN THE KALIMNA TO SWAN REACH SURVEY AREA

DESCRIPTION	AHD LEVEL	LOCATION
PM 39	26.842	on Princes H' way, west of Punt Road
PM 40	20.056	corner of Princes H' way & Swan Reach - Bruthen Road
PM 19	6.825	corner of Princes H' way & Metung Road
PM 51	3.838	corner of Metung & Rosherville Roads
PM 9	36.540	corner of Metung & Punt Roads
	2.520	spike in SEC pole at end of Reynold Road
PM 21	0.802	Shaving Point, Metung
PM 20	1.621	Metung Road, near jetty
PM 53	20.704	corner of Metung & Stirling Road
PM 25	20.412	Wood Street corner, Metung
PM 52	53.462	Metung Road, near Currawong Court
PM 54	51.473	corner of Rosherville & Nungurner Road
PM 42	21.101	Princes H' way, Swan Reach
PM 11	28.942	Princes H' way, Swan Reach
PM 43	67.840	Princes H' way, Swan Reach
PM 122	73.423	Princes H' way, south of Scrivener Road
PM 141	57.840	corner of Princes H' way and Kalimna West Road
PM 115	57.860	corner of Princes H' way and Kalimna West Road
PM 129	79.748	on Nungurner Road, south of Cornwells Road
PM 18	62.631	corner of Nungurner & Fergys Roads
PM 130	67.962	on Nungurner Road, near fire shed
PM 147	74.052	corner of Nungurner & Nungurner Jetty Roads
PM 55	53.962	on Nungurner Road, west of Rosherville Road

**HUNTERS LANE-1 WELL COMPLETION
REPORT**

APPENDIX V

WATER ANALYSIS

BY AMDEL



61 8 82342933

Hunter Lane - 1
903249 072

A.C.N. 008 127 802



FACSIMILE TRANSMISSION FROM:

AMDEL LIMITED PETROLEUM SERVICES
35-37 STIRLING STREET, THEBARTON SA 5031
FACSIMILE NO: (08) 8234 2933 or (08) 8234 2760
TELEPHONE NO: (08) 8416 5240

TO: Jack Mulready

COMPANY: Lakes Oil NL

FAX NO: 03 9629 1624

DATE: 1 April, 1999

COPY TO:

FROM: Jason Mitchell

TOTAL PAGES: 3

Jack,

Please find attached results for standard water analysis of HUNTERS LANE-1 water samples received on 23rd March 1999.

Regards,


Jason Mitchell
Petroleum Chemist
Petroleum Services



Petroleum Services

61 8 82342933

903249 073

TABLE 1 - WATER ANALYSIS

JOB NUMBER: LQ7813

WELL / ID: HUNTERS LANE-1
 SAMPLE TYPE: Formation Water
 SAMPLE POINT: PEP135
 DATE COLLECTED: September-98 ←
 DATE RECEIVED: 23/03/99

FORMATION:
 INTERVAL:
 COLLECTED BY: Client

Pre drilling out basal sand

PROPERTIES:

pH (measured) = 9.6
 Resistivity (Ohm.M @ 25°C) = 4.1
 Electrical Conductivity (µS/cm @ 25°C) = 2450
 Specific Gravity (S.G. @ 20°C) = na
 Measured Total Dissolved Solids(Evap@180°C) mg/L = na
 Measured Total Suspended Solids mg/L = na

CHEMICAL COMPOSITION

CATIONS		mg/l.	meq/l.	ANIONS		mg/L	meq/L.
Ammonium	as NH ₄	na	na	Bromide	as Br	na	na
Potassium	as K	42	1.07	Chloride	as Cl	456	12.85
Sodium	as Na	551	23.97	Fluoride	as F	na	na
Barium	as Ba	na	na	Hydroxide	as OH	nd	nd
Calcium	as Ca	nd	nd	Nitrite	as NO ₂	na	na
Iron	as Fe	nd	nd	Nitrate	as NO ₃	1	0.02
Magnesium	as Mg	nd	nd	Sulphide	as S	na	na
Strontium	as Sr	na	na	Bicarbonate	as HCO ₃	616	10.10
Boron	as B	na	na	Carbonate	as CO ₃	102	3.40
				Sulphite	as SO ₃	na	na
				Sulphate	as SO ₄	29	0.60
Total Cations		593	25.04	Total Anions		1204	26.96

DERIVED PARAMETERS

a) Ion Balance (Diff*100/Sum) (%) = 3.69
 b) Total Alkalinity (calc as CaCO₃) (mg/l.) = 674
 c) Total of Cations + Anions = 1797 (measured dissolved salts)
 d) Theoretical Total dissolved salts = 1568 (From Electrical Conductivity)

QUALITY CONTROL COMMENTS

Item	Actual Value	Acceptance Criteria	Satisfactory? (Yes/No)
Ion Balance (%) =	3.69	5%	Yes
Expected pH range		< 8.3	Yes
% difference between measured total dissolved solids and calc total dissolved salts (from ionic comp) =	na	5%	na

na = not applicable
 nd = not detected
 is = insufficient sample

If No - what action is recommended by Amdel



Petroleum Services

61 8 82342933

903249 074

TABLE 1 - WATER ANALYSIS

JOB NUMBER: LQ7813

WELL / ID: HUNTERS LANE-1
SAMPLE TYPE: Formation Water
SAMPLE POINT: PEP135
DATE COLLECTED: January-99
DATE RECEIVED: 23/03/99

FORMATION:
INTERVAL:
COLLECTED BY: Client

Post drilling and based sand.

PROPERTIES:

pH (measured) = 9.6
Resistivity (Ohm.M @ 25°C) = 4.7
Electrical Conductivity (µS/cm @ 25°C) = 2150
Specific Gravity (S.G. @ 20°C) = na
Measured Total Dissolved Solids (TDS @ 180°C) mg/L = na
Measured Total Suspended Solids mg/L = na

CHEMICAL COMPOSITION

Table with 4 columns: CATIONS, mg/L, meq/L, ANIONS, mg/L, meq/L. Lists various ions like Ammonium, Potassium, Sodium, Barium, Calcium, Iron, Magnesium, Strontium, Boron, Bromide, Chloride, Fluoride, Hydroxide, Nitrite, Nitrate, Sulphide, Bicarbonate, Carbonate, Sulphite, Sulphate.

DERIVED PARAMETERS

a) Ion Balance (Diff*100/Sum) (%) = 1.55
b) Total Alkalinity (calc as CaCO3) (mg/l.) = 659
c) Total of Cations + Anions = 1652 (measured dissolved salts)
d) Theoretical Total dissolved salts = 1376 (From Electrical Conductivity)

QUALITY CONTROL COMMENTS

Table with 4 columns: Item, Actual Value, Acceptance Criteria, Satisfactory? (Yes/No). Rows include Ion Balance (%), Expected pH range, and % difference between measured total dissolved solids and calc total dissolved salts.

na = not applicable
nd = not detected
is = insufficient sample

If No - what action is recommended by Amdel

903249 075

**HUNTERS LANE-1 WELL COMPLETION
REPORT**

APPENDIX VI

OIL ANALYSIS

BY AMDEL

13 September 2002

Lakes Oil NL
Level 11
500 Collins St
MELBOURNE VIC

Attention: Jack Mulready

REPORT LQ11910

CLIENT REFERENCE: Letter dated 9/8/02

WELL NAME/RE: Hunters Lane 1

MATERIAL: Crude Oil

WORK REQUIRED: Physical testing

AUTHOR'S NAME: Mohammad Massoumi

Please direct technical enquiries regarding this work, to the signatory below, under whose supervision the work was carried out. This report relates specifically to the sample or samples submitted for testing.



Diane Cass
Operations Manager
Petroleum Services

dc.jh

G:\Secretary\petroleum\Docs-02\11910.doc

Amdel Limited shall not be liable for loss, cost, damages or expenses incurred by the client, or any other person or company, resulting from the use of any information or interpretation given in this report. In no case shall Amdel Limited be liable for consequential damages including, but not limited to, lost profits, damages for failure to meet deadlines and lost production arising from this report. This document shall not be reproduced except in full and relates only to the items tested.

1. INTRODUCTION

Amdel Limited received a sample of liquid for qualitative gas chromatography on 12 August 2002. This report is a formal presentation of results forwarded by e-mailed on 20 August 2002.

2. PROCEDURE

The sample was analysed on a Perkin Elmer 8500 Gas Chromatograph equipped with a capillary column, flame ionisation detector and nitrogen carrier gas.

3. RESULTS

The gas chromatogram is presented on the following page.

The sample appears to be naphthenic hydrocarbons that are extensively bio-degraded.

PHYSICAL PROPERTIES

Client: Lakes Oil N.L.

Report: LQ11910

Sample: Crude oil (Hunters Lane-1)
Collected in Late 1997

Method	Description	Units	Crude Oil H.Lane-1	
IP2	ASTM D611	Aniline Point	°C	-
IP143		Asphaltenes	% wt	-
IP364	ASTM D976	Calculated Cetane Index		-
IP219	ASTM D2500	Cloud Point	°C	-
IP17		Colour by Lovibond Tintometer		-
IP274	ASTM D2624	Conductivity of Fuels	pS/m	-
IP13	ASTM D189	Conradson C Residue on 10% Dis Residue	% wt	-
IP154	ASTM D130	Copper Corrosion (100°C, 3 hrs)		-
IP365	ASTM D4052	Density @ 15°C	g/mL	0.9578
IP21		Diesel Index		-
IP123	ASTM D86	Distillation		-
		IBP	°C	-
		10% Rec	°C	-
		20% Rec	°C	-
		30% Rec	°C	-
		40% Rec	°C	-
		50% Rec	°C	-
		60% Rec	°C	-
		70% Rec	°C	-
		80% Rec	°C	-
		90% Rec	°C	-
		95% Rec	°C	-
		Decomposition Point	°C	-
		Residue	% vol	-
		Loss	% vol	-
		Evaporated @ 75°C, 105°C, 135°C	% vol	-
IP131	ASTM D381	Existent Gum by Evaporation	mg/100mL	-
IP170		Flash Point Abel Closed Cup	°C	-
IP34	ASTM D93	Flash Point Pensky Martens Closed Cup	°C	-
IP156	ASTM D1319	Fluorescent Indicator Absorption Aromatics	% vol	-
IP16	ASTM D2386	Freezing Point	°C	-
IP71	ASTM D445	Kinematic Viscosity @ 40°C	cSt	78.16
IP71	ASTM D445	Kinematic Viscosity @ 100°C	cSt	-
IP15	ASTM D97	Pour Point	°C	-18
	ASTM D5185	Aluminium	mg/kg	-
	ASTM D5185	Vanadium	mg/kg	-
	ASTM D5185	Sodium	mg/kg	-
IP365	ASTM D4052	Specific Gravity @ 60/60°F		0.9584
IP354	ASTM D3242	Total Acidity in Aviation Fuel	mgKOH/g	-
IP216		Total Contaminant	mg/L	-
	ASTM D2270	Viscosity Index		-
IP289	ASTM D1094	Water Reaction	Interface Rating	-
	ASTM D1796	Total Percent Water and Sediment	%vol	0.20
	ASTM D1796	Water and Sediment (Tube 1)	mL	0.10
	ASTM D1796	Water and Sediment (Tube 2)	mL	0.10
	ASTM D1298	API Gravity	degrees	16.14

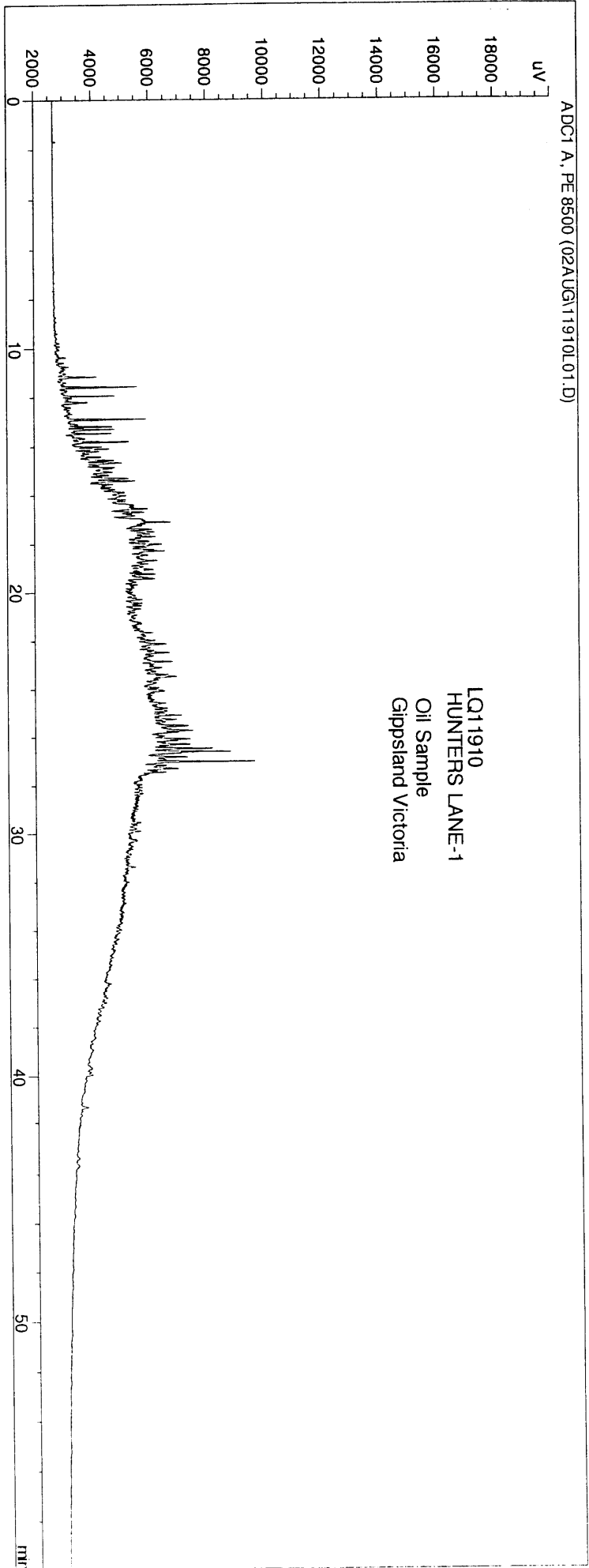
- = not determined

Approved Signatory: _____
Mohammad Massoumi

Date: 20/08/02

Accreditation No: 2013

This report relates specifically to the sample submitted for testing.



PHYSICAL PROPERTIES

Client: Lakes Oil N.L.

Report: LQ11910

Sample: Crude oil (Hunters Lane-1)
Collected in Late 1997

Method	Description	Units	Crude Oil H.Lane-1	
IP2	ASTM D611	Aniline Point	°C	-
IP143		Asphaltenes	% wt	-
IP364	ASTM D976	Calculated Cetane Index		-
IP219	ASTM D2500	Cloud Point	°C	-
IP17		Colour by Lovibond Tintometer		-
IP274	ASTM D2624	Conductivity of Fuels	pS/m	-
IP13	ASTM D189	Conradson C Residue on 10% Dis Residue	% wt	-
IP154	ASTM D130	Copper Corrosion (100°C, 3 hrs)		-
IP365	ASTM D4052	Density @ 15°C	g/mL	0.9578
IP21		Diesel Index		-
IP123	ASTM D86	Distillation		
		IBP	°C	-
		10% Rec	°C	-
		20% Rec	°C	-
		30% Rec	°C	-
		40% Rec	°C	-
		50% Rec	°C	-
		60% Rec	°C	-
		70% Rec	°C	-
		80% Rec	°C	-
		90% Rec	°C	-
		95% Rec	°C	-
		Decomposition Point	°C	-
		Residue	% vol	-
		Loss	% vol	-
		Evaporated @ 75°C, 105°C, 135°C	% vol	-
IP131	ASTM D381	Existent Gum by Evaporation	mg/100mL	-
IP170		Flash Point Abel Closed Cup	°C	-
IP34	ASTM D93	Flash Point Pensky Martens Closed Cup	°C	-
IP156	ASTM D1319	Fluorescent Indicator Absorption Aromatics	% vol	-
IP16	ASTM D2386	Freezing Point	°C	-
IP71	ASTM D445	Kinematic Viscosity @ 40°C	cSt	78.16
IP71	ASTM D445	Kinematic Viscosity @ 100°C	cSt	-
IP15	ASTM D97	Pour Point	°C	-18
	ASTM D5185	Aluminium	mg/kg	-
	ASTM D5185	Vanadium	mg/kg	-
	ASTM D5185	Sodium	mg/kg	-
IP365	ASTM D4052	Specific Gravity @ 60/60°F		0.9584
IP354	ASTM D3242	Total Acidity in Aviation Fuel	mgKOH/g	-
IP216		Total Contaminant	mg/L	-
	ASTM D2270	Viscosity Index		-
IP289	ASTM D1094	Water Reaction	Interface Rating	-
	ASTM D1796	Total Percent Water and Sediment	% vol	0.20
	ASTM D1796	Water and Sediment (Tube 1)	mL	0.10
	ASTM D1796	Water and Sediment (Tube 2)	mL	0.10
	ASTM D1298	API Gravity	degrees	16.14

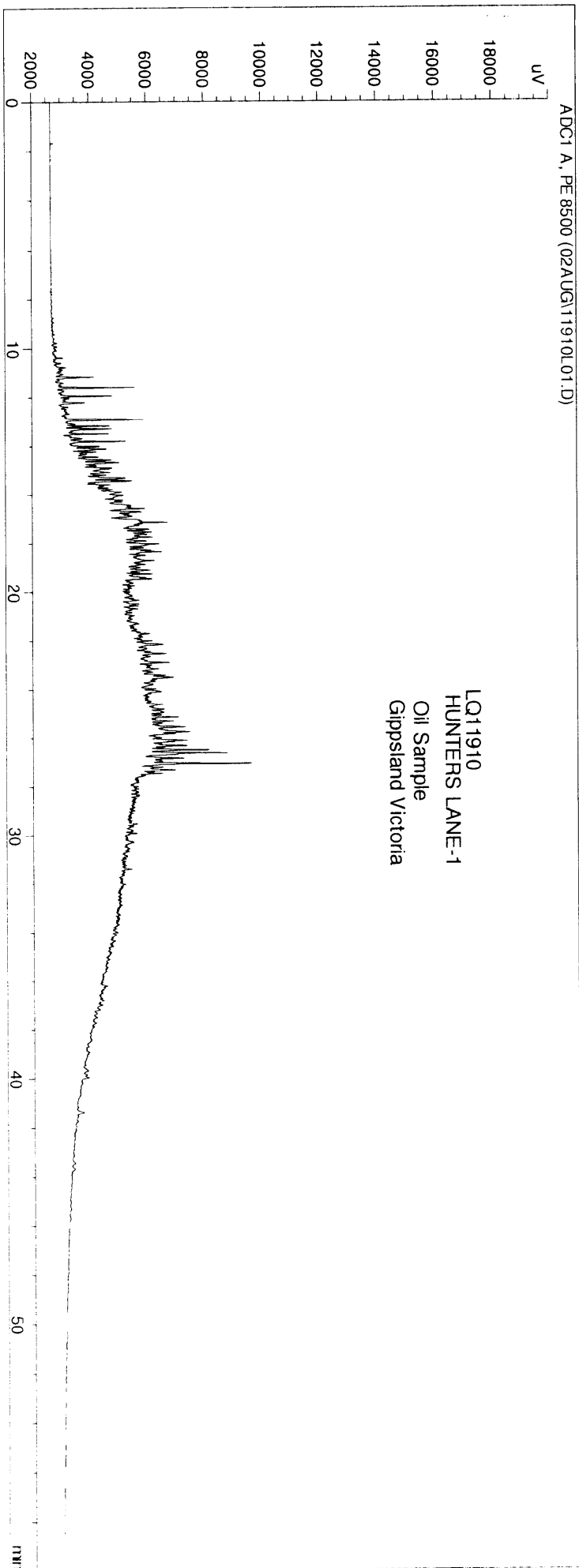
- = not determined

Approved Signatory: _____
Mohammad Massoumi

Date: 20/08/02

Accreditation No. 2013

This report relates specifically to the sample submitted for testing.



903249 083

**HUNTERS LANE-1 WELL COMPLETION
REPORT**

APPENDIX VII

THERMAL HISTORY RECONSTRUCTION

BY DR. I. DUDDY

Geotrack International



903249 085

HUNTERS LANE-1 GIPPSLAND BASIN

THERMAL HISTORY RECONSTRUCTION USING APATITE FISSION TRACK ANALYSIS

GEOTRACK REPORT #684A

**A report prepared for
Mulready Consulting Services on behalf of Lakes Oil NL
Melbourne**

Report prepared by: I. R. Duddy
AFTA determinations by: I. R. Duddy

JUNE 1998



903249 086

Geotrack International Pty Ltd and its officers and employees assume no responsibility and make no representation as to the productivity or profitability of any mineralisation, oil, gas or other material in connection with which this report may be used.

**THERMAL HISTORY RECONSTRUCTION FOR
HUNTERS LANE-1,
GIPPSLAND BASIN
USING APATITE FISSION TRACK ANALYSIS**

CONTENTS

	Page
Summary Report	i-iii
Schematic illustration of thermal history - Figure 1	iv
AFTA parameters plotted against sample depth and present temperature - Figure 2	v
Reconstructed burial - Figure 3	vi
Maturation with time - Figure 4	vii
Paleotemperature analysis summary from AFTA samples - Table 1	viii
Removed section estimates - Table 2	ix
Summary of AFTA data - Table 3	x
Summary of thermal history interpretation - Table 4	xi
Estimates of timing and magnitude of elevated paleotemperatures from AFTA data - Table 5	xii

1.	Background to Thermal history reconstruction	
1.1	Thermal history reconstruction and use of thermal gradient vs heat flow	1
1.2	Outline of our approach to interpretation of AFTA and VR data	2
1.3	Paleogeothermal gradients	4
1.4	Eroded section	5
	References	7

**CONTENTS** *continued*

	Page
Appendix A - Sample Details, Apatite Compositions and Geological Data	
A.1 Sample details	A.1
A.2 Stratigraphic details	A.1
A.3 Present temperatures	A.1
A.4 Sample preparation and Apatite yield	A.2
A.5 Apatite quality and grain morphologies	A.2
A.6 Apatite compositions	A.2
References	A.4
Appendix B - Sample Preparation, Analytical Details and Data Presentation	
B.1 Sample preparation	B.1
B.2 Analytical details	B.1
B.3 Data presentation	B.4
B.4 A note on terminology	B.8
References	B.9
Appendix C - Principles of Interpretation of AFTA Data in Sedimentary Basins	
C.1 Introduction	C.1
C.2 Basic principles of Apatite Fission Track Analysis	C.1
C.3 Quantitative understanding of fission track annealing in apatite	C.4
C.4 Evidence for elevated paleotemperatures from AFTA	C.7
C.5 Quantitative determination of the magnitude of maximum paleotemperature and the timing of cooling using AFTA	C.8
C.6 Qualitative assessment of AFTA parameters	C.10
C.7 Allowing for tracks inherited from source areas	C.10
C.8 Plots of fission track age and mean track length vs depth and temperature	C.11
C.9 Determining paleogeothermal gradients and amount of section removed on unconformities	C.13
References	C.15
Appendix D - Vitrinite Reflectance Measurements	
D.1 Integration of vitrinite reflectance data with AFTA	D.1
References	D.2

**TABLES**

	Page
Table 1 - Paleotemperature analysis summary	viii
Table 2 - Removed section estimates	ix
Table 3 - Summary of AFTA data	x
Table 4 - Summary of thermal history interpretation of AFTA data	xi
Table 5 - Estimates of timing and magnitude of elevated paleotemperatures from AFTA data	xii
Table A.1 - Details of AFTA samples and apatite yields	A.5
Table A.2 - Summary of present temperature measurements	A.6
Table A.3 - Lower limits of Detection for Apatite Analyses	A.7
Table A.4 - Per cent errors in chlorine content	A.7
Table B.1 - Apatite fission track analytical results	B.10
Table B.2 - Length distribution summary data	B.11
Data Sheets Glossary	B.17
Analytical data	B.18
Table D.1 - Paleotemperature - vitrinite reflectance nomogram	D.3

FIGURES

	Page
Figure 1 - Schematic illustration of thermal history	iv
Figure 2 - AFTA parameters plotted against sample depth and present temperature	v
Figure 3 - Possible burial history	vi
Figure 4 - Maturation with time	vii
Figure A.1 - Distributions of chlorine content	A.8
Figure B.1 - Construction of a radial plot	B.12
Figure B.2 - Simplified structure of radial plots	B.13
Figure B.3 - Distribution of single grain ages	B.14
Figure B.4 - Distributions of confined track lengths	B.15
Figure B.5 - Age vs Chlorine plots	B.16
Figure C.1a - Comparison of mean length in Otway Basin reference wells with predictions of Laslett et al. (1987) model	C.16
Figure C.1b - Comparison of mean length in apatites of the same Cl content as Durango from Otway Group samples with predictions of Laslett et al. (1987) model	C.16
Figure C.2 - Comparison of mean length in apatites of differing chlorine compositions	C.17
Figure C.3 - Comparison of mean length in Otway Basin reference wells with predictions of new multi-compositional annealing model	C.17
Figure C.4 - Histogram of Cl contents in typical samples	C.18
Figure C.5 - Comparison of mean length in Otway Basin reference wells with predictions of Crowley et al. (1991) model or F-apatite	C.19
Figure C.6 - Comparison of mean length in Otway Basin reference wells with predictions of Crowley et al. (1991) model for Durango apatite	C.19

**FIGURES** *continued*

	Page
Figure C.7 - Changes in radial plots of post-depositional annealing	C.20
Figure C.8 - Typical AFTA parameters	
a Maximum temperatures now	
b Hotter in the past	C.21
Figure C.9 - Constraint of paleogeothermal gradient	C.22
Figure C.10 - Estimation of section removed	C.23



HUNTERS LANE-1 WELL PEP 135, GIPPSLAND BASIN

THERMAL HISTORY RECONSTRUCTION USING AFTA® APATITE FISSION TRACK ANALYSIS

SUMMARY REPORT

Aims and objectives

This study of the **Hunters Lane-1** well was carried out for **Mulready Consulting Services** on behalf of **Lakes Oil N.L.** and completed in June 1998. The principal objective of the study was to apply Geotrack's thermal history reconstruction methodology based on AFTA® to determine the timing and nature of any episodes of heating and cooling affecting the Paleozoic granite basement in the **Hunters Lane-1 well, PEP 135, Gippsland Basin.**

Thermal history results are summarised in Tables 1 and 2 with a schematic illustration of the main features of the thermal history reconstruction presented in Figure 1. In this summary-style report, AFTA results are presented and discussed in detail in Tables 3 to 5, and illustrated in Figures 2 to 4. Supporting information is presented in four Appendices.

Geological Background

The **Hunters Lane-1** well in Gippsland Basin PEP 135 drilled to a total depth of 422 m encountered a thin Oligocene to Recent sedimentary section overlying Late Devonian granite basement. Granite was intersected at 409 m and was overlain Oligocene Lakes Entrance Formation (containing the oil-bearing Greensand member), Miocene Gippsland Limestone and Tambo River Formations and Pliocene to recent Jemmy's Point formation. The generalised stratigraphy is shown in Figure 2. The present-day geothermal gradient is calculated from corrected BHT data at 51.6°C/km for a surface temperature of 15°C (Appendix A).

Summary Conclusions

Thermal History

1. The AFTA thermal history results from the granite basement in **Hunters Lane-1** show clear evidence for **two heating and cooling events, with a third, earlier event,**

allowed but not required: the first cooling from 85 to 95°C began between 160 and 10 Ma and the second from paleotemperatures of 40 to 85°C began within the last 40 Ma (Table 1 and Figure 1). Cooling from around 100°C in the period prior to 200 Ma is also allowed but not required by the AFTA results.

Burial History

2. As only one AFTA sample was processed from Hunters Lane-1, it has not been possible to determine paleogeothermal gradients for each heating episode. Nevertheless for any realistic value of paleogeothermal gradient kilometre-scale uplift and erosion is required to account for the degree of cooling observed in each episode. Indicative values are listed in Table 2 and illustrated in Figure 3.

Geological implications

3. The considerable cooling required by AFTA indicates significant uplift and erosion has occurred on the unconformity separating the Late Devonian granite from the overlying Oligocene to Recent sedimentary section.
4. The early *allowed* cooling episode (prior to 200 Ma) may have resulted from either protracted unroofing (uplift and erosion) of the granite following initial intrusion (at ~370 Ma), or a period of uplift and erosion following burial under a Carboniferous-Permian sedimentary cover now totally eroded. The presence of Permian sediments in the Duck-Bay-1 well is consistent with such sediments in the general region and may support the latter possibility.
5. Both of the more recent cooling episodes (beginning between 160 and 10 Ma and between 40 and 0 Ma) are considered to have resulted from kilometre-scale uplift and erosion, probably preceded by deposition of Strzelecki Group and possibly Golden Beach Group sediments, now completely eroded. This event most likely relates to opening of the Tasman Sea at ~80 Ma, represented offshore by an unconformity separating the Golden Beach and Latrobe Groups (Lowry, 1988).
6. There is some evidence in the AFTA data for possible minor cooling after deposition of the overlying Oligocene to Recent sedimentary section, as indicated by the paleotemperatures of 40 to 85°C required within the last 40 Ma. However, the timing constraint allows cooling during this event to have occurred prior to Oligocene deposition and this is the preferred



interpretation (Figure 1). Note, however, that cooling less than $\sim 10^{\circ}\text{C}$ is difficult to constrain, and therefore post-Oligocene uplift and erosional events of the order of 100 m or so may not be observed.

Maturation History

7. The preferred interpretation of the AFTA thermal history results imply that the Oligocene sedimentary section is immature for hydrocarbon generation, predicting a maximum VR level of $\sim 0.30\%$ $R_o(\text{max})$ (Figure 4). Oil recovered in this well must therefore result from relatively long distance migration from the offshore Gippsland Basin, probably at some within the last 15 Ma based on offshore maturation patterns.

Recommendations

8. Vitrinite reflectance analyses from the Oligocene section would be useful to confirm the maturity assessment made from AFTA results.
9. Additional AFTA and VR results from a series of samples over a range of depths of a kilometre or more from deeper wells in the region would enable the paleogeothermal gradient to be directly determined. Additional AFTA from regional basement samples would also enable greater confidence to be placed in the identification of a significant post-Golden Beach Group (~ 80 Ma) erosional event.

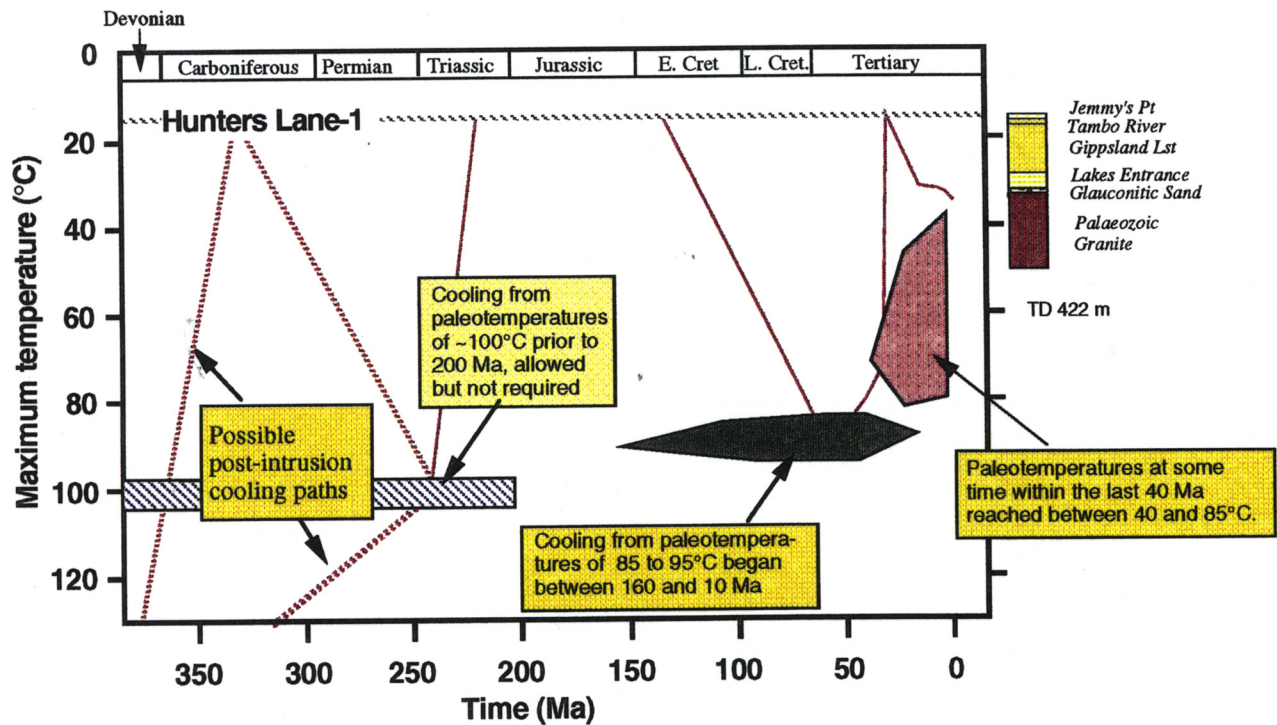


Figure 1: Schematic illustration of the thermal history of the Late Devonian granite basement in the **Hunters Lane-1** well, **Gippsland Basin**, derived from AFTA[®] results. The first cooling episode from $\sim 100^{\circ}\text{C}$ at some time prior to 200 Ma is allowed, but not required by the results. This event may represent either protracted cooling due to unroofing of the granite after initial intrusion, or a period of uplift and erosion following burial under a Carboniferous-Permian sedimentary cover. The second cooling episode, beginning between 160 and 10 Ma from ~ 85 to 95°C , is considered to result from kilometre-scale uplift and erosion, probably preceded by Early Cretaceous Strzelecki Group deposition. This event most likely relates to opening of the Tasman Sea at ~ 80 Ma, represented offshore by an unconformity separating the Golden Beach and Latrobe Groups. The AFTA data also would allow minor cooling after deposition of the overlying Oligocene to Recent sedimentary section (i.e within the last 40 Ma), but this third episode is considered most likely to have occurred prior to the Oligocene as illustrated by the red line in the figure.



Hunters Lane -1

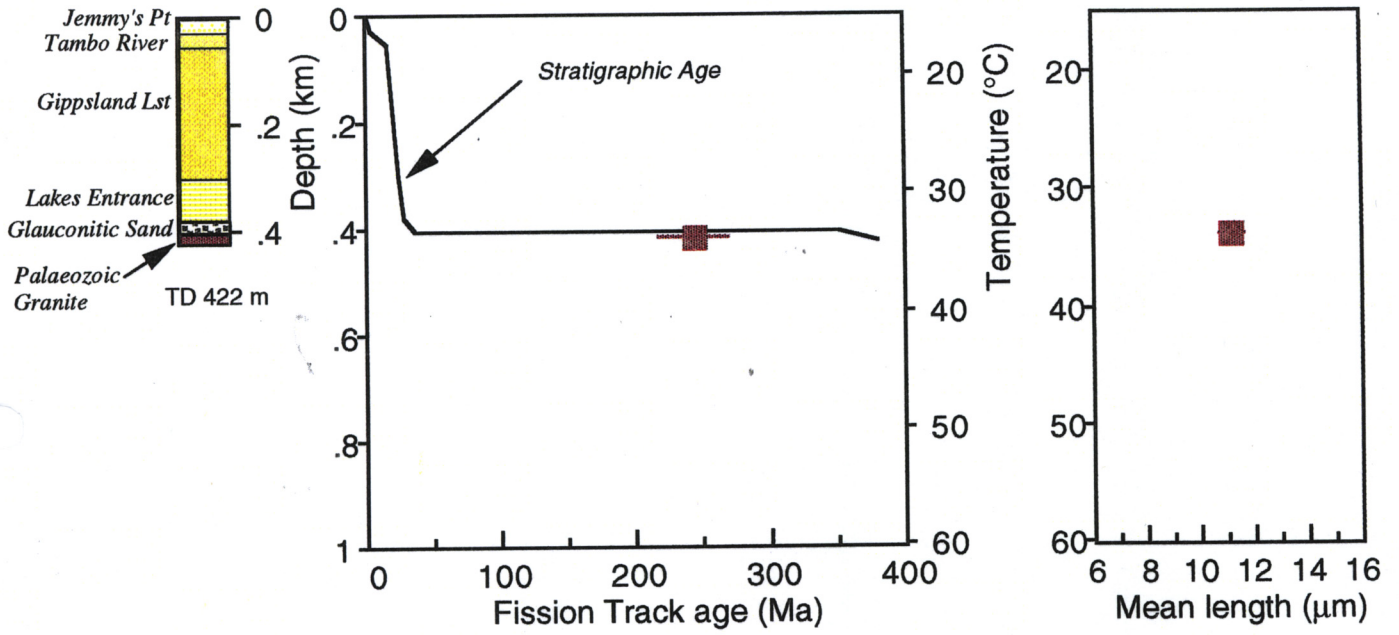


Figure 2: AFTa parameters plotted against sample depth and present temperature for a sample of granitic basement from the **Hunters Lane-1 well, Lake Entrance, Gippsland Basin**. The variation of stratigraphic age with depth is also shown, as the solid line in the central panel.

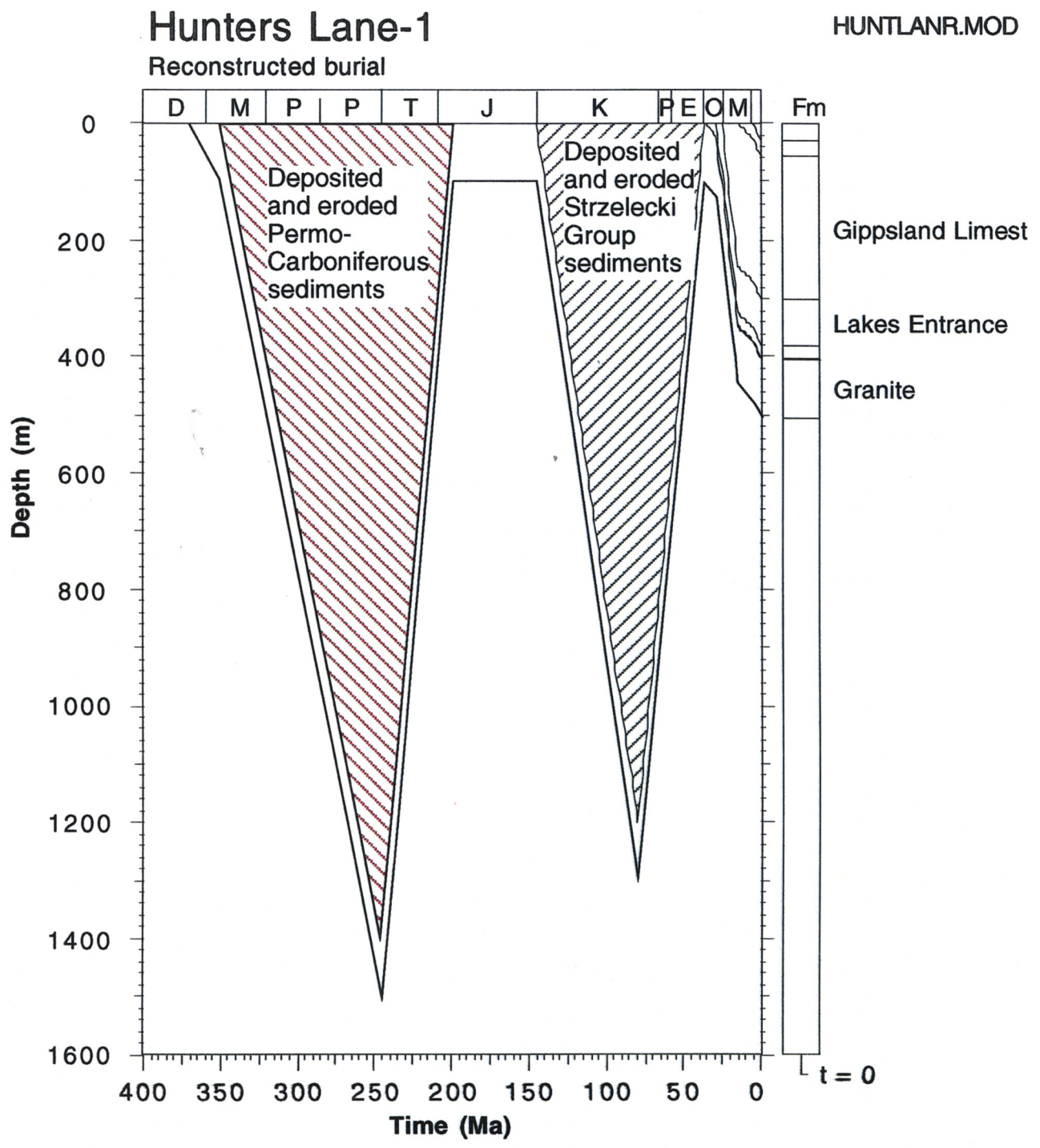


Figure 3: Possible burial history consistent with the thermal history reconstruction in the **Hunters Lane-1** well. The history involves cooling from maximum paleotemperatures at 245 Ma by uplift and erosion of 1400 m of previously deposited Carboniferous-Permian section and cooling from peak paleotemperatures at 80 Ma by uplift and erosion of 1200 m of previously deposited Cretaceous Strzelecki and Golden Beach Group sections (as allowed by the AFTA results). The protracted uplift period shown from 80 to ~30 Ma incorporates the minor cooling revealed by AFTA within the last 40 Ma (Figure 1). The paleogeothermal gradient prior to 80 Ma is assumed to have been 60°C/km compared with the present-day value of 51.6°C/km (see Table 2).

Hunters Lane-1

Maturation with time

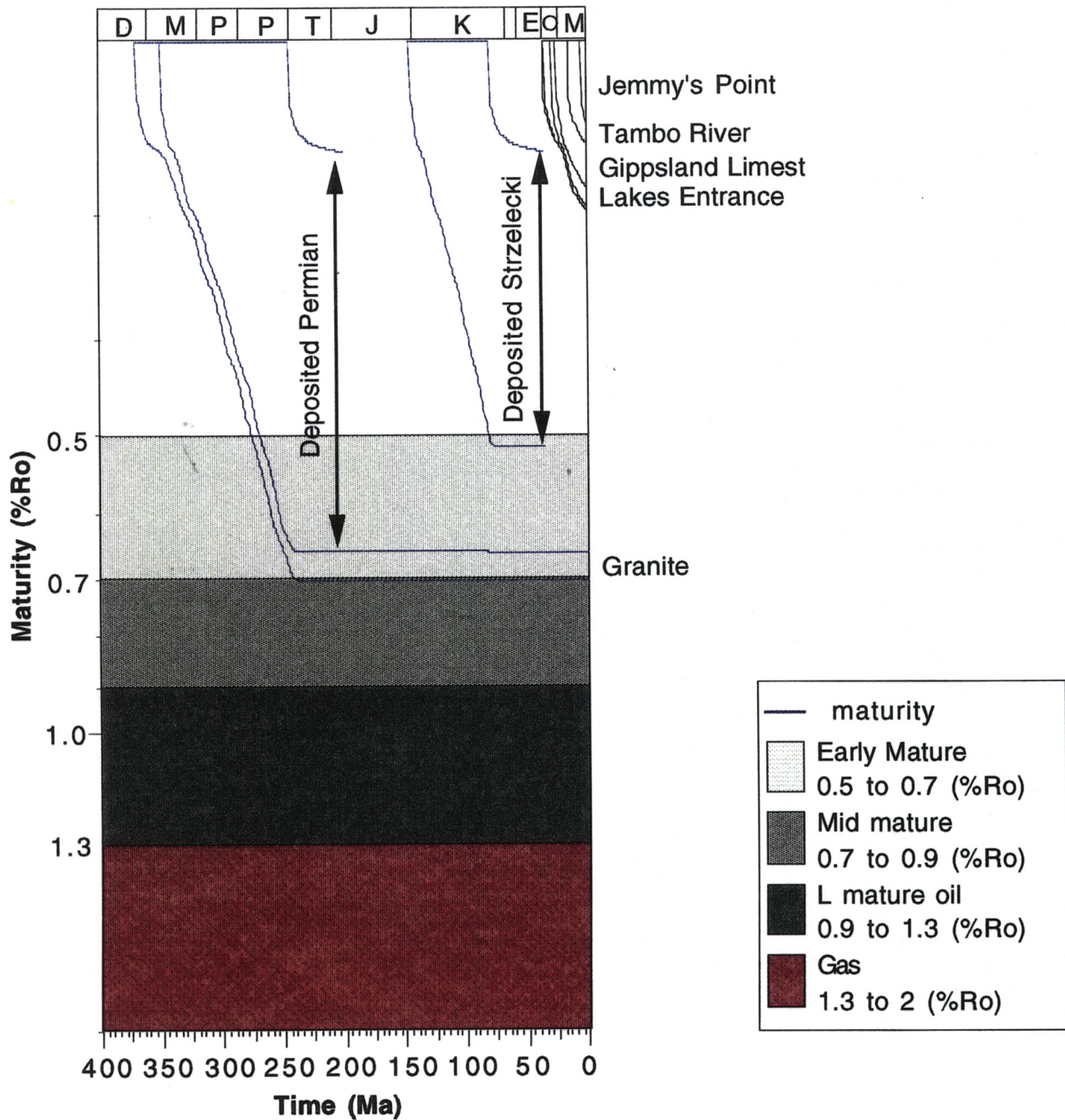


Figure 4: Predicted development of maturity with time (using Burnham and Sweeney, 1989) in the **Hunters Lane-1 well**, controlled by the AFTA results. Maximum maturity of $\sim 0.30\%$ in the Oligocene is reached at the present-day. Any source rocks in deposited Strzelecki Group sediments would have only reached a maximum maturity of $\sim 0.5\%$ (immature for oil) prior to cooling at 80 Ma. Higher maturities may have been reached by source rocks in Carboniferous-Permian sediments prior to erosion of this section prior to 200 Ma.



Table 1: Paleotemperature analysis summary from AFTA samples from the Hunters Lane-1 well, Gippsland Basin (Geotrack Report #684A)

AFTA sample number (GC-)	Mean depth (mKB)	Stratigraphic age* ¹ (Ma)	Present temperature* ² (°C)	----- from AFTA -----			
				Early episode Maximum paleotemperature* ³ (°C)	Onset of cooling (Ma)	Late episode Peak paleotemperature* ³ (°C)	Onset of cooling (Ma)
684-2	419	370	36	85-95	165 to 10	40-85	40 to 0

*1 Present temperature estimates are based on a mean surface temperature of 15°C and a linear present-day geothermal gradient of 51.6°C/km (Appendix A).
 *2 Intrusion age of granite assumed to be 370 Ma based on regional information.
 *3 AFTA paleotemperature estimates are derived assuming a heating rate of 1°C/Ma and a cooling rate of 10°C/Ma. (See Section 1.2.)



Table 2: Removed section estimates consistent with AFTA results for a range of assumed paleogeothermal gradients in the Hunters Lane-1 well, Gippsland Basin (Geotrack Report #684A)

Assumed ^{*1} paleogeothermal gradient	Section removed (km) with respect to the top of the granite basement ^{*2}	
	-- Early Episode -- (165 to 10 Ma) ^{*3} (km)	-- Late Episode -- (40 to 0 Ma) ^{*3} (km)
45°C/km (present-day)	1.6 - 1.8	0.6 - 1.6
60°C/km	1.2 - 1.3	0.4 - 1.2
75°C/km	0.9 - 1.1	0.33 - 0.9
90°C/km	0.8 - 0.9	0.28 - 0.8

*1 Paleogeothermal gradient assumed because no independent estimates are possible from a single AFTA sample.

*2 A constant surface temperature of 15°C is assumed in order to determine the degree of cooling.

*3 Timing based on AFTA timing constraints on the single granite basement sample (see Table 1)

Notes: Estimation of section removed depends on the assumption that the paleogeothermal gradient is linear and can be extrapolated through the removed section to the paleo-surface temperature. If this assumption is not valid (e.g., if the paleo-thermal effects were due to fluid flow, with a higher paleogeothermal gradient in the shallower [removed] section), the estimated section removed will not be accurate.

The paleotemperature constraints (Table 1) and the estimated paleogeothermal gradient through the preserved section are not affected by any of the assumptions required in order to estimate the amount of section removed, and can be regarded as reliable.

The amount of section removed has been estimated for an assumed paleo-surface temperature of 15°C. The resulting estimate can be adjusted to refer to other values of paleo-surface temperature simply by adding or subtracting the depth interval corresponding to the difference between the preferred value and 15°C, as appropriate, for the paleogeothermal gradient value used.



Table 3: Summary of AFTA data in samples from the Hunters Lane-1 well, Gippsland basin (Geotrack Report #684A)

Sample number	Ave depth ^{*1}	Present temperature ^{*2}	Stratigraphic Age	Measured Mean track length	Default mean track length ^{*3}	Measured apatite fission track age ^{*4}	Default fission track age ^{*3}
GC	(m)	(°C)	(Ma)	(µm)	(µm)	(Ma)	(Ma)
684-2	419	36	370	11.05±0.22	14.3	244.8±21.8	357

*1 All depths quoted are true vertical depth (TVD) with respect to KB.

*2 See Appendix A for a discussion of present temperature estimation.

*3 AFTA values predicted from the "Default Thermal History" (Section 1.2); i.e., assuming that each sample is now at its maximum temperature since deposition. The values refer only to tracks formed after deposition. Samples may also contain tracks inherited from sediment provenance areas. Calculation of the Default values refer to actual measured compositions of apatites analysed within a particular sample, which is discussed in Appendix A.

*4 Pooled fission track age or central fission track age (*italics*).



Table 4: Summary of thermal history interpretation of AFTA data in samples from the Hunters Lane-1 well, Gippsland basin (Geotrack Report #684A)

Sample number	Do AFTA data require any revision of present temperature?	Evidence of higher temperatures in the past from length data?	Evidence of higher temperatures in the past from fission track age data?	Conclusion
684-2 419 m	No 36°C	Yes [Mean track length is ~3 µm less than predicted on the basis of the Default Thermal History. Modelling the AFTA parameters through likely thermal history scenarios shows that measured lengths can be explained only by paleotemperatures higher than present temperatures in the period between intrusion and the present-day.]	Yes [Central fission track age and the majority of single grain ages are significantly younger than that predicted on the basis of the Default Thermal History]	Sample has been subjected to paleotemperatures higher than present temperatures after initial intrusion.

Note: Interpretation of AFTA data is based on comparison of measured AFTA parameters with values predicted from "Default Thermal History" (Section 1.2); i.e., assuming that each sample is now at its maximum temperature since deposition. The predicted values for each sample are summarised in Table 3, and refer only to tracks formed after deposition. Samples may also contain tracks inherited from sediment provenance areas, which must be allowed for in interpreting the data. Calculations refer to apatites with the compositional range appropriate to each sample, as explained in Appendix A.

Table 5: Estimates of timing and magnitude of elevated paleotemperatures from AFTA data in a sample from the Hunters Lane-1 well, Gippsland Basin (Geotrack Report #684A)

Sample number	Stratigraphic Age (Ma)	Present temperature (°C)	Early episode		Late episode		Comments
			Maximum paleo-temperature (°C)	Onset of cooling (Ma)	Peak paleo-temperature (°C)	Onset of cooling (Ma)	
684-2 419 m	370 Late Devonian	36	(~100)	prior to 200)	85 - 95 and 40 to 85	160 to 10 and 40 to 0	AFTA requires that the granitic basement cooled from post-intrusive paleotemperatures of 85 to 95°C beginning between 160 and 10 Ma and from 40 to 85°C, beginning at some time within the last 40 Ma. The AFTA results also allow, but do not require, cooling from paleotemperatures around 100°C prior to 200 Ma. The results are consistent with the Tertiary sedimentary section overlying the granite basement being at maximum temperatures at the present day, and suggest a maximum VR level at the base of the Oligocene sediment of ~0.30%.

HUNTERS LANE-1 WELL PEP 135, GIPPSLAND BASIN

THERMAL HISTORY RECONSTRUCTION USING AFTA® APATITE FISSION TRACK ANALYSIS

1. Background to Thermal history reconstruction

1.1 Thermal history reconstruction and use of thermal gradient vs heat flow

Most approaches to thermal history reconstruction in sedimentary basins are based on consideration of the variation of heat flow through time, using models often based solely on theoretical grounds. However, this approach is beset by problems, particularly in sections which have been hotter in the past. Use of a heat flow-based approach depends critically on knowledge of thermal conductivities through the section. When considerable section has been removed, no information is available on lithologies (and hence thermal conductivities) in the removed section. In addition, large variation in thermal conductivities within similar lithological units (e.g. Corrigan, 1991) introduces considerable uncertainty into the relationship between heat flow and thermal gradient, even in relatively simple cases. For further illustration of these problems, see Waples et al. (1992). The influence of factors such as porosity, compaction and diagenesis is difficult to assess quantitatively, and the effects of greater depth of burial are unpredictable in a sequence affected by uplift and erosion, particularly when the magnitude of burial is unknown before the analysis. A heat flow-based approach to determining amounts of removed section is subject to considerable uncertainty because of problems such as these. This point has been discussed in greater detail by Duddy et al. (1991).

It is also important to realise the validity of theoretical heat-flow models is largely untested. High heat flow associated with rifting and early subsidence leaves no measurable effect if subsidence later in the basin's history has caused higher temperatures than those attained during the assumed high heat-flow episode. In many sedimentary basins, deep burial late in the subsidence history has caused maximum temperatures, and no record of earlier heat-flow variation is preserved either in the level of measured source rock maturity or in the AFTA parameters, as these data are dominated by the effects of maximum paleotemperature. Elevated heat-flow episodes associated with rifting are known to leave a measurable signature only where cooling

has occurred shortly after the initial rifting phase, and where temperatures have subsequently remained low through to the present day (Duddy et al. 1991).

We have adopted an alternative approach, based on measurement of thermal gradients (present and past), using an integrated AFTA and VR methodology, because of these problems with a heat flow-based approach to thermal history reconstruction. This approach yields direct measurement of the time at which cooling from maximum paleotemperatures began (from AFTA), and the paleogeothermal gradient at that time (from AFTA and VR). The style of cooling from maximum paleotemperatures to present temperatures can also be constrained (from AFTA). This approach allows definition of all the major facets of the thermal history of a sedimentary section through time, and is based on *directly measurable parameters*, rather than on *assumed* values of highly unpredictable factors. The information provided can still ultimately be interpreted in terms of paleo-heat flow if desired.

It should also be appreciated that the thermal history prior to the time at which cooling from maximum paleotemperatures begins, cannot be constrained from any of the available in-situ paleotemperature indicators based on thermally activated reactions. This arises because of the dominance of temperature over time in the kinetics of the systems employed in this way (i.e. fission track annealing, vitrinite reflectance, etc). For this reason, these data can only constrain the thermal history from the onset of cooling from maximum paleotemperatures to the present day. Information on the earlier history can only be obtained indirectly, e.g. from geological information, perhaps by reconstructing patterns of burial based on section preserved in neighbouring regions, from theoretical heat-flow models (given the above caveats), or possibly by more subtle means, such as the presence of residual hydrocarbon products generated during earlier heating to lower peak paleotemperatures.

1.2 Outline of our approach to interpretation of AFTA and VR data

Interpretation of AFTA and VR data in this report begins by assessing whether the AFTA and/or VR data in each sample could have been produced if the sample has never been hotter than its present temperature at any time since deposition. The burial history derived from the stratigraphy of the preserved sedimentary section and the present geothermal gradient are used to predict a "Default Thermal History" for each sample, which forms the basis of interpretation.

If the data show a greater degree of fission track annealing and/or a higher VR value than expected on the basis of this history, the sample must have been hotter at some time in the past. In this case, the AFTA data are analysed to provide estimates of the magnitude of the maximum paleotemperature in that sample, and the timing of cooling from the thermal maximum. VR data provide an independent estimate of maximum paleotemperature. Paleotemperature estimates from both AFTA and VR are then used to reconstruct a paleogeothermal gradient and, where appropriate, to estimate the amount of section removed by uplift and erosion.

The heating rate assumed in calculating paleotemperatures affects the magnitude of paleotemperature required to produce a given set of data. As AFTA and VR data do not independently constrain the heating rate, paleotemperatures are estimated by assuming simple linear heating between a point on the Default Thermal History and the maximum paleotemperature. This will not give the actual paleotemperature in general, but this procedure at least allows AFTA and VR data to be analysed within a common thermal history framework in the absence of any other constraint on heating rate. If any evidence of the real time-scale of heating is available, this can easily be incorporated into the analysis. Note AFTA data provide some constraint on cooling rates, as explained in more detail in Appendix C.

Estimates of maximum paleotemperature from AFTA are often quoted in terms of a range of paleotemperatures, as the data can often be explained by a variety of scenarios. Paleotemperature estimates from VR are usually quoted to the nearest degree Celsius as the value which predicts the measured reflectance. This is not meant to imply VR data can be used to estimate paleotemperatures to this degree of precision. VR data from individual samples typically show a scatter equivalent to a range of between ± 5 and $\pm 10^\circ\text{C}$. Estimates from a series of samples are normally used to define a paleotemperature profile in samples from a well or a regional trend in paleotemperatures from outcrop samples.

If the data show a lower degree of fission track annealing and/or a lower VR value than expected on the basis of the Default Thermal History, this suggests either present temperatures may be overestimated or temperatures have increased very recently. In such cases, the data may allow an estimate of the true thermal gradient, or some estimate of the time over which temperatures have increased.



Further discussion of the methodology employed in interpreting AFTA and VR data are given in Appendices C and D.

AFTA data are interpreted using a new multi-compositional kinetic model for fission track annealing in apatite developed by Geotrack, details of which are provided in Appendix C. Vitrinite reflectance data are interpreted using the distributed activation energy model describing the evolution of VR, with temperature and time developed by Burnham and Sweeney (1989) (see also Sweeney and Burnham, 1990), as implemented in the BasinMod[®] software package of Platte River Associates (using version 3.15).

1.3 Paleogeothermal gradients

Basic principles

A series of paleotemperature estimates from AFTA and/or VR over a range of depths can be used to reconstruct a paleotemperature profile through the preserved section. The slope of this profile defines the paleogeothermal gradient. As explained by Bray et al. (1992), the shape of the paleotemperature profile and the magnitude of the paleogeothermal gradient provides unique insights into the origin and nature of the heating and cooling episodes expressed in the observed paleotemperatures.

Linear paleotemperature profiles with paleogeothermal gradients close to the present-day geothermal gradient provide strong evidence that heating was caused by greater depth of burial with no significant increase in basal heat-flow, implying in turn that cooling was due to uplift and erosion. Paleogeothermal gradients significantly higher than the present-day geothermal gradient suggest that heating was due, at least in part, to increased basal heat flow, while a component of deeper burial may also be important as discussed in the next section. Paleogeothermal gradients significantly lower than the present-day geothermal gradient suggest that a simple conductive model is inappropriate, and more complex mechanisms must be sought for the observed heating. One common cause of low paleogeothermal gradients is transport of hot fluids shallow in the section. However, the presence of large thicknesses of sediment with uniform lithology dominated by high thermal conductivities can produce similar paleotemperature profiles, and each case has to be considered individually.

A paleotemperature profile can only be characterised by a single value of paleogeothermal gradient when the profile is linear. Departures from linearity may

occur where strong contrasts in thermal conductivities are present within the section, or where hot fluid movement or intrusive bodies have produced localised heating effects. In such cases, a single value of paleogeothermal gradient cannot be calculated. However, it is important to recognise that the validity of the paleotemperatures determined from AFTA and/or VR are independent of these considerations, and can still be used to control possible thermal history models.

Estimation of paleogeothermal gradients in this report

Paleogeothermal gradients have been assumed in this report as independent estimates require a vertical suite of samples, and only one sample from Hunters Lane-1 was analysed. Normally, paleogeothermal gradients are estimated where paleotemperature estimates are available over a range of depths using methods outlined in Appendix C. These methods provide a best estimate of the gradient ("maximum likelihood value") and upper and lower 95% confidence limits on this estimate (analogous to $\pm 2\sigma$ limits). The "goodness of fit" is displayed in the form of a log-likelihood profile, which is expected to show good quadratic behaviour for a dataset which agrees with a linear profile. This analysis depends on the assumption that the paleogeothermal gradient through the preserved section is linear. Visual inspection is usually sufficient to confirm or deny this assumption.

1.4 Eroded section

Basic principles

Subject to a number of important assumptions, extrapolation of a linear paleotemperature profile to a paleo-surface temperature allows estimation of the amount of eroded section represented by an unconformity, as explained in more detail in Section C.9 (Appendix C).

Specifically, this analysis assumes:

- The paleotemperature profile through the preserved section is linear;
- The paleogeothermal gradient through the preserved section can be extrapolated linearly through the missing section;
- The paleo-surface temperature is known; and,



- The heating rate used to estimate the paleotemperatures defining the paleogeothermal gradient is correct.

It is important to realise that any method of determining the amount of eroded section based on thermal methods is subject to these and/or additional assumptions. For example, methods based on heat-flow modelling must assume values of thermal conductivities in the eroded section, which can never be known with confidence. Such models also require some initial assumption of the amount of eroded section to allow for the effect of compaction on thermal conductivity. Methods based on geothermal gradients, as used in this study, are unaffected by this consideration, and can therefore provide independent estimates of the amount of eroded section. However, these estimates are always subject to the assumptions set out above and should be considered with this in mind.

Estimation of eroded section in this report

In this report eroded section has been calculated from the degree of cooling indicated by AFTA for a range of assumed paleogeothermal gradients. Where a number of samples over a range of depths is available, the formal analysis used to estimate paleogeothermal gradients is extended to provide maximum likelihood values of eroded section for a given paleo-surface temperature, together with $\pm 95\%$ confidence limits. These parameters are quoted for each well in which the paleotemperature profile suggests that heating may have been due, at least in part, to deeper burial.

However, it is emphasised that such interpretations are not unique and alternative interpretations are always possible. For instance, the paleogeothermal gradient through the missing section may have been much higher than in the preserved section where the eroded section was dominated by units with high thermal conductivities, and extrapolation of a linear gradient will lead to overestimation of the eroded section.

For the well analysed in this report, the estimates of eroded section are conditional on:

- Heating rates of $1^\circ\text{C}/\text{Ma}$ and cooling rates of $10^\circ\text{C}/\text{Ma}$ in each episode, and
- A paleo-surface temperature equal to the present value of 15°C ,

as well as the other assumptions outlined above. The effects of higher paleo-surface temperatures can be simply allowed for by subtracting the depth increment corresponding to the increase in temperature, for the appropriate value of



paleogeothermal gradient. For instance, if the paleogeothermal gradient was 45°C/km and the paleo-surface temperature was 10°C higher than the value assumed in this report, the estimated eroded section should be reduced by 222 metres. Different heating rates can be allowed for in similar fashion, with an order of magnitude change in heating rate equivalent to a 10°C change in paleotemperature (paleotemperatures increase for higher heating rates, and decrease for lower heating rates). For typical values, the assumed value of heating rate will not affect the shape or slope of the paleotemperature profile significantly.

References

- Burnham, A. K. and Sweeney, J. J. (1989) A chemical kinetic model of vitrinite reflectance maturation. *Geochimica et Cosmochimica Acta.*, 53, 2649-2657.
- Bray, R. J., Green, P. T. and Duddy, I. R. (1992) Thermal History Reconstruction using apatite fission track analysis and vitrinite reflectance: a case study from the UK East Midlands and the Southern North Sea. In: Hardman, R.F.P. (ed), *Exploration Britain: Into the next decade. Geological Society Special Publication*, 67, 3-25.
- Corrigan, J. D. (1991) Thermal anomalies in the Central Indian Ocean: Evidence for de-watering of the Bengal Fan. *Journal of Geophysical Research*, 96, 14263 - 14275.
- Green, P. F., Duddy, I. R., Gleadow, A. J. W., Tingate, P. R. and Laslett, G. M. (1985) Fission track annealing in apatite: Track length measurements and the form of the Arrhenius Plot. *Nuclear Tracks*, 10, 323-328.
- Duddy, I. R., Green, P. F., Hegarty, K. A. and Bray, R. J. (1991) Reconstruction of thermal history in basin modelling using Apatite Fission Track Analysis: what is really possible? *Proceedings of the First Offshore Australia Conference (Melbourne)*. III-49 - III-61.
- Lowry, D.C. (1988) Alternative Cretaceous history of the Gippsland Basin. *Australian Journal of Earth Sciences*, 35, 1995, 181-194.
- Sweeney, J. J. and Burnham, A. K. (1990) Evaluation of a simple model of vitrinite reflectance based on chemical kinetics. *The American Association of Petroleum Geologists' Bulletin*, 74, 1559 - 1570.
- Waples, D. W., Kamata, H. and Suizu, M. (1992) The art of maturity modelling. Part 1: Finding a satisfactory geologic model. *The American Association of Petroleum Geologists' Bulletin*, 76, 31 - 46.



APPENDIX A

Sample Details, Apatite Compositions and Geological Data

A.1 Sample details

The study involves THR using Apatite Fission Track Analysis (AFTA[®]) on a cuttings sample of Late Devonian granite from 419 m in the Hunters Lane-1 well, PEP 135, onshore Gippsland Basin. The study was carried out for Mulready Consulting Services (M.C.S.) on behalf of Lakes Oil N.L.

Details of the AFTA samples, including depths, stratigraphic ages and present temperatures supplied by M.C.S. are listed for each sample in Table A.1.

A.2 Stratigraphic details

The details of each stratigraphic interval in the preserved section of the well were supplied by M.C.S. as listed in Table A.2. Also supplied were the depths (mKB) of each AFTA sample. Based on the chronostratigraphic age, a numerical age (Ma) was assigned for each sample using Harland et al. (1989). The stratigraphic ages, or age ranges, of each AFTA sample are summarised in Table A.1. Any errors in this procedure will not have any significant effect on the results presented in this report.

A.3 Present temperatures

In application of any technique involving estimation of paleotemperatures it is critical to control the present temperature profile, since estimation of maximum paleotemperatures proceeds from trying to see how much of the observed effect could be explained by the magnitude of present temperatures.

Temperature data were supplied as raw measured BHT values (Table A.3). Full circulation time data were not available to allow Horner-correction procedures, and therefore raw measured BHT data were corrected using a simplified correction procedure adapted from the literature (Oxburgh and Andrews-Speed, 1981; Andrews-Speed et al. 1984). Quoted BHT data were corrected by increasing the difference between the sea-bed temperature (assumed to be 15°C) and the uncorrected BHT value by 20% for uncorrected temperatures below 150°F (66°C), and by 25% above 150°F. The first recorded BHT value was used where multiple temperature measurements were available at a given depth. While no doubt simplistic, this procedure has the advantage of allowing a common approach in all wells in a region, and appears to give consistent results in other studies.

Uncorrected and corrected BHT data from each well are summarised in Table A.2.



The single corrected temperature value for Hunters Lane-1 was used to estimate a linear geothermal gradient of 51.6°C/km using a surface temperature of 15°C.

A.4 Sample preparation and Apatite yield

The cuttings sample supplied from the Devonian granite basement in **Hunters Lane-1** was clearly significantly contaminated with limestone and marl sediments from the overlying Tertiary section. To ensure that apatite possibly associated with these Tertiary sediments was not attributed to the granite, the bulk cuttings sample was treated with concentrated hydrochloric acid until all activity ceased. This pre-treatment ensures that all carbonate and potential contaminating apatite was dissolved. After dissolution the sample was washed to remove fine material, leaving a residue of largely coherent cuttings fragments of granite with no free apatite. This residue was then crushed and subjected to our normal heavy liquid and magnetic separation procedures to recover apatite locked within the granite fragments.

The yield of detrital apatite obtained after mineral separation was excellent as summarised in Table A.1. The quality of the etched surfaces of those apatites obtained for analysis was high and the AFTA data collected from this key basement sample has resulted in a reliable interpretation of key aspects of the thermal history of the region.

A.5 Apatite quality and grain morphologies

Apatite grains in all samples are generally characterised by euhedral forms, consistent with derivation from a granitic rock.

A.6 Apatite compositions

The annealing kinetics of fission tracks in apatite are affected by chemical composition, specifically the Chlorine content, as explained in more detail in Appendix C. Compilation of data from a wide variety of geological environments from around the world suggests that apatites from common sedimentary rocks (such as quartz-feldspathic sandstones) are characterised by a distribution of chlorine contents similar to the distribution shown in Figure C.4b. The majority of grains from quartzo-feldspathic sandstones have chlorine contents between 0 and 0.1 wt% (typical of basement granitic rocks), while a smaller number of grains give values up to ~0.5 wt%, close to the value found in the Durango apatite, on which Geotrack's original kinetic model of fission track behaviour was based (Appendix C). Occasional grains may give Cl contents up to ~1 wt %, but higher amounts are unusual. On the other hand, apatite grains from volcanogenic sandstones have Cl contents between 0 and ~3 wt%, as shown in Figure C.4c, indicative of derivation from a wide range of original volcanic rock types.



For this study, Cl compositions were determined for all individual apatite grains in which fission track ages were determined and/or lengths were measured. Cl contents were measured using a semi-automated Jeol JXA-5A electron microprobe equipped with three wavelength dispersive crystal spectrometers, with an accelerating voltage of 15 KV and beam current of 25 nA. The beam was defocussed to 20 μm to avoid the problems associated with apatite decomposition, which occur under a fully focussed 1 μm - 2 μm beam. The X-Y co-ordinates of apatite grains within the grain mount were transferred from the Autoscan Fission Track Stage to a file suitable for direct input into the electron microprobe. Pure rock salt (NaCl) was used to peak the spectrometer for chlorine, which was the only element determined in each apatite grain. Cl count rates were converted to wt% Cl by reference to measured count rates for a Durango Apatite standard (Melbourne University Standard APT151), analysed at regular intervals during an analysis session. A value of 0.43 wt% Cl was used for Durango APT151, based on repeated measurements of the same fragment using pure rock salt (NaCl) as the ultimate standard for Cl. This approach gives essentially identical results to Cl determined from full compositional measurements of apatite, but has the advantage of reducing measurement time by a factor of ten or more.

Using this approach, lower limits of detection for chlorine content have been calculated for typical analytical conditions (beam current, counting time, etc.), and are listed in Table A.4. Errors in wt% composition are given as a percentage and quoted at 1σ for chlorine determinations. A generalised summary of error values for various values of wt% Cl is presented in Table A.5.

The measured range of Cl contents of apatites (both age and length grains) in all samples from each well are shown in histogram format in Figures A.1.

Plots of single grain age versus wt% chlorine for each sample are shown in Figure B.5. Chlorine contents, which are presented in numerical format for dated grains only, appear in the fission track age summary sheets in Appendix B. The Cl data are employed in interpreting the AFTA data for each sample using methods outlined in Appendix C.



References

- Andrews-Speed, C. P., Oxburgh, E. R. and Cooper, B. A. (1984) Temperatures and depth-dependent heat flow in the Western North Sea. *AAPG Bulletin*, 68, 1764-1781.
- Harland, W. B., Armstrong, R. L., Cox, A. V., Craig, L. E., Smith, A. G. and Smith, D. G. (1989) A geologic time scale 1989, Cambridge University Press.
- Oxburgh, E. R. and Andrews-Speed, C. P. (1981) Temperatures, thermal gradients and heat flow in the Southwestern North Sea. *In: L. V. and Hobson, G. D. (eds.), The petroleum geology of the continental shelf of NW Europe*, 3, 141-151.



Table A.1: Details of AFTA samples and apatite yields - sample from the Hunter Lane-1 well, PEP 135, Gippsland Basin (Geotrack Report #684A)

Sample number	Depth (m)	Sample type	Stratigraphic Age (Ma)	Present temperature* ¹ (°C)	Raw weight* ² (g)	Washed weight (g)	Apatite yield* ³
GC684-2	419	cuttings	370	36	100	40	Excellent

*¹ See Appendix A for discussion of present temperature data.

*² Following acid dissolution - see Section A.4 Appendix A.

*³ Yield based on quantity of mineral suitable for age determination. Excellent: >20 grains; Very Good: ~20 grains; Good: 15-20 grains; Fair: 10-15 grains; Poor: 5-10 grains; Very Poor: <5 grains



Table A.2: Summary of present temperature measurements - Hunters Lane-1 well, PEP 135, Gippsland Basin (Geotrack Report #684A)

	Ground surface (m)	Depth (m)	Measured temperature (°C)	Corrected temperature (°C)	Geothermal gradient (°C/km)
Hunters Lane-1	4.6	400	32	35.4	51.6

A surface temperature of 15°C has been assumed.
All depths are quoted with respect to ground level.



**Table A.3: Lower Limits of Detection for Apatite Analyses
(Geotrack Report #684A)**

Element	LLD (95% c.l.)		LLD (99% c.l.)	
	(wt%)	(ppm)	(wt%)	(ppm)
Cl	0.01	126	0.02	182

**Table A.4: Per cent errors in chlorine content
(Geotrack Report #684A)**

Chlorine content (wt%)	Error (%)
0.01	9.3
0.02	8.7
0.05	7.3
0.10	6.1
0.20	4.7
0.50	3.2
1.00	2.3
1.50	1.9
2.00	1.7
2.50	1.5
3.00	1.4

Errors quoted are at 1σ . See Appendix A for more details.

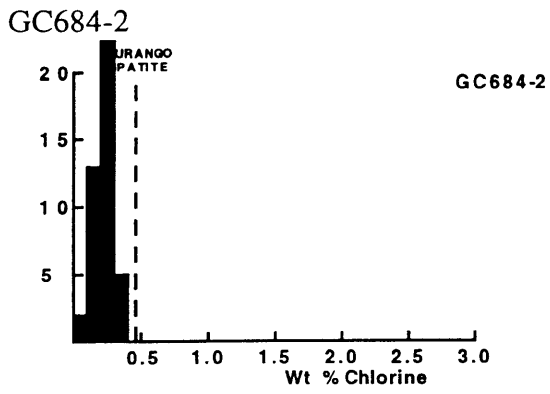


Figure A.1: Distributions of chlorine content in samples from well **Hunters Lane-1, Gippsland Basin.**

APPENDIX B

Sample Preparation, Analytical Details and Data Presentation

B.1 Sample Preparation

Core and outcrop samples are crushed in a jaw crusher and then ground to sand grade in a rotary disc mill. Cuttings samples are washed and dried before grinding to sand grade. The ground material is then washed to remove dust, dried and processed by conventional heavy liquid and magnetic separation techniques to recover heavy minerals. Apatite grains are mounted in epoxy resin on glass slides, polished and etched for 20 sec in 5M HNO₃ at 20°C to reveal the fossil fission tracks.

After etching, all mounts are cut down to 1.5 X 1 cm, and cleaned in detergent, alcohol and distilled water. The mounts are then sealed in intimate contact with low-uranium muscovite detectors within heat-shrink plastic film. Each batch of mounts is stacked between two pieces of uranium standard glass, which has been prepared in similar fashion. The stack is then inserted into an aluminium can for irradiation.

After irradiation, the mica detectors are removed from the grain mounts and standard glasses and etched in hydrofluoric acid to reveal the fission tracks produced by induced fission of ²³⁵U in the apatite and standard glass.

B.2 Analytical Details

Fission track ages

Fission track ages are calculated using the standard fission track age equation using the zeta calibration method (equation five of Hurford and Green, 1983), viz:

$$\text{F.T. AGE} = \frac{1}{\lambda_D} \ln \left[1 + \left(\frac{\zeta \lambda_D \rho_s g \rho_D}{\rho_i} \right) \right] \quad \text{B.1}$$

where: λ_D = Total decay constant of ²³⁸U (= 1.55125 x 10⁻¹⁰)
 ζ = Zeta calibration factor
 ρ_s = Spontaneous track density
 ρ_i = Induced track density
 ρ_D = Track density from uranium standard glass



$g = A$ geometry factor (= 0.5)

Fission track ages are determined by the external detector method or EDM (Gleadow, 1981). The EDM has the advantage of allowing fission track ages to be determined on single grains. In apatite, tracks are counted in 20 grains from each mount wherever possible. In those samples where the desired number is not present, all available grains are counted, the actual number depending on the availability of suitably etched and oriented grains. Only grains oriented with surfaces parallel to the crystallographic c-axis are analysed. Such grains can be identified on the basis of the etching characteristics, as well as from morphological evidence in euhedral grains. The grain mount is scanned sequentially, and the first 20 suitably oriented grains identified are analysed.

Tracks are counted within an eyepiece graticule divided into 100 grid squares. In each grain, the number of spontaneous tracks (N_s) within a certain number of grid squares (N_a) is recorded. The number of induced tracks (N_i) in the corresponding location within the mica external detector is then counted. Spontaneous and induced track densities (ρ_s and ρ_i , respectively) are calculated by dividing the track counts by the total area counted, given by the product of N_a and the area of each grid square (determined by calibration against a ruled stage graticule or diffraction grating). Fission track ages may be calculated by substituting track counts (N_s and N_i) for track densities (ρ_s and ρ_i) in equation B.1, since the areas cancel in the ratio.

Translation between apatite grains in the grain mount and external detector locations corresponding to each grain is carried out using AutoscanTM microcomputer-controlled automatic stages (Smith and Leigh Jones, 1985). This system allows repeated movement between grain and detector, and all grain locations are stored for later reference if required.

Neutron irradiations are carried out in a well-thermalised flux (X-7 facility; Cd ratio for Au ~98) in the Australian Atomic Energy Commission's HIFAR research reactor. Total neutron fluence is monitored by counting tracks in mica external detectors attached to two pieces of Corning Glass Works standard glass CN5 (containing ~11 ppm Uranium) included in the irradiation canister at each end of the sample stack. In determining track densities in external detectors irradiated adjacent to uranium standard glasses, 25 fields are normally counted in each detector. The total track count (N_D) is divided by the total area counted to obtain the track density (ρ_D). The positions of the counted fields are arranged in a 5 X 5 grid covering the whole area of the detector. For typical track densities of between $\sim 5 \times 10^5$ and 5×10^6 , this is a convenient arrangement to sample across the detector while gathering sufficient counts to achieve a precision of $\sim \pm 2\%$ in a reasonable time.



A small flux gradient is often present in the irradiation facility over the length of the sample package. If a detectable gradient is present, the track count in the external detector adjacent to each standard glass is converted to a track density (ρ_D) and a value for each mount in the stack is calculated by linear interpolation. When no detectable gradient is present, the track counts in the two external detectors are pooled to give a single value of ρ_D , which is used to calculate fission track ages for each sample.

A Zeta calibration factor (ζ) has been determined empirically for each observer by analysing a set of carefully chosen age standards with independently known K-Ar ages, following the methods outlined by Hurford and Green (1983) and Green (1985).

All track counting is carried out using Zeiss^(R) Axioplan microscopes, with an overall linear magnification of 1068 x using dry objectives.

For further details and background information on practical aspects of fission track age determination, see e.g., Fleischer, Price and Walker (1975), Naeser (1979) and Hurford (1986).

Track length measurements

For track length studies in apatite, the full lengths of "confined" fission tracks are measured. Confined tracks are those which do not intersect the polished surface but have been etched from other tracks or fractures, so that the whole length of the track is etched. Confined track lengths are measured using a digitising tablet connected to a microcomputer, superimposed on the microscope field of view via a projection tube. With this system, calibrated against a stage graticule ruled in 2 μm divisions, individual tracks can be measured to a precision of $\pm 0.2 \mu\text{m}$. Tracks are measured only in prismatic grains, characterised by sharp polishing scratches with well-etched tracks of narrow cone angle in all orientations, because of the anisotropy of annealing of fission tracks in apatite (as discussed by Green et al., 1986). Tracks are also measured following the recommendations of Laslett et al. (1982), the most important of which is that only horizontal tracks should be measured. One hundred tracks are measured whenever possible. In apatite samples with low track density, or in those samples in which only a small number of apatite grains are obtained, fewer confined tracks may be available. In such cases, the whole mount is scanned to measure as many confined tracks as possible.

Integrated fission track age and length measurement

Fission track age determination and length measurement are now made in a single pass of the grain mount, in an integrated approach. The location of each grain in which tracks are

either counted or measured is recorded for future reference. Thus, track length measurements can be tied to age determination in individual grains. As a routine procedure we do not measure the age of every grain in which lengths are determined, as this would be much too time-consuming. Likewise we do not only measure ages in grain in which lengths are measured, as this would bias the age data against low track density grains. Nevertheless, the ability to determine the fission track age of certain grains from which length data originate can be a particularly useful aid to interpretation in some cases. Grain location data are not provided in this report, but are available on request.

B.3 Data Presentation

Fission track age data

Data sheets summarising the apatite fission track age data, including full details of fission track age data for individual apatite grains in each sample, together with the primary counting results and statistical data, are given in the following pages. Individual grain fission track ages are calculated from the ratio of spontaneous to induced fission track counts for each grain using equation B.1, and errors in the single grain ages are calculated using Poissonian statistics, as explained in more detail by Galbraith (1981) and Green (1981). All errors are quoted as $\pm 1\sigma$ throughout this report, unless otherwise stated.

The variability of fission track ages between individual apatite grains within each sample can be assessed using a chi-squared (χ^2) statistic (Galbraith, 1981), the results of which are summarised for each sample in the data sheets. If all the grains counted belong to a single age population, the probability of obtaining the observed χ^2 value, for ν degrees of freedom (where $\nu = \text{number of crystals} - 1$), is listed in the data sheets as $P(\chi^2)$ or $P(\text{chi squared})$.

A $P(\chi^2)$ value greater than 5% can be taken as evidence that all grains are consistent with a single population of fission track age. In this case, the best estimate of the fission track age of the sample is given by the "pooled age", calculated from the ratio of the total spontaneous and induced track counts in all grains analysed. Errors for the pooled age are calculated using the "conventional" technique outlined by Green (1981), based on the total number of tracks counted for each track density measurement (see also Galbraith, 1981).

A $P(\chi^2)$ value of less than 5% denotes a significant spread of single grain ages, suggesting real differences exist between the fission track ages of individual apatite grains. A significant spread in grain ages can result either from inheritance of detrital grains from



mixed source areas (in sedimentary rocks), or from differential annealing in apatite grains of different composition, within a narrow range of temperature.

Calculation of the pooled age inherently assumes that only a single population of ages is present, and is thus not appropriate to samples containing a significant spread of fission track ages. In such cases Galbraith, has recently devised a means of estimating the modal age of a distribution of single grain fission track ages which is referred to as the "central age". Calculation of the central age assumes that all single grain ages belong to a Normal distribution of ages, with a standard deviation (σ) known as the "age dispersion". An iterative algorithm (as yet unpublished) is used to provide estimates of the central age with its associated error, and the age dispersion, which are all quoted in the data sheets. Note that this treatment replaces use of the "mean age", which has used been in the past for those samples in which $P(\chi^2) < 5\%$. For samples in which $P(\chi^2) > 5\%$, the central age and the pooled age should be equal, and the age dispersion should be less than $\sim 10\%$.

Table B.1 summarises the fission track age data in apatite from each sample analysed.

Construction of radial plots of single grain age data

Single grain age data are best represented in the form of radial plot diagrams (Galbraith, 1988, 1990). As illustrated in Figure B.1, these plots display the variation of individual grain ages in a plot of y against x , where:

$$y = (z_j - z_0) / \sigma_j \quad x = 1/\sigma_j \quad \text{B.2}$$

and; z_j = Fission track age of grain j
 z_0 = A reference age
 σ_j = Error in age for grain j

In this plot, all points on a straight line from the origin define a single value of fission track age, and, at any point, the value of x is a measure of the precision of each individual grain age. Therefore, precise individual grain ages fall to the right of the plot (small error, high x), which is useful, for example, in enabling precise, young grains to be identified. The age scale is shown radially around the perimeter of the plot (in Ma). If all grains belong to a single age population, all data should scatter between $y = +2$ and $y = -2$, equivalent to scatter within $\pm 2\sigma$. Scatter outside these boundaries shows a significant spread of individual grain ages, as also reflected in the values of $P(\chi^2)$ and age dispersion.

In detail, rather than using the fission track age for each grain as in equation B.2, we use:



$$z_j = \frac{N_{sj}}{N_{ij}} \sigma_j = \{1/N_{sj} + 1/N_{ij}\} \quad \text{B.3}$$

as we are interested in displaying the scatter within the data from each sample in comparison with that allowed by the Poissonian uncertainty in track counts, without the additional terms which are involved in determination of the fission track age (ρ_D , ζ , etc).

Zero ages cannot be displayed in such a plot. This can be achieved using a modified plot, (Galbraith, 1990) with:

$$z_j = \text{arc sin} \sqrt{\left\{ \frac{N_{sj} + 3/8}{N_{sj} + N_{ij} + 3/4} \right\}} \sigma_j = \frac{1}{2} \sqrt{\left\{ \frac{1}{N_{sj} + N_{ij}} \right\}} \quad \text{B.4}$$

Note that the numerical terms in the equation for z_j are standard terms, introduced for statistical reasons. Using this arc-sin transformation, zero ages plot on a diagonal line which slopes from upper left to lower right. Note that this line does not go through the origin. Figure B.2 illustrates this difference between conventional and arc-sin radial plots, and also provides a simple guide to the structure of radial plots.

Use of arc-sin radial plots is particularly useful in assessing the relative importance of zero ages. For instance, grains with $N_s = 0$, $N_i = 1$ are compatible with ages up to ~900 Ma (at the 95% confidence level), whereas grains with $N_s = 0$, $N_i = 50$ are only compatible with ages up to ~14 Ma. The two data would readily be distinguishable on the radial plot as the 0,50 datum would plot well to the right (high x) compared to the 0,1 datum.

In this report the value of z corresponding to the stratigraphic age of each sample (or the midpoint of the range where appropriate) is adopted as the reference value, z_0 . This allows rapid assessment of the fission track age of individual grains in relation to the stratigraphic age, which is a key component in the interpretation of AFTA data, as explained in more detail in Appendix C.

Note that the x axis of the radial plot is normally not labelled, as this would obscure the age scale around the plot. In general labelling is not considered necessary, as we are concerned only with relative variation within the data, rather than absolute values of precision.

Radial plots of the single grain age data in apatite from each sample analysed in this report are shown in Figure B.3. Use of radial plots to provide thermal history information is explained in Appendix C and Figure C.7.



Smoothed probability distributions

The single grain ages within each sample are also shown in Figure B.3 in histogram form and also as smoothed probability distributions (Hurford et al., 1984). In constructing these distributions, each grain is represented by a normal probability curve, with mean equal to the single grain age, standard deviation given by the error on the single grain age and the contributions from all grains analysed in each sample summed to produce the plotted curve. These distributions are generally not as informative as the radial plot presentation of single grain age data as they convey little assessment of the relative precision of the fission track ages of different grains. However, they can be useful for portraying the general form of the distribution of ages within a sample.

Track length data

Distributions of confined track lengths in apatite from each sample are shown as simple histograms in Figure B.4. For every track length measurement, the length is recorded to the nearest 0.1 μm , but the measurements have been grouped into 1 μm intervals in the histograms in Figure B.4. Each distribution has been normalised to 100 tracks for each sample to facilitate comparison. A summary of the length distribution in each sample is presented in Table B.2, which also shows the mean track length in each sample and its associated error, the standard deviation of each distribution and the number of tracks (N) measured in each sample. The angle which each confined track makes with the crystallographic c-axis is also routinely recorded, as is the width of each fracture within which tracks are revealed. These data are not provided in this report, but can be supplied on request.

Breakdown of data into compositional groups

In Table B.3, AFTA data are grouped into compositional intervals of 0.1 wt% Cl width. Parameters for each interval represent the data from all grains with Cl contents within each interval. Also shown are the parameters for each compositional interval predicted from the Default Thermal History (see Section 2.1). These data form the basis of interpretation of the AFTA data, which takes full account of the influence of Cl content on annealing kinetics, as described in Appendix C.

Plots of fission track age against Cl content for individual apatite grains

In Figure B.5, fission track ages of single apatite grains within individual samples are plotted against the Cl content of each grain. These plots are useful in assessing the degree of annealing, as expressed by the fission track age data. For example, if grains with a



range of Cl contents from zero to some upper limit all give similar fission track ages which are significantly less than the stratigraphic age, then grains with these compositions must have been totally annealed. Alternatively, if fission track age falls rapidly with decreasing Cl content, the sample displays a high degree of partial annealing.

B.4 A note on terminology

Note that throughout this report, the term "fission track age" is understood to denote the parameter calculated from the fission track age equation, using the observed spontaneous and induced track counts (either pooled for all grains or for individual grains). The resulting number (with units of Ma) should not be taken as possessing any significance in terms of events taking place at the time indicated by the measured fission track age, but should rather be regarded as a measure of the integrated thermal history of the sample, and should be interpreted in that light using the principles outlined in Appendix C. Use of the term "apparent age" is not considered to be useful in this regard, as almost every fission track age should be regarded as an apparent age, in the classic sense, and repeated use becomes cumbersome.



References

- Fleischer, R. L., Price, P. B., and Walker, R. M. (1975) Nuclear tracks in solids, University of California Press, Berkeley.
- Galbraith, R. F. (1981) On statistical models for fission-track counts. *Mathematical Geology*, 13, 471-488.
- Galbraith, R. F. (1988) Graphical display of estimates having differing standard errors. *Technometrics*, 30, 271-281.
- Galbraith, R. F. (1990) The radial plot: graphical assessment of spread in ages. *Nuclear Tracks*, 17, 207-214.
- Gleadow, A. J. W. (1981) Fission track dating methods; what are the real alternatives? *Nuclear Tracks*, 5, 3-14.
- Green, P. F. (1981) A new look at statistics in fission track dating. *Nuclear Tracks* 5, 77-86.
- Green, P. F. (1985) A comparison of zeta calibration baselines in zircon, sphene and apatite. *Chem. Geol. (Isot. Geol. Sect.)*, 58, 1-22.
- Green, P. F., Duddy, I. R., Gleadow, A. J. W., Tingate, P. R. and Laslett, G. M. (1986) Thermal annealing of fission tracks in apatite 1. A qualitative description. *Chem. Geol. (Isot. Geosci. Sect.)*, 59, 237-253.
- Hurford, A. J. (1986) Application of the fission track dating method to young sediments: Principles, methodology and Examples. In: Hurford, A. J., Jäger, E. and Ten Cate, J. A. M. (eds), Dating young sediments, CCOP Technical Publication 16, CCOP Technical Secretariat, Bangkok, Thailand.
- Hurford, A. J., Fitch, F. J. and Clarke, A. (1984) Resolution of the age structure of the detrital zircon populations of two Lower Cretaceous sandstones from the Weald of England by fission track dating. *Geological Magazine*, 121, 269-396.
- Hurford, A. J. and Green, P. F. (1982) A user's guide to fission track dating calibration. *Earth. Planet. Sci Lett.* 59, 343-354.
- Hurford, A. J. and Green, P. F. (1983) The zeta age calibration of fission track dating. *Isotope Geoscience* 1, 285-317.
- Laslett, G. M., Kendall, W. S., Gleadow, A. J. W. and Duddy, I. R. (1982) Bias in measurement of fission track length distributions. *Nuclear Tracks*, 6, 79-85.
- Naeser, C. W. (1979) Fission track dating and geologic annealing of fission tracks. In: Jäger, E. and Hunziker, J. C. (eds), Lectures in Isotope Geology, Springer Verlag, Berlin.
- Smith, M. J. and Leigh-Jones, P. (1985) An automated microscope scanning stage for fission-track dating. *Nuclear Tracks*, 10, 395-400.



Table B.1: AFTA[®] analytical results - sample from the Hunters Lane-1 well, PEP 135, Gippsland Basin (Geotrack Report #684A)

Sample number	Number of grains (m)	Rho D x 10 ⁶ (ND)	Rho S x 10 ⁶ (Ns)	Rho I x 10 ⁶ (Ni)	Uranium content (ppm)	P (chi squared) (%)	Age dispersion (%)	Fission track Age (Ma)
GC684-2	34	1.598	0.959	1.177	8.4	<0.1	34.8	<i>244.8±21.8</i>

Rho S = spontaneous track density; Rho I = induced track density; Rho D = track density in glass standard external detector. All track densities quoted in units of millions of tracks per square cm. Brackets show numbers of tracks counted. Rho D and Rho I are measured in mica external detectors; Rho S measured in internal surfaces of the mineral.

Ages calculated using dosimeter glass CN 5, with a zeta of 380.4±5.7 (Analyst: C.E. O'Brien). Central fission track age quoted (in italics) where P Chi square) < 5%.

Table B.2: Length distribution summary data - Hunters Lane-1 #1, PEP 135, Gippsland Basin

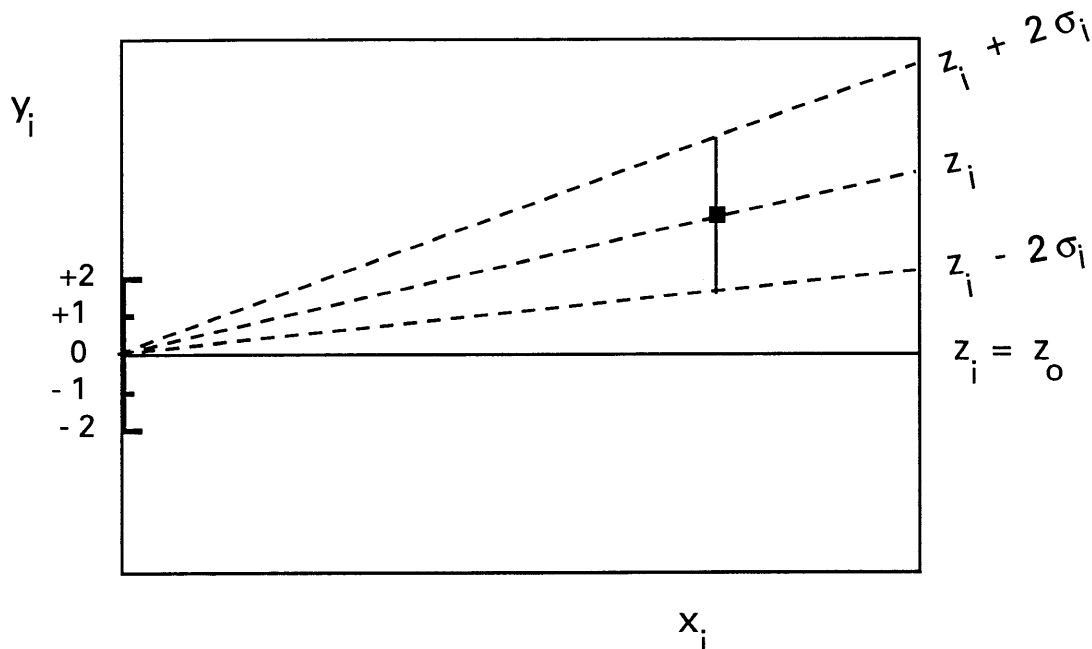
Sample Number GC	Depth (m)*1	Mean Track Length (μm)	Std. Dev. (μm)	Number of Tracks (N)	1	2	3	4	5	6	7	8	9	10	11	12	13	14	15	16	17	18	19	20
684-2	419	11.05 \pm 0.22	1.51	48	-	-	-	-	-	-	-	1	3	7	16	5	10	5	1	-	-	-	-	-

*1 Average depth.

Length measurements by C.E. O'Brien

Estimates	z_i
Standard errors	s_i
Reference value	z_o
Standardised estimates	$y_i = (z_i - z_o) / s_i$
Precision	$x_i = 1 / s_i$

PLOT y_i against x_i



Slope of line from origin through data point

$$= y_i / x_i$$

$$= \{(z_i - z_o) / \sigma_i\} / \{1 / \sigma_i\}$$

$$= z_i - z_o$$

Key Points:

Radial lines emanating from the origin correspond to fixed values of z

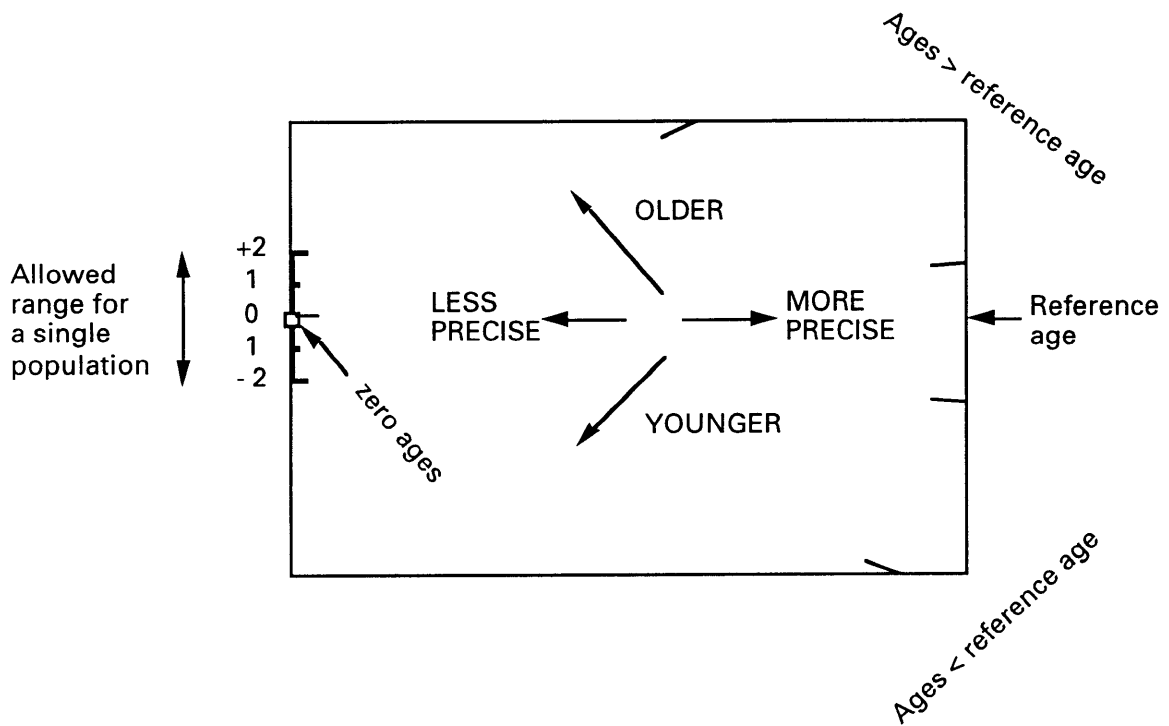
Data points with higher values of x_i have greater precision.

Error bars on all points are the same size in this plot.

Figure B.1 Basic construction of a radial plot. In AFTA, the estimates z_i correspond to the fission track age values for individual apatite grains. Any convenient value of age can be chosen as the reference value corresponding to the horizontal in the radial plot. Radial lines emanating from the origin with positive slopes correspond to fission track ages greater than the reference value. Lines with negative slopes correspond to fission track ages less than the reference value.



Normal radial plot (equations B.2 and B.3)



Arc-sin radial plot (equations B.2 and B.4)

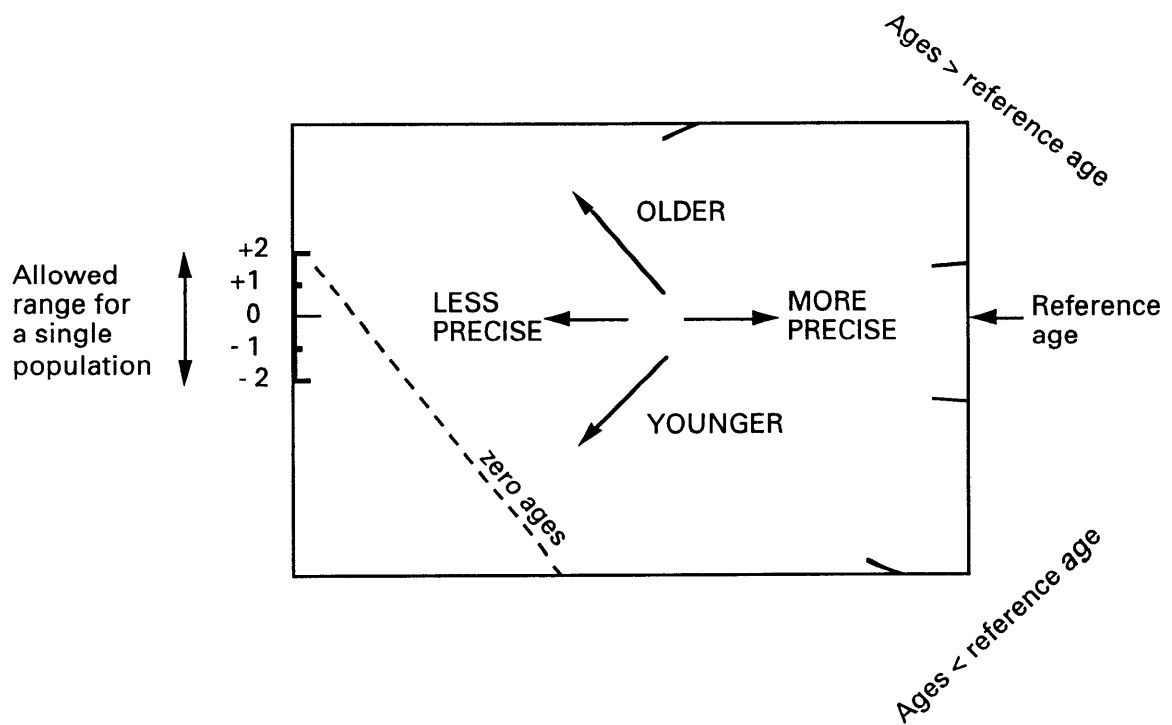


Figure B.2 Simplified structure of Normal and Arc-sin radial plots.

HUNTERS LANE -1

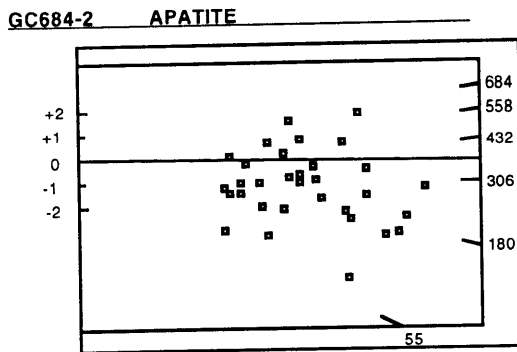
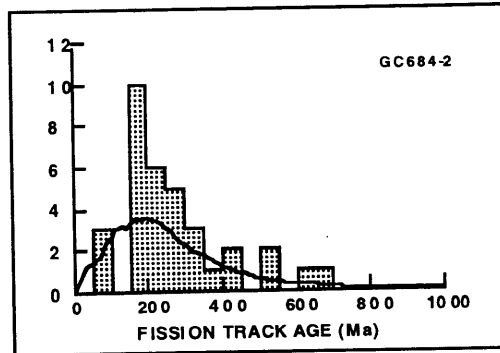


Figure B.3: Distributions of single grain ages with smoothed probability functions (top) and radial plots of single grain age data (bottom) in sample GC684-2 from the **Hunters Lane-1 well, Gippsland Basin**. The horizontal line or shaded area in the radial plot shows the stratigraphic age of the sample. The construction of radial plots is described in the Appendix B text.

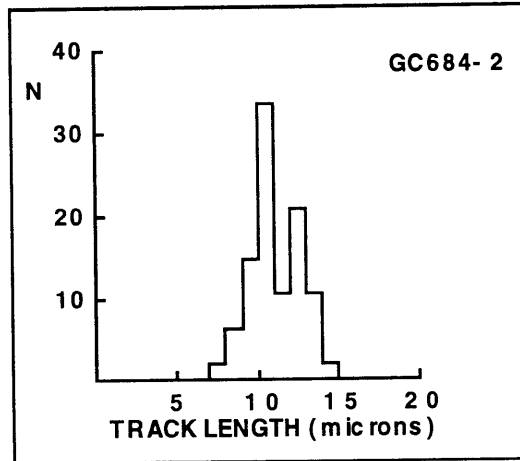


Figure B.4: Distribution of confined fission track lengths in sample GC684-2 from the **Hunters Lane-1 well, Gippsland Basin.**

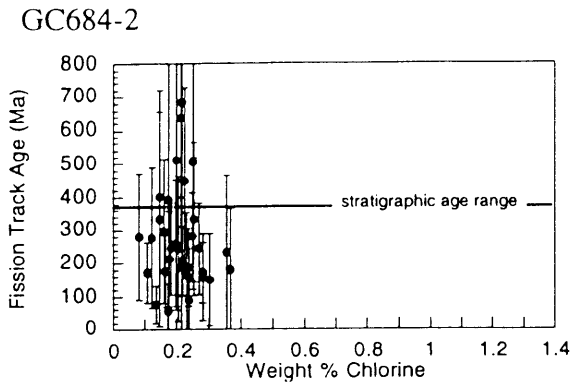


Figure B.5: Plots of single grain age against weight per-cent chlorine for samples from well **Hunters Lane-1, Gippsland Basin.**



Fission Track Age Data Sheets - Glossary

Ns	=	Number of spontaneous tracks in Na grid squares
Ni	=	Number of induced tracks in Na grid squares
Na	=	Number of grid squares counted in each grain
RATIO	=	Ns/Ni
U (ppm)	=	Uranium content of each grain (= U content of standard glass * ρ_i/ρ_D)
Cl (wt%)	=	Weight percent chlorine content of each grain
RHOs	=	Spontaneous track density (ρ_s) = Ns/ (Na*area of basic unit)
RHOi	=	Induced track density (ρ_i) = Ni/(Na*area of basic unit)
F.T. AGE	=	Fission track age, calculated using equation B.1
Area of basic unit	=	Area of one grid square
Chi squared	=	χ^2 parameter, used to assess variation of single grain ages within the sample
P(chi squared)	=	Probability of obtaining observed χ^2 value for the relevant number of degrees of freedom, if all grains belong to a single population
Correlation coefficient	=	Correlation coefficient between Ns and Ni
Variance of SQR(Ns)	=	Variance of square root of Ns values - should be ~ 0.25 for Poisson distribution; greater if additional variation present
Variance of SQR(Ni)	=	Variance of square root of Ni values - should be ~ 0.25 for Poisson distribution; greater if additional variation present
Age Dispersion	=	% variation in single grain ages - see discussion in text re "Central age"
Ns/Ni	=	Pooled ratio, total spontaneous tracks divided by total induced tracks for all grains
Mean ratio	=	Mean of (Ns/Ni) for individual grains
Zeta	=	Calibration constant, determined empirically for each observer
RhoD	=	Track density (ρ_D) from uranium standard glass (interpolated from values at each end of stack)
ND	=	Total number of tracks counted for determining ρ_D
POOLED AGE	=	Fission track age calculated from pooled ratio Ns/Ni. Valid only when $\chi^2 > 5\%$
CENTRAL AGE	=	Alternative to pooled age when $\chi^2 < 5\%$



GC684-2 APATITE
IRRADIATION G730
SLIDE NUMBER 1
COUNTED BY: COB

Current grain no.	Ns	Ni	Na	RHOs	RHOi	RATIO	U (ppm)	Cl (wt%)	F.T. AGE (Ma)
3	36	38	32	1.788E+06	1.887E+06	0.947	13.5	0.25	281.7 ± 65.9
4	33	15	24	2.185E+06	9.932E+05	2.200	7.1	0.21	636.2 ± 198.7
5	18	16	24	1.192E+06	1.059E+06	1.125	7.6	0.26	333.1 ± 114.8
6	23	28	42	8.702E+05	1.059E+06	0.821	7.6	0.18	244.9 ± 69.2
7	23	40	40	9.137E+05	1.589E+06	0.575	11.3	0.11	172.4 ± 45.3
9	9	36	40	3.575E+05	1.430E+06	0.250	10.2	0.14	75.5 ± 28.2
10	7	14	27	4.120E+05	8.240E+05	0.500	5.9	0.30	150.2 ± 69.6
12	27	39	35	1.226E+06	1.771E+06	0.692	12.6	0.22	207.0 ± 52.1
13	2	11	15	2.119E+05	1.165E+06	0.182	8.3	0.17	55.0 ± 42.3
14	9	8	16	8.938E+05	7.945E+05	1.125	5.7	0.15	333.1 ± 162.1
15	9	11	30	4.767E+05	5.827E+05	0.818	4.2	0.21	244.0 ± 109.8
16	5	17	30	2.648E+05	9.005E+05	0.294	6.4	0.24	88.8 ± 45.2
17	5	8	12	6.621E+05	1.059E+06	0.625	7.6	0.22	187.2 ± 106.8
20	27	24	48	8.938E+05	7.945E+05	1.125	5.7	0.26	333.1 ± 93.8
53	6	10	20	4.767E+05	7.945E+05	0.600	5.7	0.37	179.8 ± 93.0
55	9	17	24	5.959E+05	1.126E+06	0.529	8.0	0.28	158.9 ± 65.6
57	15	15	20	1.192E+06	1.192E+06	1.000	8.5	0.16	297.0 ± 108.7
58	19	11	24	1.258E+06	7.283E+05	1.727	5.2	0.25	504.7 ± 191.6
60	17	27	18	1.501E+06	2.384E+06	0.630	17.0	0.24	188.6 ± 58.6
62	19	8	20	1.510E+06	6.356E+05	2.375	4.5	0.22	684.2 ± 288.9
63	17	18	27	1.001E+06	1.059E+06	0.944	7.6	0.08	280.8 ± 95.2
64	17	29	30	9.005E+05	1.536E+06	0.586	11.0	0.17	175.7 ± 53.9
65	14	16	24	9.270E+05	1.059E+06	0.875	7.6	0.20	260.6 ± 95.6
66	20	38	15	2.119E+06	4.026E+06	0.526	28.7	0.24	158.0 ± 43.8
69	14	8	21	1.059E+06	6.054E+05	1.750	4.3	0.20	511.0 ± 226.9
70	8	6	24	5.297E+05	3.973E+05	1.333	2.8	0.18	393.0 ± 212.5
71	23	28	36	1.015E+06	1.236E+06	0.821	8.8	0.27	244.9 ± 69.2
73	5	9	28	2.838E+05	5.108E+05	0.556	3.6	0.23	166.7 ± 93.1
76	15	21	36	6.621E+05	9.270E+05	0.714	6.6	0.18	213.5 ± 72.4
77	13	14	12	1.721E+06	1.854E+06	0.929	13.2	0.12	276.2 ± 106.6
78	26	17	20	2.066E+06	1.351E+06	1.529	9.6	0.23	448.8 ± 140.4
79	15	11	15	1.589E+06	1.165E+06	1.364	8.3	0.15	401.6 ± 159.8
80	23	40	42	8.702E+05	1.513E+06	0.575	10.8	0.28	172.4 ± 45.3
81	7	9	16	6.952E+05	8.938E+05	0.778	6.4	0.36	232.1 ± 117.1
535		657		9.585E+05	1.177E+06		8.4		

Area of basic unit = 6.293E-07 cm²

Chi Squared = 68.000 with 33 degrees of freedom

P(chi squared) = 0.0 %

Correlation Coefficient = 0.587

Variance of SQR(Ns) = 1.24

Variance of SQR(Ni) = 1.45

Age Dispersion = 34.881 %

Ns/Ni = 0.814 ± 0.047

Mean Ratio = 0.924 ± 0.088

Ages calculated using a zeta of 380.4 ± 5.7 for CN5 glass

Rho D = 1.598E+06cm⁻²; ND = 2460

Rho D interpolated between top of can; Rho D = 1.598E+06cm⁻², ND = 1257

bottom of can; Rho D = 1.529E+06cm⁻², ND = 1203

POOLED AGE = 242.8 ± 15.4 Ma

CENTRAL AGE = 244.8 ± 21.8 Ma



APPENDIX C

Principles of Interpretation of AFTA Data in Sedimentary Basins

C.1 Introduction

Detrital apatite grains are incorporated into sedimentary rocks from three dominant sources - crystalline basement rocks, older sediments and contemporaneous volcanism. Apatites derived from the first two sources will, in general, contain fission tracks when they are deposited, with AFTA parameters characteristic of the source regions. However, apatites derived from contemporaneous volcanism, or from rapidly uplifted basement, will contain no tracks when they are deposited. For now, we will restrict discussion to this situation, and generalise at a later point to cover the case of apatites which contain tracks that have been inherited from source regions.

C.2 Basic principles of Apatite Fission Track Analysis

Fission tracks are trails of radiation damage, which are produced within apatite grains at a more or less constant rate through geological time, as a result of the spontaneous fission of ^{238}U impurity atoms. Therefore, the number of fission events which occur within an apatite grain during a fixed time interval depends on the magnitude of the time interval and the uranium content of the grain. Each fission event leads to the formation of a single fission track, and the proportion of tracks which can intersect a polished surface of an apatite grain depends on the length of the tracks. Therefore, the number of tracks which are etched in unit area of the surface of an apatite grain (the "spontaneous track density") depends on three factors - (i) The time over which tracks have been accumulating; (ii) The uranium content of the apatite grain; and, (iii) The distribution of track lengths in the grain. In sedimentary rocks which have not been subjected to temperatures greater than $\sim 50^\circ\text{C}$ since deposition, spontaneous fission tracks have a characteristic distribution of confined track lengths, with a mean length in the range $14\text{-}15\ \mu\text{m}$ and a standard deviation of $\sim 1\ \mu\text{m}$. In such samples, by measuring the spontaneous track density and the uranium content of a collection of apatite grains, a "fission track age" can be calculated which will be equal to the time over which tracks have been accumulating. The technique is calibrated against other isotopic systems using age standards which also have this type of length distribution (see Appendix B).

In samples which have been subjected to temperatures greater than $\sim 50^\circ\text{C}$ after deposition, fission tracks are shortened because of the gradual repair of the radiation damage which constitutes the unetched tracks. In effect, the tracks shrink from each end, in a process which



is known as fission track "annealing". The final length of each individual track is essentially determined by the maximum temperature which that track has experienced. A time difference of an order of magnitude produces a change in fission track parameters which is equivalent to a temperature change of only $\sim 10^{\circ}\text{C}$, so temperature is by far the dominant factor in determining the final fission track parameters. As temperature increases, all existing tracks shorten to a length determined by the prevailing temperature, regardless of when they were formed. After the temperature has subsequently decreased, all tracks formed prior to the thermal maximum are "frozen" at the degree of length reduction they attained at that time. Thus, the length of each track can be thought of as a maximum-reading thermometer, recording the maximum temperature to which it has been subjected.

Therefore, in samples for which the present temperature is maximum, all tracks have much the same length, resulting in a narrow, symmetric distribution. The degree of shortening will depend on the temperature, with the mean track length falling progressively from $\sim 14\ \mu\text{m}$ at 50°C , to zero at around $110^{\circ}\text{--}120^{\circ}\text{C}$ - the precise temperature depending on the timescale of heating and the composition of the apatites present in the sample (see below). Values quoted here relate to times of the order of 10^7 years (heating rates around 1 to $10^{\circ}\text{C}/\text{Ma}$) and average apatite composition. If the effective timescale of heating is shorter than 10^7 years, the temperature responsible for a given degree of track shortening will be higher, depending in detail on the kinetics of the annealing process (Green et al., 1986; Laslett et al., 1987; Duddy et al., 1988; Green et al., 1989b). Shortening of tracks produces an accompanying reduction in the fission track age, because of the reduced proportion of tracks which can intersect the polished surface. Therefore, the fission track age is also highly temperature dependent, falling to zero at around 120°C due to total erasure of all tracks.

Samples which have been heated to a maximum paleotemperature less than $\sim 120^{\circ}\text{C}$ at some time in the past and subsequently cooled will contain two populations of tracks, and will show a more complex distribution of lengths and ages. If the maximum paleotemperature was less than $\sim 50^{\circ}\text{C}$ then the two components will not be resolvable, but for maximum paleotemperatures between $\sim 50^{\circ}$ and 120°C the presence of two components can readily be identified. Tracks formed prior to the thermal maximum will all be shortened to approximately the same degree (the precise value depending on the maximum paleotemperature), while those formed during and after cooling will be longer, due to the lower prevailing temperatures. The length distribution in such samples will be broader than in the simple case, consisting of a shorter and a longer component, and the fission track age will reflect the amount of length reduction shown by the shorter component (determined by the maximum paleotemperature).

If the maximum paleotemperature was sufficient to shorten tracks to between 9 and $11\ \mu\text{m}$, and cooling to temperatures of $\sim 50^{\circ}\text{C}$ or less was sufficiently rapid, tracks formed after cooling will have lengths of $14\text{--}15\ \mu\text{m}$ and the resulting track length distribution will show a characteristic bimodal form. If the maximum paleotemperature was greater than ~ 110 to



120°C, all pre-existing tracks will be erased, and all tracks now present will have formed after the onset of cooling. The fission track age in such samples relates directly to the time of cooling.

In thermal history scenarios in which a heating episode is followed by cooling and then temperature increases again, the tracks formed during the second heating phase will undergo progressive shortening. The tracks formed prior to the initial cooling, which were shortened in the first heating episode, will not undergo further shortening until the temperature exceeds the maximum temperature reached in the earlier heating episode. (In practice, differences in timescale of heating can complicate this simple description. In detail, it is the integrated time-temperature effect of the two heating episodes which should be considered.) If the maximum and peak paleotemperatures in the two episodes are sufficiently different ($> \sim 10^\circ\text{C}$), and the later peak paleotemperature is less than the earlier maximum value, then the AFTA parameters allow determination of both episodes. As the peak paleotemperature in the later episode approaches the earlier maximum, the two generations of tracks become increasingly more difficult to resolve, and when the two paleotemperatures are the same, both components are shortened to an identical degree and all information on the earlier heating phase will be lost.

No information is preserved on the approach to maximum paleotemperature because the great majority of tracks formed up to that time have the same mean track length. Only those tracks formed in the last few per cent of the history prior to the onset of cooling are not shortened to the same degree (because temperature dominates over time in the annealing kinetics). These form a very small proportion of the total number of tracks and therefore cannot be resolved within the length distribution because of the inherent spread of several μm in the length distribution.

To summarise, AFTA allows determination of the magnitude of the maximum temperature and the time at which cooling from that maximum began. In some circumstances, determination of a subsequent peak paleotemperature and the time of cooling is also possible.



C.3 Quantitative understanding of fission track annealing in apatite

Annealing kinetics and modelling the development of AFTA parameters

Our understanding of the behaviour of fission tracks in apatite during geological thermal histories is based on study of the response of fission tracks to elevated temperatures in the laboratory (Green et al., 1986; Laslett et al., 1987; Duddy et al., 1988; Green et al., 1989b), in geological situations (Green et al., 1989a), observations of the lengths of spontaneous tracks in apatites from a wide variety of geological environments (Gleadow et al., 1986), and the relationship between track length reduction and reduction in fission track age observed in controlled laboratory experiments (Green, 1988).

These studies resulted in the capability to simulate the development of AFTA parameters resulting from geological thermal histories for an apatite of average composition (Durango apatite, ~0.43 wt% Cl). Full details of this modelling procedure have been explained in Green et al. (1989b). The following discussion presents a brief explanation of the approach.

Geological thermal histories involving temperatures varying through time are broken down into a series of isothermal steps. The progressive shortening of track length through sequential intervals is calculated using the extrapolated predictions of an empirical kinetic model fitted to laboratory annealing data. Contributions from tracks generated throughout the history (remembering that new tracks are continuously generated through time as new fissions occur) are summed to produce the final distribution of track lengths expected to result from the input history. In summing these components, care is taken to allow for various biases which affect revelation of confined tracks (Laslett et al., 1982). The final length reduction of each component of tracks is converted to a contribution of fission track age, using the relationship between track length and density reduction determined by Green (1988). These age contributions are summed to generate the final predicted fission track age.

This approach depends critically on the assumption that extrapolation of the laboratory-based kinetic model to geological timescales, over many orders of magnitude in time, is valid. This was assessed critically by Green et al. (1989b), who showed that predictions from this approach agree well with observed AFTA parameters in apatites of the appropriate composition in samples from a series of reference wells in the Otway Basin of south-east Australia (Gleadow and Duddy, 1981; Gleadow et al., 1983; Green et al., 1989a). This point is illustrated in Figure C.1. Green et al. (1989b) also quantitatively assessed the errors associated with extrapolation of the Laslett et al. (1987) model from laboratory to geological timescales (i.e., precision, as opposed to accuracy). Typical levels of precision are ~0.5 μm for mean lengths <~10 μm , and ~0.3 μm for lengths >~10 μm . These figures are equivalent to an uncertainty in estimates of maximum paleotemperature derived using this approach of ~10°C. Precision is largely independent of thermal history for any reasonable geological

history. Accuracy of prediction from this model is limited principally by the effect of apatite composition on annealing kinetics, as explained in the next section.

Compositional effects

Natural apatites essentially have the composition $\text{Ca}_5(\text{PO}_4)_3(\text{F},\text{OH},\text{Cl})$. Most common detrital and accessory apatites are predominantly Fluor-apatites, but may contain appreciable amounts of chlorine. The amount of chlorine in the apatite lattice exerts a subtle compositional control on the degree of annealing, with apatites richer in fluorine being more easily annealed than those richer in chlorine. The result of this effect is that in a single sample, individual apatite grains may show a spread in the degree of annealing (i.e., length reduction and fission track age reduction). This effect becomes most pronounced in the temperature range 90 - 120°C (assuming a heating timescale of ~10 Ma), and can be useful in identifying samples exposed to paleotemperatures in this range. At temperatures below ~80°C, the difference in annealing sensitivity is less marked, and compositional effects can largely be ignored.

Our original quantitative understanding of the kinetics of fission track annealing, as described above, relates to a single apatite (Durango apatite) with ~0.43 wt% Cl, on which most of our original experimental studies were carried out. Recently, we have extended this quantitative understanding to apatites with Cl contents up to ~3 wt%. This new, multi-compositional kinetic model is based both on new laboratory annealing studies on a range of apatites with different F-Cl compositions (Figure C.2), and on observations of geological annealing in apatites from a series of samples from exploration wells in which the section is currently at maximum temperature since deposition. A composite model for Durango apatite composition was first created by fitting a common model to the old laboratory data (from Green et al., 1986) and the new geological data for a similar composition. This was then extended to other compositions on the basis of the multi-compositional laboratory and geological data sets. Details of the multi-compositional model are contained in a Technical Note, available from Geotrack in Melbourne.

The multi-compositional model allows prediction of AFTA parameters for any Cl content between 0 and 3 wt%, using a similar approach to that used in our original single composition modelling, as outlined above. Then, for an assumed or measured distribution of Cl contents within a sample, the composite parameters for the sample can be predicted. The range of Cl contents from 0 to 3 wt% spans the range of compositions commonly encountered, as discussed in the next section.

Predictions of the new multi-compositional model are in good agreement with the geological constraints on annealing rates provided by the Otway Basin reference wells, as shown in Figure C.3. However, note that the AFTA data from these Otway Basin wells were among



those used in construction of the new model, so this should not be viewed as independent verification, but rather as a demonstration of the overall consistency of the model.

Distributions of Cl content in common AFTA samples

Figure C.4a shows a histogram of Cl contents, measured by electron microprobe, in apatite grains from more than 100 samples of various types. Most grains have Cl contents less than ~0.5 wt%. The majority of grains with Cl contents greater than this come from volcanic sources and basic intrusives, and contain up to ~2 wt% Cl. Figure C.4b shows the distribution of Cl contents measured in randomly selected apatite grains from 61 samples of "typical" quartzo-feldspathic sandstone. This distribution is similar to that in Figure C.4a, except for a more rapid fall-off as Cl content increases. Apatites from most common sandstones give distributions of Cl content which are very similar to that in Figure C.4b. Volcanogenic sandstones typically contain apatites with higher Cl contents, with a much flatter distribution for Cl contents up to ~1.5%, falling to zero at ~2.5 to 3 wt%, as shown in Figure C.4c. Cl contents in granitic basement samples and high-level intrusives are typically much more dominated by compositions close to end-member Fluorapatite, although many exceptions occur to this general rule.

Information about the spread of Cl contents in samples analysed in this report can be found in Appendix A.

Alternative kinetic models

Recently, both Carlson (1990) and Crowley et al. (1991) have published alternative kinetic models for fission track annealing in apatite. Carlson's model is based on our laboratory annealing data for Durango apatite (Green et al., 1986) and other (unpublished) data. In his abstract, Carlson claims that because his model is "based on explicit physical mechanisms, extrapolations of annealing rates to the lower temperatures and longer timescales required for the interpretation of natural fission track length distributions can be made with greater confidence than is the case for purely empirical relationships fitted to the experimental annealing data". As explained in detail by Green et al. (1993), all aspects of Carlson's model are in fact purely empirical, and his model is inherently no "better" for the interpretation of data than any other. In fact, detailed inspection shows that Carlson's model does not fit the laboratory data set at all well. Therefore, we recommend against use of this model to interpret AFTA data.

The approach taken by Crowley et al. (1991) is very similar to that taken by Laslett et al., (1987). They have fitted models to new annealing data in two apatites of different composition - one close to end-member Fluorapatite (B-5) and one having a relatively high Sr content (113855). The model developed by Crowley et al. (1991) from their own annealing data for the B-5 apatite gives predictions in geological conditions which are consistently higher

than measured values, as shown in Figure C.5. Corrigan (1992) reported a similar observation in volcanogenic apatites in samples from a series of West Texas wells. Since the B-5 apatite is close to end-member Fluor-apatite, while the Otway Group apatites contain apatites with Cl contents from zero up to ~3 wt% (and the West Texas apatites have up to 1 wt%), the fluorapatites should have mean lengths rather less than the measured values, which should represent a mean over the range of Cl contents present. Therefore, the predictions of the Crowley et al. (1991) B-5 model appear to be consistently high.

We attribute this to the rather restricted temperature-time conditions covered by the experiments of Crowley et al. (1991), with annealing times between one and 1000 hours, in contrast to times between 20 minutes and 500 days in the experiments of Green et al. (1986). In addition, few of the measured length values in Crowley et al.'s study fall below 11 μm (in only five out of 60 runs in which lengths were measured in apatite B-5) and their model is particularly poorly defined in this region.

Crowley et al. (1991) also fitted a new model to the annealing data for Durango apatite published by Green et al. (1986). Predictions of their fit to our data are not very much different to those from the Laslett et al. (1987) model (Figure C.6). We have not pursued the differences between their model and ours in detail because the advent of our multi-compositional model has rendered the single compositional approach obsolete.

C.4 Evidence for elevated paleotemperatures from AFTA

The basic principle involved in the interpretation of AFTA data in sedimentary basins is to determine whether the degree of annealing shown by tracks in apatite from a particular sample could have been produced if the sample has never been hotter than its present temperature at any time since deposition. To do this, the burial history derived from the stratigraphy of the preserved sedimentary section is used to calculate a thermal history for each sample using the present geothermal gradient and surface temperature (i.e., assuming these have not changed through time). This is termed the "Default Thermal History". For each sample, the AFTA parameters predicted as a result of the Default Thermal History are then compared to the measured data. If the data show a greater degree of annealing than calculated on the basis of this history, the sample must have been hotter at some time in the past. In this case, the AFTA data are analysed to provide estimates of the magnitude of the maximum paleotemperature in that sample, and the time at which cooling commenced from the thermal maximum.

The degree of annealing is assessed in two ways - from fission track age and track length data. The stratigraphic age provides a basic reference point for the interpretation of fission track age, because reduction of the fission track age below the stratigraphic age unequivocally reveals that appreciable annealing has taken place after deposition of the host sediment. Large degrees of fission track age reduction, with the pooled or central fission track age very much less than



the stratigraphic age, indicate severe annealing, which requires paleotemperatures of at least $\sim 100^{\circ}\text{C}$ for any reasonable geological time-scale of heating ($> \sim 1$ Ma). Note that this applies even when apatites contain tracks inherited from source areas. More moderate degrees of annealing can be detected by inspection of the single grain age data, as the most sensitive (fluorine-rich) grains will begin to give fission track ages significantly less than the stratigraphic age before the central or pooled age has been reduced sufficiently to give a noticeable signal. Note that this aspect of the single grain age data can also be used for apatites which have tracks inherited from source areas. If signs of moderate annealing (from single grain age reduction) or severe annealing (from the reduction in pooled or central age) are seen in samples in which the Default Thermal History predicts little or no effect, the sample must have been subjected to elevated paleotemperatures at some time in the past. Figure C.7 shows how increasing degrees of annealing are observable in radial plots of the single grain fission track age data.

Similarly, the present temperature from which a sample is taken, and the way in which this has been approached (as inferred from the preserved sedimentary section), forms a basic point of reference for track length data. The observed mean track length is compared with the mean length predicted from the Default Thermal History. If the observed degree of track shortening in a sample is greater than that expected from the Default Thermal History (i.e., the mean length is significantly less than the predicted value), either the sample must have been subjected to higher paleotemperatures at some time after deposition, or the sample contains shorter tracks which were inherited from sediment source areas at the time the sediment was deposited. If shorter tracks were inherited from source areas, the sample should still contain a component of longer tracks corresponding to the tracks formed after deposition. In general, the fission track age should be greater than the stratigraphic age. This can be assessed quantitatively using the computer models for the development of AFTA parameters described in an earlier section. If the presence of shorter tracks cannot be explained by their inheritance from source areas, the sample must have been hotter in the past.

C.5 Quantitative determination of the magnitude of maximum paleotemperature and the timing of cooling using AFTA

Values of maximum paleotemperature and timing of cooling in each sample are determined using a forward modelling approach based on the quantitative description of fission track annealing described in earlier sections. The Default Thermal History described above is used as the basis for this forward modelling, but with the addition of episodes of elevated paleotemperatures as required to explain the data. AFTA parameters are modelled iteratively through successive thermal history scenarios in order to identify thermal histories that can account for observed parameters. The range of values of maximum paleotemperature and timing of cooling which can account for the measured AFTA parameters (fission track age and track length distribution) are defined using a maximum likelihood-based approach. In this



way, best estimates ("maximum likelihood values") can be defined together with $\pm 95\%$ confidence limits.

In samples in which all tracks have been totally annealed at some time in the past, only a minimum estimate of maximum paleotemperature is possible. In such cases, AFTA data provide most control on the time at which the sample cooled to temperatures at which tracks could be retained. The time at which cooling began could be earlier than this time, and therefore the timing also constitutes a minimum estimate.

Comparison of the AFTA parameters predicted by the multi-compositional model with measured values in samples which are currently at their maximum temperatures since deposition shows a good degree of consistency, suggesting the uncertainty in application of the model should be less than $\pm 10^\circ\text{C}$. This constitutes a significant improvement over earlier approaches, since the kinetic models used are constrained in both laboratory and geological conditions. It should be appreciated that relative differences in maximum paleotemperature can be identified with greater precision than absolute paleotemperatures, and it is only the estimation of absolute paleotemperature values to which the $\pm 10^\circ\text{C}$ uncertainty relates.

Cooling history

If the data are of high quality and provided that cooling from maximum paleotemperatures began sufficiently long ago (so that the history after this time is represented by a significant proportion of the total tracks in the sample), determination of the magnitude of a subsequent peak paleotemperature and the timing of cooling from that peak may also be possible (as explained in Section C.2). A similar approach to that outlined above provides best estimates and corresponding $\pm 95\%$ confidence limits for this episode. Such estimates may simply represent part of a protracted cooling history, and evidence for a later discrete cooling episode can only be accepted if this scenario provides a significantly improved fit to the data. Geological evidence and consistency of estimates between a series of samples can also be used to verify evidence for a second episode.

In practise, most typical AFTA datasets are only sufficient to resolve two discrete episodes of heating and cooling. One notable exception to this is when a sample has been totally annealed in an early episode, and has then undergone two (or more) subsequent episodes with progressively lower peak paleotemperatures in each. But in general, complex cooling histories involving a series of episodes of heating and cooling will allow resolution of only two episodes, and the results will depend on which episodes dominate the data. Typically this will be the earliest and latest episodes, but if multiple cooling episodes occur within a narrow time interval the result will represent an approximation to the actual history.



C.6 Qualitative assessment of AFTA parameters

Various aspects of thermal history can often be assessed by qualitative assessment of AFTA parameters. For example, samples which have reached maximum paleotemperatures sufficient to produce total annealing, and which only contain tracks formed after the onset of cooling, can be identified from a number of lines of evidence. In a vertical sequence of samples showing increasing degrees of annealing, the transition from rapidly decreasing fission track age with increasing depth to more or less the same age over a range of depth denotes the transition from partial to total annealing of all tracks formed prior to the thermal maximum. In samples in which all tracks have been totally annealed, the single grain age data should show that none of the individual grain fission track ages are significantly older than the time of cooling, and grains in all compositional groups should give the same fission track age unless the sample has been further disturbed by a later episode. If the sample cooled rapidly to sufficiently low temperatures, little annealing will have taken place since cooling, and all grains will give ages which are compatible with a single population around the time of cooling, as shown in Figure C.7.

Inspection of the distribution of single grain ages in partially annealed samples can often yield useful information on the time of cooling, as the most easily annealed grains (those richest in fluorine) may have been totally annealed prior to cooling, while more retentive (Cl-rich) compositions were only partially annealed (as in Figure C.7, centre). The form of the track length distribution can also provide information, from the relative proportions of tracks with different lengths. All of these aspects of the data can be used to reach a preliminary thermal history interpretation.

C.7 Allowing for tracks inherited from source areas

The effect of tracks inherited from source areas, and present at the time the apatite is deposited in the host sediment, is often posed as a potential problem for AFTA. However, this can readily be allowed for in analysing both the fission track age and length data.

In assessing fission track age data to determine the degree of annealing, the only criterion used is the comparison of fission track age with the value expected on the basis of the Default Thermal History. From this point of view, inherited tracks do not affect the conclusion: if a grain or a sample gives a fission track age which is significantly less than expected, the grain or sample has clearly undergone a higher degree of annealing than can be accounted for by the Default Thermal History, and therefore must have been hotter in the past, whether the sample contained tracks when it was deposited or not.

The presence of inherited tracks does impose a limit on our ability to detect post-depositional annealing from age data alone, as in samples which contain a fair proportion of inherited

tracks, moderate degrees of annealing may reduce the fission track age from the original value, but not to a value which is significantly less than the stratigraphic age. This is particularly noticeable in the case of Tertiary samples containing apatites derived from Paleozoic basement. In such cases, although fission track age data may show no evidence of post-depositional annealing, track length data may well show such evidence quite clearly.

The influence of track lengths inherited from source areas can be allowed for by comparison of the fission track age with the value predicted by the Default Thermal History combined with inspection of the track length distribution. If the mean length is much less than the length predicted by the Default Thermal History, either the sample has been subjected to elevated paleotemperatures, sufficient to produce the observed degree of length reduction, or else the sample contains a large proportion of shorter tracks inherited from source areas. However, in the latter case, the sample should give a pooled or central fission track age correspondingly older than the stratigraphic age, while the length distribution should contain a component of longer track lengths corresponding to the value predicted by the Default Thermal History. It is important in this regard that the length of a track depends primarily on the maximum temperature to which it has been subjected, whether in the source regions or after deposition in the sedimentary basin. Thus, any tracks retaining a provenance signature will have lengths towards the shorter end of the distribution where track lengths will not have "equilibrated" with the temperatures attained since deposition.

In general, it is only in extreme cases that inherited tracks render track length data insensitive to post-depositional annealing. For example, if practically all the tracks in a particular sample were formed prior to deposition, perhaps in a Pliocene sediment in which apatites were derived from a stable Paleozoic shield with fission track ages of ~300 Ma or more, the track length distribution will, in general, be dominated by inheritance, as only ~2% of tracks would have formed after deposition. Post-depositional heating will not be detectable as long as the maximum paleotemperature is insufficient to cause greater shortening than that which occurred in the source terrain. Even in such extreme cases, once a sample is exposed to temperatures sufficient to produce greater shortening than that inherited from source areas, the inherited tracks and those formed after deposition will all undergo the same degree of shortening, and the effects of post-depositional annealing can be recognised. In such cases, the presence of tracks inherited from source areas is actually very useful, because the number of tracks formed after deposition is so small that little or no information would be available without the inherited tracks.

C.8 Plots of fission track age and mean track length vs depth and temperature

AFTA data from well sequences are usually plotted as shown in Figure C.8. This figure shows AFTA data for two scenarios: one in which deposition has been essentially continuous from the Carboniferous to the present and all samples are presently at their maximum

paleotemperature since deposition (Figure C.8a); and, one in which the section was exposed to elevated paleotemperatures prior to cooling in the Early Tertiary (Figure C.8b).

In both figures, fission track age and mean track length are plotted against depth and present temperature. Presentation of AFTA data in this way often provides insight into the thermal history interpretation, following principles outlined earlier in this Appendix.

In Figure C.8a, for samples at temperatures below $\sim 70^{\circ}\text{C}$, the fission track age is either greater than or close to the stratigraphic age, and little fission track age reduction has affected these samples. Track lengths in these samples are all greater than $\sim 13\ \mu\text{m}$. In progressively deeper samples, both the fission track age and mean track length are progressively reduced to zero at a present temperature of around 110°C , with the precise value depending on the spread of apatite compositions present in the sample. Track length distributions in the shallowest samples would be a mixture of tracks retaining information on the thermal history of source regions, while in deeper samples, all tracks would be shortened to a length determined by the prevailing temperature. This pattern of AFTA parameters is characteristic of a sequence which is currently at maximum temperatures.

The data in Figure C.8b show a very different pattern. The fission track age data show a rapid decrease in age, with values significantly less than the stratigraphic age at temperatures of ~ 40 to 50°C , at which such a degree of age reduction could not be produced in any geological timescale. Below this rapid fall, the fission track ages do not change much over $\sim 1\ \text{km}$ (30°C). This transition from rapid fall to consistent ages is diagnostic of the transition from partial to total annealing. Samples above the "break-in slope" contain two generations of tracks: those formed prior to the thermal maximum, which have been partially annealed (shortened) to a degree which depends on the maximum paleotemperature; and, those formed after cooling, which will be longer. Samples below the break-in slope contain only one generation of tracks, formed after cooling to lower temperatures at which tracks can be retained. At greater depths, where temperatures increase to $\sim 90^{\circ}\text{C}$ and above, the effect of present temperatures begins to reduce the fission track ages towards zero, as in the "maximum temperatures now" case.

The track length data also reflect the changes seen in the fission track age data. At shallow depths, the presence of the partially annealed tracks shortened prior to cooling causes the mean track length to decrease progressively as the fission track age decreases. However, at depths below the break in slope in the age profile, the track length increases again as the shorter component is totally annealed and so does not contribute to the measured distribution of track lengths. At greater depths, the mean track lengths decrease progressively to zero once more due to the effects of the present temperature regime.



Examples of such data have been presented e.g., by Green (1989) and Kamp and Green (1990).

C.9 Determining paleogeothermal gradients and amount of section removed on unconformities

Estimates of maximum paleotemperatures in samples over a range of depths in a vertical sequence provides the capability of determining the paleogeothermal gradient immediately prior to the onset of cooling from those maximum paleotemperatures. The degree to which the paleogeothermal gradient can be constrained depends on a number of factors, particularly the depth range over which samples are analysed. If samples are only analysed over ~1 km, then the paleotemperature difference over that range may be only ~20 to 30°C. Since maximum paleotemperatures can often only be determined within a ~10°C range, this introduces considerable uncertainty into the final estimate of paleogeothermal gradient (see Figure C.9)

Another important factor is the difference between maximum paleotemperatures and present temperatures ("net cooling"). If this is only ~10°C, which is similar to the uncertainty in absolute paleotemperature determination, only broad limits can be established on the paleogeothermal gradient. In general, the control on the paleogeothermal gradient improves as the amount of net cooling increases. However, if the net cooling becomes so great that many samples were totally annealed prior to the onset of cooling - so that only minimum estimates of maximum paleotemperatures are possible - constraints on the paleogeothermal gradient from AFTA come only from that part of the section in which samples were not totally annealed. In this case, integration of AFTA data with VR measurements can be particularly useful in constraining the paleo-gradient.

Having constrained the paleogeothermal gradient at the time cooling from maximum paleotemperatures began, if we assume a value for surface temperature at that time, the amount of section subsequently removed by uplift and erosion can be calculated as shown in Figure C.10. The *net* amount of section removed is obtained by dividing the difference between the paleo-surface temperature (T_s) and the intercept of the paleotemperature profile at the present ground surface (T_i) by the estimated paleogeothermal gradient. The *total* amount of section removed is obtained by adding the thickness of section subsequently redeposited above the unconformity to the *net* amount estimated as in Figure C.10. If the analysis is performed using depths from the appropriate unconformity, then the analysis will directly yield the *total* amount of section removed.

Geotrack have developed a method of deriving estimates of both the paleogeothermal gradient and the net amount of section removed using estimated paleotemperatures derived from AFTA and VR. Perhaps more importantly, this method also provides rigorous values for upper and lower 95% confidence limits on each parameter. The method is based on maximum likelihood



estimation of the paleogeothermal gradient and the surface intercept, from a table of paleotemperature and depth values. The method is able to accept ranges for paleotemperature estimates (e.g., where the maximum paleotemperature can only be constrained to between, for example, 60 and 90°C), as well as upper and lower limits (e.g., <60°C for samples which show no detectable annealing; >110°C in samples which were totally annealed). Estimates of paleotemperature from AFTA and VR may be combined or analysed separately. Some results from this method have been reported by Bray et al. (1992). Full details of the methods employed are presented in a confidential, in-house, Geotrack research report, copies of which are available on request from the Melbourne office.

Results are presented in two forms. Likelihood profiles, plotting the log-likelihood as a function of either gradient or section removed, portray the probability of a given value of gradient or section removed. The best estimate is given by the value of gradient or section removed for which the log-likelihood is maximised. Ideally, the likelihood profiles should show a quadratic form, and values of gradient or section removed at which the log-likelihood has fallen by two from the maximum value define the upper and lower 95% confidence limits on the estimates. An alternative method of portraying this information is a crossplot of gradient against section removed, in which values which fall within 95% confidence limits (in two dimensions) are contoured. Note that the confidence limits defined by this method are rather tighter than those from the likelihood profiles, as the latter only reflect variation in one parameter, whereas the contoured crossplot takes variation of both parameters into account.

It must be emphasised that this method relies on the assumption that the paleotemperature profile was linear both throughout the section analysed and through the overlying section which has been removed. While the second part of this assumption can never be confirmed independently, visual inspection of the paleotemperature estimates as a function of depth should be sufficient to verify or deny the linearity of the paleotemperature profile through the preserved section.

Results of this procedure are shown in this report if the data allow sufficiently well-defined paleotemperature estimates to justify use of the method. Where the AFTA data suggest that the section is currently at maximum temperature since deposition, or that the paleotemperature profile was non-linear, or where data are of insufficient quality to allow rigorous paleotemperature estimation, the method is not used.



References

- Carlson, W.D. (1990) Mechanisms and kinetics of apatite fission-track annealing. *American Mineralogist*, 75, 1120 - 1139.
- Corrigan, J. (1992) Annealing models under the microscope, *On Track*, 2, 9-11.
- Crowley, K.D., Cameron, M. and Schaefer, R.L. (1991) Experimental studies of annealing of etched fission tracks in apatite. *Geochimica et Cosmochimica Acta*, 55, 1449-1465.
- Duddy, I.R., Green, P.F. and Laslett G.M. (1988) Thermal annealing of fission tracks in apatite 3. Variable temperature behaviour. *Chem. Geol. (Isot. Geosci. Sect.)*, 73, 25-38.
- Gleadow, A.J.W. and Duddy, I.R. (1981) A natural long-term track annealing experiment for apatite. *Nuclear Tracks*, 5, 169-174.
- Gleadow, A.J.W., Duddy, I.R. and Lovering, J.F. (1983) Fission track analysis; a new tool for the evaluation of thermal histories and hydrocarbon potential. *APEA J*, 23, 93-102.
- Gleadow, A.J.W., Duddy, I.R., Green, P.F. and Lovering, J.F. (1986) Confined fission track lengths in apatite - a diagnostic tool for thermal history analysis. *Contr. Min. Petr.*, 94, 405-415.
- Green, P.F. (1988) The relationship between track shortening and fission track age reduction in apatite: Combined influences of inherent instability, annealing anisotropy, length bias and system calibration. *Earth Planet. Sci. Lett.*, 89, 335-352.
- Green, P.F., Duddy, I.R., Gleadow, A.J.W., Tingate, P.R. and Laslett, G.M. (1986) Thermal annealing of fission tracks in apatite 1. A qualitative description. *Chem. Geol. (Isot. Geosci. Sect.)*, 59, 237-253.
- Green, P.F., Duddy, I.R., Gleadow, A.J.W. and Lovering, J.F. (1989a) Apatite Fission Track Analysis as a paleotemperature indicator for hydrocarbon exploration. In: Naeser, N.D. and McCulloh, T. (eds.) *Thermal history of sedimentary basins - methods and case histories*, Springer-Verlag, New York, 181-195.
- Green, P.F., Duddy, I.R., Laslett, G.M., Hegarty, K.A., Gleadow, A.J.W. and Lovering, J.F. (1989b) Thermal annealing of fission tracks in apatite 4. Quantitative modelling techniques and extension to geological timescales. *Chem. Geol. (Isot. Geosci. Sect.)*, 79, 155-182
- Green, P.F., Laslett, G.M. and Duddy, I.R. (1993) Mechanisms and kinetics of apatite fission track annealing: Discussion. *American Mineralogist*, 78, 441-445.
- Laslett, G.M., Kendall, W.S., Gleadow, A.J.W. and Duddy, I.R. (1982) Bias in measurement of fission track length distributions. *Nuclear Tracks*, 6, 79-85.
- Laslett, G.M., Green, P.F., Duddy, I.R. and Gleadow, A.J.W. (1987) Thermal annealing of fission tracks in apatite 2. A quantitative analysis. *Chem. Geol. (Isot. Geosci. Sect.)*, 65, 1-13.



Otway data and Laslett et al. (1987) predictions

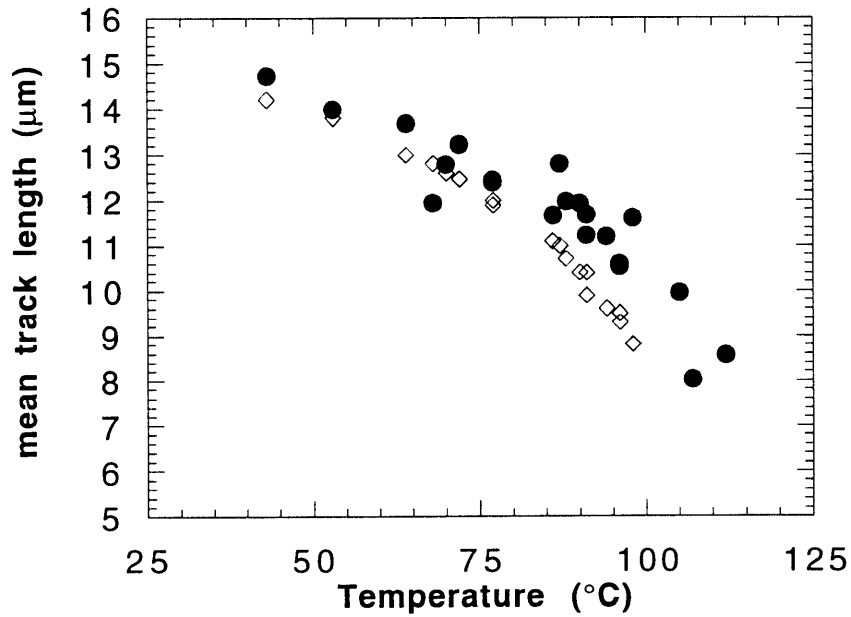


Figure C.1a Comparison of mean track length (solid circles) measured in samples from four Otway Basin reference wells (from Green et al, 1989a) and predicted mean track lengths (open diamonds) from the kinetic model of fission track annealing from Laslett et al. (1987). Although the predictions underestimate the measured values, they refer to an apatite composition that is more easily annealed than the majority of apatites in these samples, and therefore this is expected.

Otway Basin data (Durango composition) vs predictions of Laslett et al. (1987) model

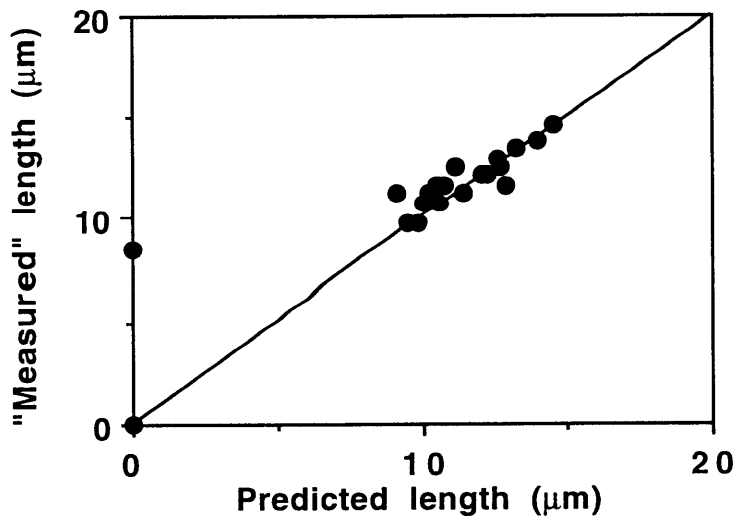


Figure C.1b Comparison of the mean track length in apatites of the same Cl content as Durango apatite from the Otway Group samples illustrated in figure C.1a, with values predicted for apatite of the same composition by the model of Laslett et al. (1987). The agreement is clearly very good except possibly at lengths below ~10 μm.

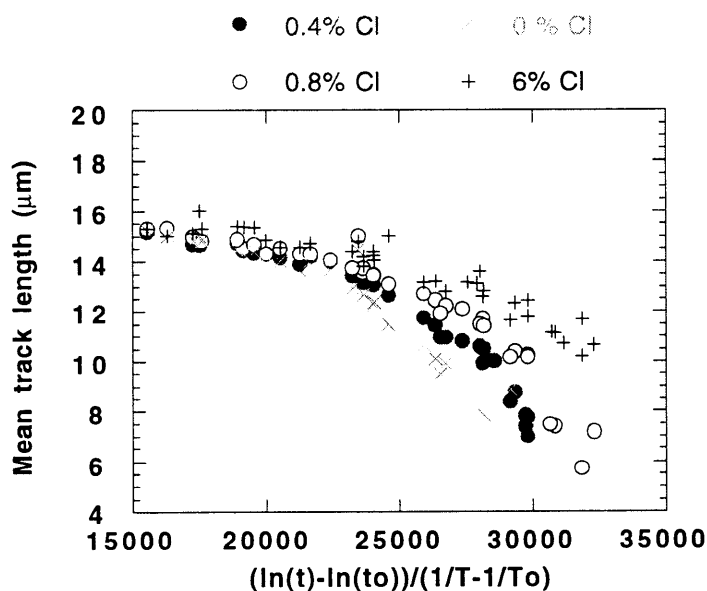


Figure C.2 Mean track length in apatites with four different chlorine contents, as a combined function of temperature and time, to reduce the data to a single scale. Fluorapatites are more easily annealed than chlorapatites, and the annealing kinetics show a progressive change with increasing Cl content.

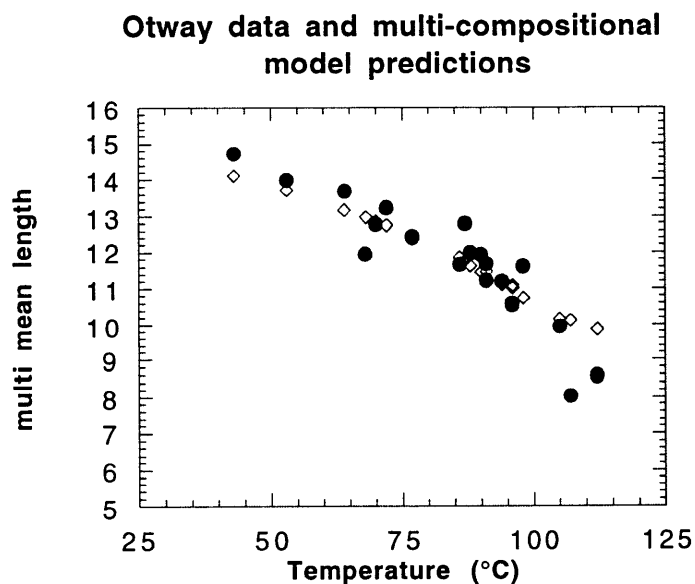
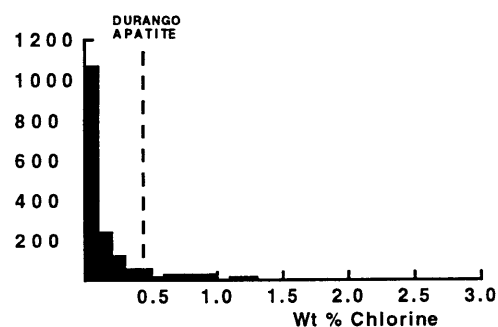


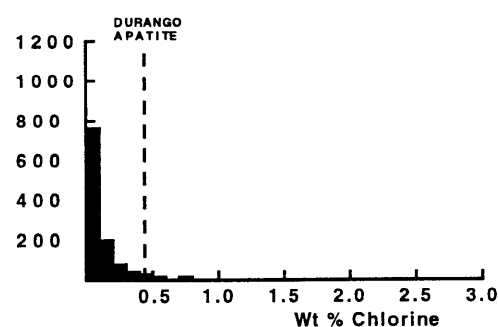
Figure C.3 Comparison of measured mean track length (solid circles) in samples from four Otway Basin reference wells (from Green et al, 1989a) and predicted mean track lengths (open diamonds) from the new multi-compositional kinetic model of fission track annealing described in Section C.3. This model takes into account the spread of Cl contents in apatites from the Otway Group samples and the influence of Cl content on annealing rate. The agreement is clearly very good over the range of the data.



All samples



"Normal sandstones"



Volcanogenic sandstones

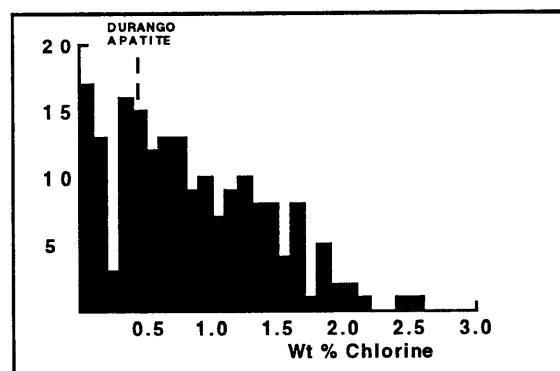


Figure C.4 a: Histogram of Cl contents (wt%) in over 1750 apatite grains from over 100 samples of various sedimentary and igneous rocks. Most samples give Cl contents below ~0.5 wt %, while those apatites giving higher Cl contents are characteristic of volcanogenic sandstones and basic igneous sources.

b: Histogram of Cl contents (wt%) in 1168 apatite grains from 61 samples which can loosely be characterised as "normal sandstone". The distribution is similar to that in the upper figure, except for a lower number of grains with Cl contents greater than ~1%.

c: Histogram of Cl contents (wt%) in 188 apatite grains from 15 samples of volcanogenic sandstone. The distribution is much flatter than the other two, with much higher proportion of Cl-rich grains.



Otway data and predictions

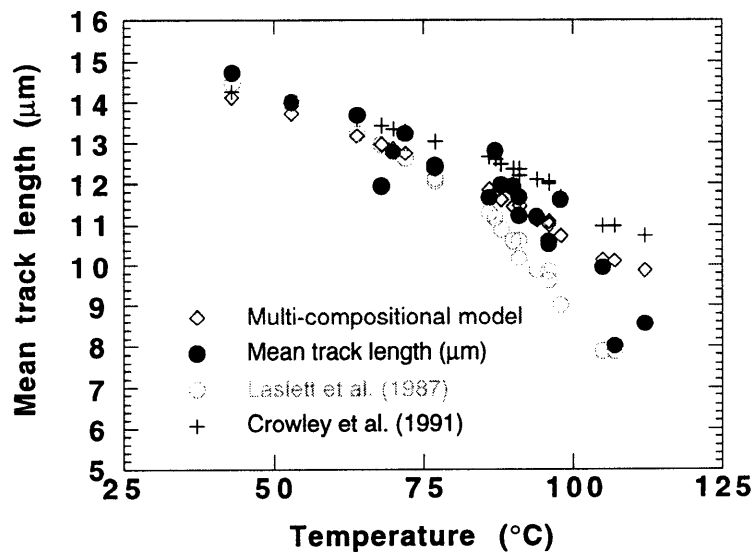


Figure C.5 Comparison of mean track length in samples from four Otway Basin reference wells (from Green et al, 1989a) and predicted mean track lengths from three kinetic models for fission track annealing. The Crowley et al. (1991) model relates to almost pure Fluorapatite (B-5), yet overpredicts mean lengths in the Otway Group samples which are dominated by Cl-rich apatites. The predictions of that model are therefore not reliable.

Otway data and predictions from Laslett et al. (1987) and Crowley et al. (1991) fits to data of Green et al. (1986)

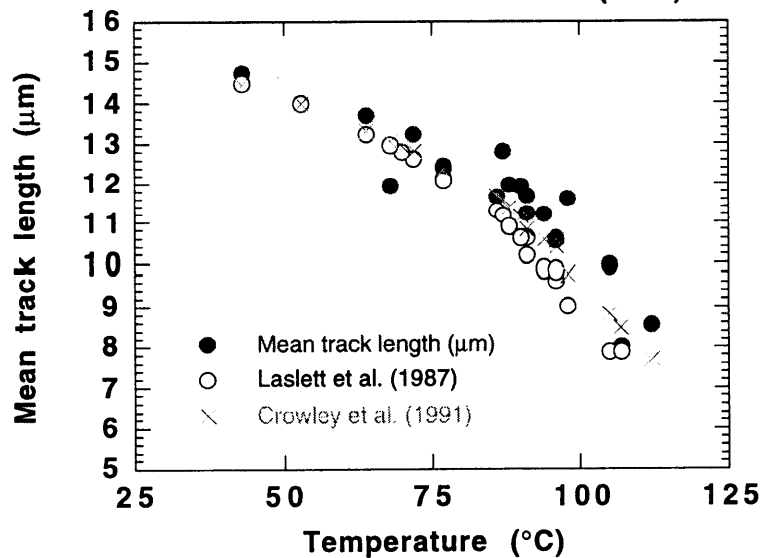
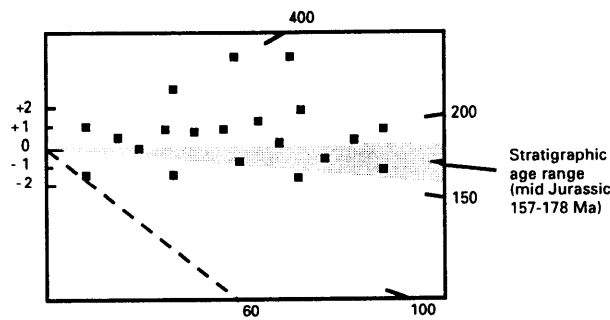


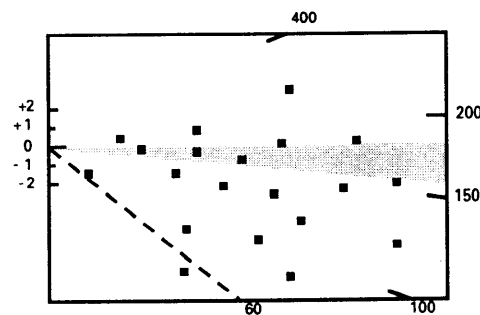
Figure C.6 Comparison of mean track length in samples from four Otway Basin reference wells with values predicted from Laslett et al. (1987) and the model fitted to the annealing data of Green et al. (1986) by Crowley et al. (1991). The predictions of the two models are not very different.



Little or no post-depositional annealing ($T < 60^\circ\text{C}$)



Moderate post-depositional annealing ($T \sim 90^\circ\text{C}$)



Total post-depositional annealing ($T > 110^\circ\text{C}$)

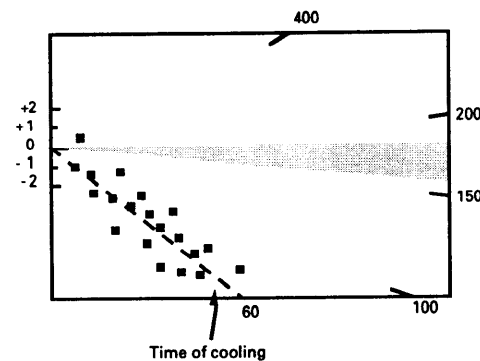


Figure C.7 Radial plots of single grain age data in three samples of mid-Jurassic sandstone that have been subjected to varying degrees of post-depositional annealing prior to cooling at ~ 60 Ma. The mid-point of the stratigraphic age range has been taken as the reference value (corresponding to the horizontal).

The upper diagram represents a sample which has remained at paleotemperatures less than $\sim 60^\circ\text{C}$, and has therefore undergone little or no post-depositional annealing. All single grain ages are either compatible with the stratigraphic age (within $y = \pm 2$ in the radial plot) or older than the stratigraphic age ($y_i > 2$).

The centre diagram represents a sample which has undergone a moderate degree of post-depositional annealing, having reached a maximum paleotemperature of around $\sim 90^\circ\text{C}$ prior to cooling. While some of the individual grain ages are compatible with the stratigraphic age ($-2 < y_i < +2$) and some may be significantly greater than the stratigraphic age ($y_i > 2$), a number of grains give ages which are significantly less than the stratigraphic age ($y < 2$).

The lower diagram represents a sample in which all apatite grains were totally annealed, at paleotemperatures greater than $\sim 110^\circ\text{C}$, prior to rapid cooling at ~ 60 Ma. All grains give fission track ages compatible with a fission track age of ~ 60 Ma (i.e., all data plot within ± 2 of the radial line corresponding to an age of ~ 60 Ma), and most are significantly younger than the stratigraphic age.

MAXIMUM TEMPERATURES NOW

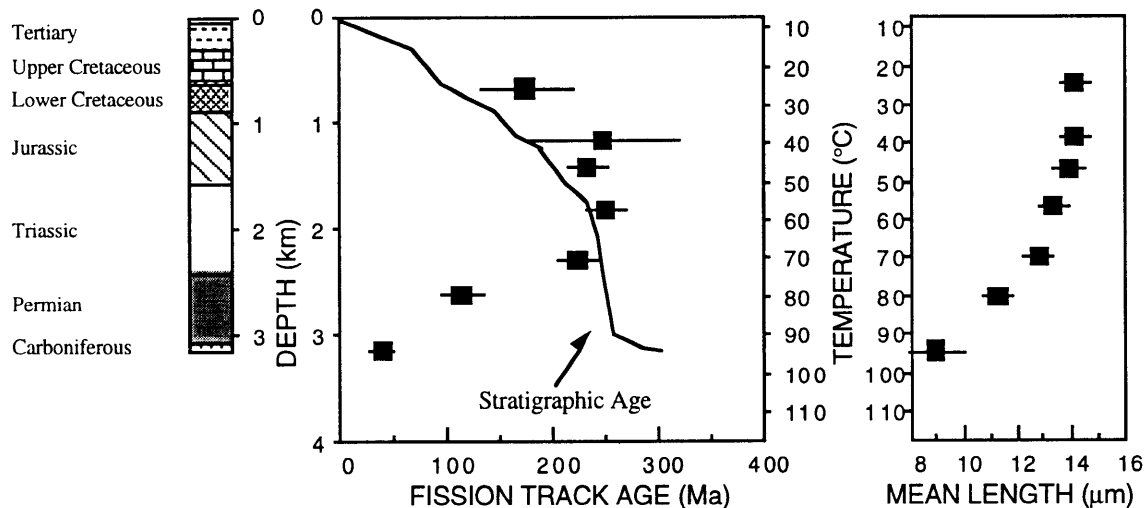


Figure C.8a Typical pattern of AFTA parameters in a well in which samples throughout the entire section are currently at their maximum temperatures since deposition. Both the fission track age and mean track length undergo progressive reduction to zero at temperatures of ~100 - 110°C, the actual value depending on the range of apatite compositions present.

HOTTER IN THE PAST

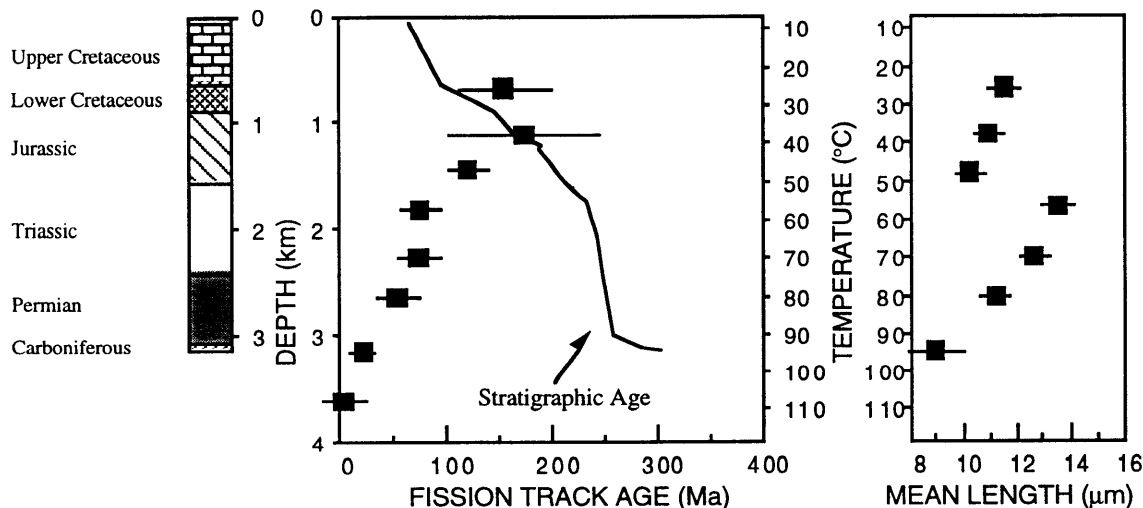


Figure C.8b Typical pattern of AFTA parameters in a well in which samples throughout the section were exposed to elevated paleotemperatures after deposition (prior to cooling in the Early Tertiary, in this case). Both the fission track age and mean track length show more reduction at temperatures of ~40 to 50°C than would be expected at such temperatures. At greater depths (higher temperatures), the constancy of fission track age and the increase in track length are both diagnostic of exposure to elevated paleotemperatures. See Appendix C for further discussion

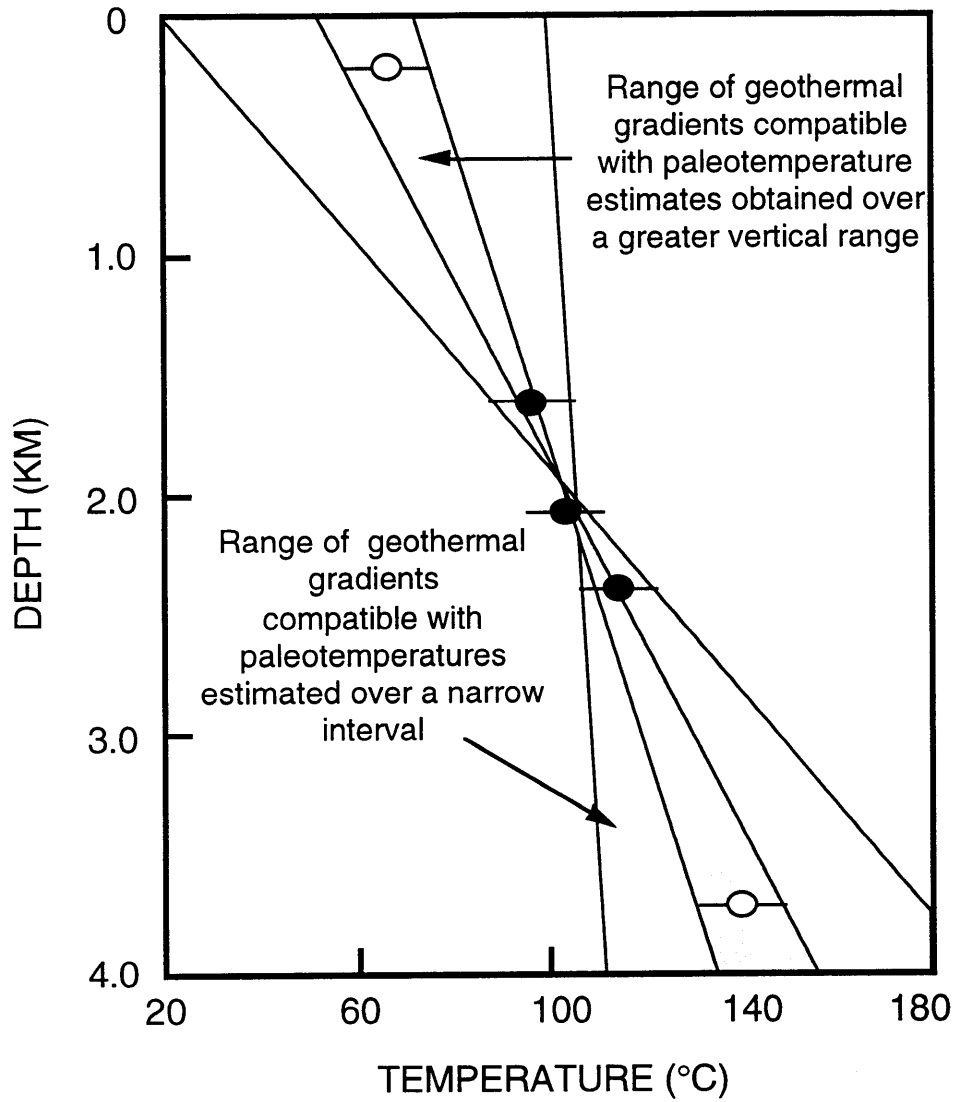


Figure C.9 It is important to obtain paleotemperature constraints over as great a range of depths as possible in order to provide a reliable estimate of paleogeothermal gradient. If paleotemperatures are only available over a narrow depth range, then the paleogeothermal gradient can only be very loosely constrained.

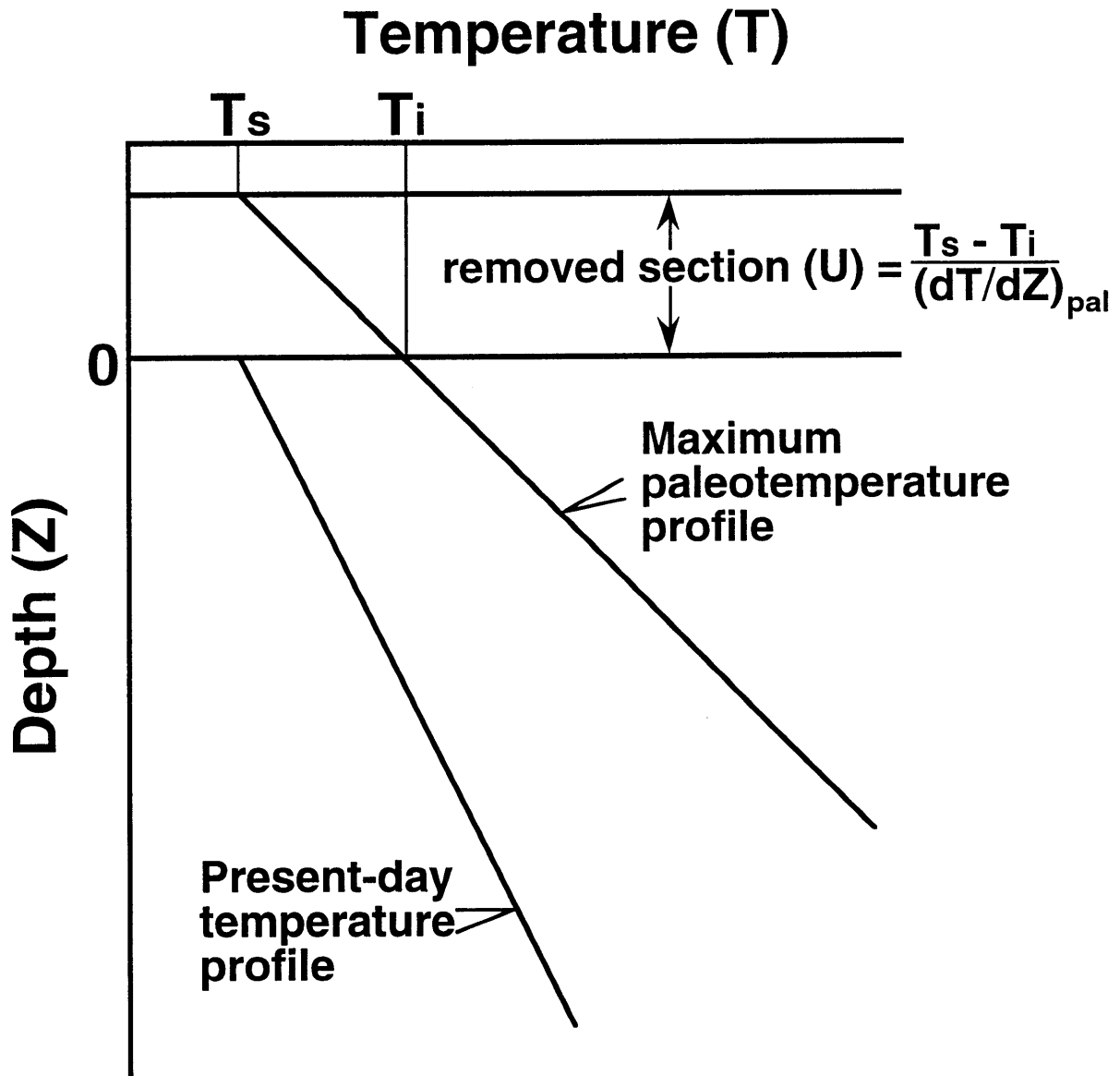


Figure C.10 If the paleogeothermal gradient can be constrained by AFTA and VR, as explained in the text, then for an assumed value of surface temperature, T_s , the amount of section removed can be estimated, as shown.



APPENDIX D

Vitrinite Reflectance Measurements

D.1 Integration of vitrinite reflectance data with AFTA

Vitrinite reflectance is a time-temperature indicator governed by a kinetic response in a similar manner to the annealing of fission tracks in apatite as described in Appendix C. In this study, vitrinite reflectance data are interpreted on the basis of the distributed activation energy model describing the evolution of VR with temperature and time described by Burnham and Sweeney (1989), as implemented in the BasinModTM software package of Platte River Associates. In a considerable number of wells from around the world, in which AFTA has been used to constrain the thermal history, we have found that the Burnham and Sweeney (1989) model gives good agreement between predicted and observed VR data, in a variety of settings.

As in the case of fission track annealing, it is clear from the chemical kinetic description embodied in equation 2 of Burham and Sweeney (1989) that temperature is more important than time in controlling the increase of vitrinite reflectance. If the Burham and Sweeney (1989) distributed activation energy model is expressed in the form of an Arrhenius plot (a plot of the logarithm of time versus inverse absolute temperature), then the slopes of lines defining contours of equal vitrinite reflectance in such a plot are very similar to those describing the kinetic description of annealing of fission tracks in Durango apatite developed by Laslett et al. (1987), which is used to interpret the AFTA data in this report. This feature of the two quite independent approaches to thermal history analysis means that for a particular sample, a given degree of fission track annealing in apatite of Durango composition will be associated with the same value of vitrinite reflectance regardless of the heating rate experienced by a sample. Thus paleotemperature estimates based on either AFTA or VR data sets should be equivalent, regardless of the duration of heating. As a guide, Table D.1 gives paleotemperature estimates for various values of VR for two different heating times.

One practical consequence of this relationship between AFTA and VR is, for example, that a VR value of 0.7% is associated with total annealing of all fission tracks in apatite of Durango composition, and that total annealing of all fission tracks in apatites of more Chlorine-rich composition is accomplished between VR values of 0.7 and ~0.9%.



Furthermore, because vitrinite reflectance continues to increase progressively with increasing temperature, VR data allow direct estimation of maximum paleotemperatures in the range where fission tracks in apatite are totally annealed (generally above $\sim 110^{\circ}\text{C}$) and where therefore AFTA only provides minimum estimates. Maximum paleotemperature estimates based on vitrinite reflectance data from a well in which most AFTA samples were totally annealed will allow constraints on the paleogeothermal gradient that would not be possible from AFTA alone. In such cases the AFTA data should allow tight constraints to be placed on the time of cooling and also the cooling history, since AFTA parameters will be dominated by the effects of tracks formed after cooling from maximum paleotemperatures. Even in situations where AFTA samples were not totally annealed, integration of AFTA and VR can allow paleotemperature control over a greater range of depth, e.g. by combining AFTA from sand-dominated units with VR from other parts of the section, thereby providing tighter constraint on the paleogeothermal gradient.

References

- Burnham, A.K. and Sweeney, J.J. (1989). A chemical kinetic model of vitrinite reflectance maturation. *Geochim. et Cosmochim. Acta*, 53, 2649-2657.
- Laslett, G.M., Green, P.F., Duddy, I.R. and Gleadow, A.J.W. (1987). Thermal annealing of fission tracks in apatite 2. A quantitative analysis. *Chem. Geol. (Isot. Geosci.Sect.)*, 65, 1-13.

**Table D.1: Paleotemperature - vitrinite reflectance nomogram based on Equation 2 of Burnham and Sweeney (1989)**

Paleotemperature (°C/°F)	Vitrinite Reflectance (%)	
	1 Ma Duration of heating	10 Ma Duration of heating
40 / 104	0.29	0.32
50 / 122	0.31	0.35
60 / 140	0.35	0.40
70 / 158	0.39	0.45
80 / 176	0.43	0.52
90 / 194	0.49	0.58
100 / 212	0.55	0.64
110 / 230	0.61	0.70
120 / 248	0.66	0.78
130 / 266	0.72	0.89
140 / 284	0.81	1.04
150 / 302	0.92	1.20
160 / 320	1.07	1.35
170 / 338	1.23	1.55
180 / 356	1.42	1.80
190 / 374	1.63	2.05
200 / 392	1.86	2.33
210 / 410	2.13	2.65
220 / 428	2.40	2.94
230 / 446	2.70	3.23

PE608056

This is an enclosure indicator page.
The enclosure PE608056 is enclosed within the
container PE908249 at this location in this
document.

The enclosure PE608056 has the following characteristics:

ITEM_BARCODE = PE608056
CONTAINER_BARCODE = PE908249
 NAME = Hunters Lane-1 Composite Well Log
 BASIN = GIPPSLAND
 ONSHORE? = N
 DATA_TYPE = WELL
 DATA_SUB_TYPE = COMPOSITE_LOG
 DESCRIPTION = Hunters Lane-1 Composite Well Log,
 Scale 1:605, Enclosure of Hunters
 Lane-1 Well Completion Report. Replaces
 PE908250 with the addition of Age and
 Formation columns.
 REMARKS = See Correspondence File PE909806 for
 letter dated 16 December 2002
 DATE_WRITTEN =
 DATE_PROCESSED =
 DATE_RECEIVED = 16-DEC-2002
 RECEIVED_FROM = Lakes Oil N.L.
 WELL_NAME = Hunters Lane-1
 CONTRACTOR =
 AUTHOR =
 ORIGINATOR = Lakes Oil N.L.
 TOP_DEPTH = 7
 BOTTOM_DEPTH = 422
 ROW_CREATED_BY = GT17_SW

(Inserted by DNRE - Vic Govt Mines Dept)

PE908251

This is an enclosure indicator page.
The enclosure PE908251 is enclosed within the
container PE908249 at this location in this
document.

The enclosure PE908251 has the following characteristics:

ITEM_BARCODE = PE908251
CONTAINER_BARCODE = PE908249
NAME = Hunters Lane-1 Formation Evaluation Log
BASIN = GIPPSLAND
ONSHORE? = Y
DATA_TYPE = WELL
DATA_SUB_TYPE = MUD_LOG
DESCRIPTION = Hunters Lane-1 Formation Evaluation
(Mud Log) Log, Scale 1:500, Enclosure
of Hunters Lane-1 Well Completion
Report
REMARKS =
DATE_WRITTEN =
DATE_PROCESSED =
DATE_RECEIVED = 30-OCT-2002
RECEIVED_FROM = Lakes Oil N.L.
WELL_NAME = Hunters Lane-1
CONTRACTOR = Lakes Oil N.L.
AUTHOR =
ORIGINATOR = Lakes Oil N.L.
TOP_DEPTH = 7
BOTTOM_DEPTH = 422
ROW_CREATED_BY = DN07_SW

(Inserted by DNRE - Vic Govt Mines Dept)